Repression of SATB1 in regulatory T cells is required for suppressive function and inhibition of effector differentiation

Marc Beyer[1], Yasser Thabet[1], Roman Müller[2], Timothy Sadlon[3], Sabine Classen[1], Katharina Lahl[4], Samik Basu[5], Xuyu Zhou[6], Samantha L. Bailey-Bucktrout[6], Wolfgang Krebs[1], Eva Schönfeld[1], Jan Böttcher[7], Tatiana Golovina[5], Christian T. Mayer[4], Andrea Hofmann[1], Daniel Sommer[1], Svenja Debey-Pascher[1], Elmar Endl[7], Andreas Limmer[7], Keli L. Hippen[8], Bruce R. Blazar[8], Robert Balderas[9], Thomas Quast[10], Andreas Waha[11], Günter Mayer[12], Michael Famulok[12], Percy A. Knolle[7], Claudia Wickenhauser[13], Waldemar Kolanus[10], Bernhard Schermer[2], Jeffrey A. Bluestone[6], Simon C. Barry[3], Tim Sparwasser[4], James L. Riley[5], Joachim L. Schultze[1]

[1] *LIMES-Institute, Laboratory for Genomics and Immunoregulation, University of Bonn, Carl-Troll-Str. 31, D-53115 Bonn, Germany*

[2] *Internal Medicine IV, Nephrology and General Internal Medicine, University Cologne, Kerpener Str. 62, D-50937 Cologne, Germany*

[3] *Discipline of Paediatrics, Women's and Children's Health Research Institute, University of Adelaide, 72 King William Road, North Adelaide, 5006, Australia*

[4] *Institute of Infection Immunology, TWINCORE, Centre for Experimental and Clinical Infection Research; a joint venture between the Medical School Hannover (MHH) and the Helmholtz Centre for Infection Research (HZI), Feodor-Lynen-Str. 7, 30625 Hannover, Germany*

[5] *Department of Pathology and Laboratory Medicine, Translational Research Program, Abramson Family Cancer Research Institute, University of Pennsylvania, Room 556 BRB II/III, 421 Curie Blvd., Philadelphia, PA 19104-6160, USA*

[6] *Diabetes Center and the Department of Medicine, University of California, 513 Parnassus Avenue, Box 0540, San Francisco, CA 94143, USA.*

[7] *Institutes of Molecular Medicine and Experimental Immunology, University Hospital Bonn, Sigmund-Freud-Str. 25, D-53105 Bonn, Germany*

[8] *Cancer Center and Department of Pediatrics, Division of Blood and Marrow Transplantation, University of Minnesota, Mayo Mail Code 109, 420 Delaware St. SE, Minneapolis, MN 55455, USA*

[9] *BD Biosciences – Pharmingen, 10975 Torreyana Road, San Diego, CA 92121, USA*

[10] *LIMES-Institute, Laboratory for Molecular Immunology, University of Bonn, Carl-Troll-Str. 31, D-53115 Bonn, Germany*

[11] *Department of Neuropathology, University Hospital Bonn, Sigmund-Freud-Str. 25, D-53105 Bonn, Germany*

[12] *LIMES-Institute, Laboratory of Chemical Biology, University of Bonn, Gerhard-Domagk-Str. 1, D-53121 Bonn, Germany*

[13] *Department for Diagnostic, Institute for Pathology, University Hospital Leipzig, Liebigstr. 26, D-04103 Leipzig, Germany*

Regulatory T cells are essential for self tolerance and immune homeostasis. Lack of $T_{effector}$-cell function and gain of suppressive activity by T_{reg} are dependent on the transcriptional program induced by FOXP3. Here we identified the repression of SATB1, a genome organizer regulating chromatin structure and gene expression, as a critical event for T_{reg} phenotype and function. FOXP3 acts as a transcriptional repressor directly at the SATB1 locus and indirectly through induction of microRNAs binding to the 3′UTR of SATB1 as well as by maintaining a repressive chromatin state of the SATB1 locus. Release of SATB1 from FOXP3 control in T_{reg} causes loss of suppressive function, establishment of transcriptional $T_{effector}$ programs, and induction of $T_{effector}$ cytokines *in vitro* and *in vivo*. These data support that inhibition of SATB1-mediated modulation of global chromatin remodelling is pivotal for maintaining T_{reg} functionality.

T_{reg} are characterized by their suppressive function and inability to produce effector cytokines upon activation[1]. Expression of the X-linked forkhead transcription factor FOXP3 has been clearly linked to the establishment and maintenance of T_{reg} lineage, identity and suppressor function[2-7]. Moreover, FOXP3 is also associated with the control of $T_{effector}$ function in T_{reg}[4, 5]. Although, there is a growing body of evidence pointing towards plasticity amongst committed $CD4^+$ T-cell lineages including T_{reg}[8-11] the mechanism for this plasticity and its significance in normal immune responses and disease states are still to be elucidated. Naturally occurring functional deletion mutants of FOXP3 in man (IPEX (immune dysregulation, polyendocrinopathy, enteropathy, X-linked) and mice (scurfy) are associated with severe autoimmunity and excessive $T_{effector}$ function[6, 7, 12, 13]. However, it is unclear whether autoimmunity occurs because the T cells destined to become T_{reg} now have effector function (cell intrinsic) or whether there is lack of peripheral tolerance due to the lack of T_{reg} (cell extrinsic). While these mechanisms are not mutually exclusive and could both contribute to immune dysfunction, there are new studies indicating that T_{reg} can become potent mediators of autoimmunity when FOXP3 expression is lost. Multiple transgenic reporter mouse models have demonstrated that loss of FOXP3 can induce the conversion of T_{reg} into cells with a variety of $T_{effector}$ programs[2-4, 14]. In a model where FOXP3 is attenuated, a TH2 phenotype was induced in the T_{reg} compartment[2]. In other transgenic models deletion of FOXP3 induced TH1, TH2, or TH17 phenotypes in FOXP3 positive cells[4, 14]. While T_{reg} seem to be re-programmable by loss of the lineage-associated transcription factor FOXP3, there is no evidence that conventional T cells (T_{conv}) actively suppress the T_{reg} lineage program. On the contrary, only stable expression of FOXP3 in T_{conv} appears capable of inducing a T_{reg} phenotype within these cells[7]. Together these findings suggest that $T_{effector}$ programs are the default state in $CD4^+$ T cells and that transcriptional programs induced and maintained by FOXP3 overrule $T_{effector}$ function in

T_{reg}. Whether the inhibition of $T_{effector}$ differentiation in T_{reg} is critical for T_{reg} suppressive function is unclear. Such a model would be supported by the existence of FOXP3-induced mechanisms that continuously and actively control $T_{effector}$ programs in these specialized T cells.

Consistent with the active suppression of $T_{effector}$ programs in T_{reg} ablation of the transcriptional repressor Eos[15] or the FOXO transcription factors[16, 17] impart partial $T_{effector}$ characteristics to T_{reg}. Other transcription factors including IRF4[18] and STAT3[19] have also been implicated in the modulation of effector cell differentiation by T_{reg}[20]. Selectively disrupting miRNA control in T_{reg} leads to ablation of T_{reg} function and gain of effector function[21-23] suggesting that there is additional posttranscriptional control sustaining T_{reg} phenotype and function. There is also evidence that epigenetic control by DNA methylation and histone modification is important for FOXP3-mediated suppressive functions[18, 24, 25] raising the possibility that epigenetic regulation may also be involved in the repression of $T_{effector}$ functions in T_{reg}. Moreover, genome-wide assessment of histone modifications in T-cell subsets indicated an unexpectedly high degree of plasticity between different T-cell subsets including not only effector populations but also iT_{reg} and T_{reg}[26]. In summary, these findings support the existence of active regulatory mechanisms that enable committed T_{reg} to suppress $T_{effector}$ differentiation[27]. The mechanisms identified so far are mainly associated with the induction of FOXP3-specific programs involved in the maintenance of T_{reg} phenotype and function. However, complementary mechanisms preserving T_{reg} function through the repression of a global process required for triggering $T_{effector}$ function may also exist.

In this report, we specifically searched for genes repressed by FOXP3 in T_{reg} that might be central to maintaining regulatory function and suppression of $T_{effector}$ function in

T_{reg}. We identified the special AT-rich sequence-binding protein-1 (SATB1) to be amongst the most significantly repressed genes in human and murine T_{reg}. Repression was mediated directly by transcriptional control of FOXP3 at the SATB1 locus and indirectly by FOXP3-dependent miRNAs as well as repressive histone marks. Release of SATB1 from FOXP3 control was sufficient to re-program natural $FOXP3^{+}$ T_{reg} into $T_{effector}$ cells that lost suppressive function and gained $T_{effector}$ function *in vitro* an *in vivo*. These findings show that SATB1 control by FOXP3 is an essential and critical mechanism maintaining T_{reg}-cell functionality.

RESULTS

SATB1 is expressed only at low levels in human T_{reg}

To identify regulatory circuits actively suppressed by FOXP3 as a prerequisite for T_{reg} function and inhibition of $T_{effector}$ programs, whole transcriptome analysis of human resting or activated conventional $FOXP3^{-}CD25^{-}$ T cells (T_{conv}) and natural regulatory $CD25^{+}FOXP3^{+}$ T cells (T_{reg}) was performed (Supplementary Fig. 1 and Supplementary Table 1). Of the 22 genes displaying significant downregulation in T_{reg}, special AT-rich sequence-binding protein 1 (SATB1) was consistently expressed at a significantly lower level in T_{reg} compared to T_{conv} (Fig. 1a). Re-assessment of transcriptome data from previous reports confirmed our observation of SATB1 to be a potential target of FOXP3-mediated repression[28-30].

SATB1 is a chromatin organizer and transcription factor essential for controlling a large number of genes participating in T-cell development and activation[31]. SATB1 regulates gene expression by directly recruiting chromatin modifying factors[32] and anchoring matrix attachment regions to the nuclear matrix[33]. In murine TH2 clones, SATB1 has been shown to function as a global transcriptional regulator specifically anchoring the looped topology of the TH2 cytokine locus, a pre-requisite for the induction of certain TH2 cytokines[34]. Since SATB1-deficient thymocytes do not develop beyond the double-positive stage[31, 33], the role of SATB1 in peripheral T cells, particularly in T_{reg}, is still elusive. Transcriptome data were validated in an independent set of samples by qRT-PCR (Fig. 1b), western blotting (Fig. 1c), and single cell analysis by flow cytometry (Fig. 1d) clearly demonstrating reduced SATB1 mRNA and protein expression in human T_{reg}. Since similar

results were obtained by the different techniques we further analyzed on single cell level using either analytical flow cytometry or cell sorting. As increased SATB1 expression has been previously linked to activation of pan-T-cell populations[35], we assessed the dynamics of SATB1 expression in T_{conv} and T_{reg} during activation using T-cell receptor stimulation (with CD3 mAbs) in the presence of co-stimulation (CD28 mAbs) or the cytokine interleukin-2 (IL-2) (Fig. 1e) as well as mitogens (data not shown). Analysis of SATB1 expression established a stimulation dependent up-regulation of SATB1 in T_{conv} while resting T_{reg} had a significantly lower SATB1 expression than T_{conv} and this expression was only modestly upregulated after T-cell activation. Next we assessed SATB1 in induced T_{reg} (iT_{reg})[36]. Naïve human $CD25^{-}CD45RA^{+}$ T cells were activated via TCR and CD28 in the presence of TGFβ for 5 days. These iT_{reg} expressed FOXP3 mRNA and protein, and showed T-cell suppressive function (data not shown). Similar to natural T_{reg}, SATB1 was not induced in iT_{reg} under these conditions while significantly enhanced expression was observed in cells stimulated via TCR and CD28 in the absence of TGFβ (T_{stim}, Fig. 1f, g). In line with this observation, TH1 and TH2 cytokine production is significantly abrogated in the absence of SATB1 (Fig. 1h). To determine whether FOXP3 induction in iT_{reg} was necessary to suppress SATB1 we performed gain-of-function experiments ectopically over-expressing FOXP3 in T_{conv}. High expression of FOXP3 resulted in reduced expression of SATB1 (Fig. 1i), which was accompanied by a concomitant decrease in cytokine expression (Fig. 1j) and the induction of a T_{reg}-cell gene signature (Supplementary Fig. 2). Low level FOXP3 expression did not result in significant repression of SATB1 or induction of a Treg gene signature (data not shown). Taken together, reduced expression of SATB1 is

a hallmark of both iT_{reg} and T_{reg} in humans and repression of SATB1 depends on sufficiently high expression of FOXP3.

Loss of FOXP3 in T_{reg} results in high SATB1 expression

To further assess the role of FOXP3 in SATB1 repression in human T_{reg} we performed loss-of-function experiments. Silencing FOXP3 by siRNA resulted in loss of FOXP3 expression and consequently loss of suppressive function in T_{reg} (Fig. 2a, b) as well as typical T_{reg}-cell genes (Supplementary Fig.3). A small but significant increase of SATB1 expression was already evident in unstimulated FOXP3-depleted human T_{reg} (Fig. 2c), however, this was significantly enhanced when T_{reg} were stimulated via TCR together with co-stimulation or IL-2. This increase in SATB1 expression was associated with production of TH1 (IFN-γ) and TH2 (IL-4 and IL-5) cytokines (Fig. 2d, e). As this effect could have been a direct effect of FOXP3 on the cytokines themselves we developed a strategy to knockdown SATB1 and FOXP3 simultaneously in human T_{reg}. Only experiments with a sufficient knockdown efficiency for both genes were further analyzed. Additional knockdown of SATB1 in human T_{reg} with a silenced FOXP3 gene (Supplementary Fig. 4) resulted in a significantly decreased induction of T-helper cytokines (Fig. 2f) demonstrating that expression of $T_{effector}$ cytokines in FOXP3-deficient T_{reg} is governed by SATB1. Similar results were obtained when expanded human T_{reg} were transduced with lentiviruses encoding miRNA targeting FOXP3 and SATB1 (Supplementary Fig. 5). Together, these findings establish that FOXP3 negatively regulates SATB1 expression and that low SATB1

levels are required to prevent expression of $T_{effector}$ cytokines in human $T_{reg,}$ thus assigning a key function of FOXP3-SATB1 interaction to the T_{reg} phenotype.

FOXP3 expression is not linked to low levels of SATB1

To exclude the possibility that SATB1 may reciprocally repress FOXP3 in T_{conv} cells we performed siRNA mediated knockdown of SATB1 in human naïve T_{conv} to assess whether SATB1 downregulation in T_{conv} might induce FOXP3 expression and a conversion of T_{conv} into $T_{reg.}$ We did not observe increased FOXP3 expression in resting and stimulated naïve T_{conv}, including under iT_{reg}-inducing conditions after silencing of SATB1 (Supplementary Fig. 6a), suggesting that high SATB1 levels are not necessary for low levels of FOXP3 in resting T_{conv} and that FOXP3 induction in naïve T_{conv} under stimulation occurs independent of the levels of SATB1. In line with this finding, we did not observe increased induction of several T_{reg}-cell associated genes after knockdown of SATB1 (Supplementary Fig. 6b).

SATB1 expression in murine T_{reg}

To address whether SATB1 regulation is conserved between human and murine T_{reg} we analyzed SATB1 expression by qPCR, western blotting, flow cytometry, and confocal microscopy in T cells derived from two different FOXP3 reporter mice (DEREG[37], FOXP3-GFP[38]). Similar to human T_{reg} SATB1 mRNA and protein expression was lower in murine T_{reg} compared with T_{conv} cells isolated from thymus, spleen or lymph nodes (Fig. 3a, b, c, and data not shown). SATB1 expression in $CD4^+$ single-positive thymocytes was considerably higher than in peripheral $CD4^+$ T_{conv} from the spleen or lymph nodes (data not

shown) which further supports the essential role of SATB1 during early thymocyte development as established in SATB1$^{-/-}$ mice[31]. Despite this, FOXP3^{+} T_{reg} in thymus still displayed a significant downregulation of SATB1 compared with FOXP3^{-} cells s.

To establish SATB1 as a FOXP3-target gene we analyzed T_{reg} from male DEREG mice harboring a spontaneously mutated FOXP3 allele (DEREG x scurfy). Flow-sorted T_{reg} from these animals displayed a significantly increased SATB1 expression in T_{reg} compared to FOXP3-competent T_{reg} (Fig. 3d). In line with this finding an increase of TH1 and TH2 cytokines *in vivo* was observed in T_{reg} from DEREG x scurfy mice (Fig. 3e). SATB1 mRNA expression in T_{reg} versus T_{conv} cells was further validated by re-assessment of three transcriptome data sets (GSE18387, GSE6681, GSE11775)[5, 39, 40] derived from mice with a mutated FOXP3 gene in T_{reg} (data not shown).

Female heterozygous DEREG x scurfy mice harbor both FOXP3-competent and FOXP3-incompetent T_{reg}. These mice were used to determine whether SATB1 repression in T_{reg} cells is a cell-intrinsic function of FOXP3. FOXP3-competent and FOXP3-incompetent T_{reg} were isolated and compared side-by-side by immunofluorescence (Fig. 3f). Similar to previous reports we observed nuclear localization of SATB1 in FOXP3^{-} thymocytes forming a cage-like structure within the nucleus (Fig. 3c)[33]. Increased SATB1 signals in FOXP3-incompetent T_{reg} cells with unchanged localization and distribution further support that SATB1 expression is regulated by FOXP3 (Fig. 3f). Up-regulation of SATB1 in FOXP3^{sf} GFP^{+} T_{reg} was further quantified by intracellular flow cytometry (Fig. 3g). Overall, these data clearly establish increased SATB1 mRNA and protein expression as a consequence of FOXP3 deficiency in T_{reg}.

FOXP3 binds to the genomic SATB1 locus in human T_{reg}

Inverse correlation between FOXP3 and SATB1 expression in murine and human T_{reg} strongly suggested that FOXP3 might act directly as a transcriptional repressor of the SATB1 locus. We performed FOXP3-ChIP tiling arrays and promoter arrays using chromatin isolated from human natural T_{reg} (Fig. 4a and Supplementary Fig. 7a) as well as bioinformatic *in silico* prediction to identify 16 regions for qPCR validation. Binding regions identified were located upstream of the TSS as well as in the genomic locus of SATB1 (Fig. 4b and Supplementary Table 2). FOXP3 binding within the promoter region or genomic locus of SATB1 in T_{reg} was demonstrated by ChIP-coupled quantitative PCR (ChIP-qPCR) (Fig. 4c) and electrophoretic mobility-shift assays (data not shown) clearly demonstrating binding to the SATB1 locus similar to known targets of FOXP3 (Supplementary Fig. 7b-f). To probe functional consequences of FOXP3 binding to the SATB1 locus, we performed luciferase reporter assays for six of the FOXP3 binding regions. FOXP3 binding regions were cloned in between a minP promoter element and a luciferase reporter gene. Co-transfection of these reporter constructs with a human FOXP3 expression vector led to a significant decrease in activity for four of these regions with more than one FOXP3 binding motif (Fig. 4d). Mutation of predicted FOXP3 binding motifs within these regions rescued luciferase activity (Fig. 4d) indicating that SATB1 expression is actively repressed by FOXP3 binding to several regions within the genomic SATB1 locus. Further support for FOXP3 binding was derived from *in vitro* DNA-protein interaction analysis using recombinant FOXP3 protein with either wild-type or mutated FOXP3 binding motifs within the BR1 and BR2 elements demonstrating strong binding of

FOXP3 only to the wild type sequences (BR1: K_D 516.2 nM, BR2: K_D 579.8 nM) whereas the mutated motifs showed almost no interaction with FOXP3 (Fig. 4e).

Ectopic SATB1 expression in T_{reg} results in loss of suppressive function and gain of $T_{effector}$ function

To determine whether reduced SATB1 expression is required for T_{reg} to exert regulatory function we over-expressed SATB1 in human natural $CD4^+CD25^{high}$ $FOXP3^+$ T_{reg} using a lentiviral vector carrying the SATB1 full length transcript (Supplementary Fig. 8). MACS-isolated human $CD4^+CD25^{high}$ T_{reg} or $CD4^+CD25^-$ T_{conv} were stimulated for 24 hours with CD3 and CD28-coated beads in the presence of IL-2. After this initial stimulation, T_{reg} were lentivirally transduced with pELNS DsRED 2A SATB1 which expresses DsRED at a ratio of 1:1 to the transgene[41] or control virus containing only DsRED. Cells were expanded for 6 days in the presence of CD3 and CD28-coated beads and IL-2, prior to sorting DsRED-positive cells. Only SATB1 and control transduced cells showing highly similar FOXP3 and DsRED expression were used for further analysis (Supplementary Fig. 8a). In sharp contrast to control-transduced T_{reg}, SATB1 over-expressing $FOXP3^+$ T_{reg} cells lost their suppressive function (Supplementary Fig. 8b-c and Fig. 5a). At the same time, these cells gained expression of TH1 (IFN-γ), TH2 (IL-4), and TH17 (IL-17A) cytokines (Fig. 5b-e) suggesting a reprogramming of T_{reg} cells into $T_{effector}$ in the presence of high levels of SATB1 in the absence of any change in FOXP3 levels. As expected, T_{conv} transduced with SATB1 using the same approach had no suppressive

function (Supplementary Fig. 9). These data strongly support that ectopic expression of SATB1 in T_{reg} is sufficient to convert the FOXP3-mediated program into $T_{effector}$ programs.

High expression of SATB1 induces transcriptional $T_{effector}$ programs

To estimate the genome-wide re-programming in SATB1 over-expressing T_{reg} whole transcriptome analysis was performed. Using stringent filter criteria a total of 100 genes were found to be significantly increased in SATB1 expressing T_{reg} whereas 21 were decreased (Fig. 6a). Analysis of the differentially expressed genes revealed that 20% were associated with elevated expression in T_{conv} (in comparison to T_{reg}), 29% of the changed genes were primarily linked with T-cell activation, and 16% were classified as common T-cell genes. The remaining genes (35%) showed no known association with T-cell function or lineage and were classified as SATB1-induced (Fig. 6b). Furthermore, compiling gene lists previously associated with TH1, TH2, and TH17 differentiation revealed induction of many genes involved in $T_{effector}$ differentiation in SATB1-expressing T_{reg} (Fig. 6c).In contrast genes representing the human T_{reg}-cell gene signature including the T_{reg}-cell signature we identified, were unchanged in SATB1 expressing T_{reg} (Fig. 6d). Since we used polyclonal human T_{reg} for this analysis, it is not surprising that we find the three major T-cell differentiation programs simultaneously. In summary, low SATB1 expression in T_{reg} is necessary to permit suppressive function and to ensure inhibition of effector cell differentiation of regulatory T cells.

Epigenetic regulation of SATB1 transcription in T_{reg}

The strong dependency of T_{reg} function on the repression of SATB1 implies the involvement of additional regulatory mechanisms. When assessing DNA methylation, we identified three CpG-rich sites upstream of exon 1 at the SATB1 locus (Fig. 7a). However, in contrast to the FOXP3 locus itself (Supplementary Fig. 10)[24], the SATB1 locus was similarly demethylated in T_{reg} and T_{conv} (Fig. 7a) suggesting that DNA-methylation does not play a regulatory role at the SATB1 locus in T_{reg}.

Next, we examined the chromatin status of the SATB1 locus by analyzing permissive and repressive histone modifications. ChIP-sequencing of expanded human T_{reg} showed a reduction in permissive histone H3 trimethylation at Lys 4 (H3K4me3) and increased repressive histone H3 trimethylation at Lys27 (H3K27me3) in T_{reg} compared to T_{conv} in humans (Fig. 7b and Supplementary Fig. 11) as well as lower acetylation of histone 4 (H4Ac, Fig. 7b and Supplementary Fig. 11). Using CHIP-qPCR we confirmed these epigenetic differences between T_{reg} and T_{conv} (Fig. 7c). When assessing a publicly available dataset for murine T_{reg} we could establish similar histone marks at the SATB1 locus (Supplementary Fig. 12) suggesting that a conserved regulatory circuit exists that contributes to the lower expression of SATB1 in T_{reg} by inducing repressive epegenetic marks at the SATB1 locus.

MicroRNA-dependent regulation of SATB1 levels in T_{reg}

A prominent layer of post-transcriptional gene regulation is exerted by miRNAs. MiRNA profiling in human T_{reg} versus T_{conv} allowed us to identify several differentially expressed miRNAs in T_{reg} (data not shown). Using inverse correlation analysis between SATB1 and miRNA expression as well as computational prediction of miRNA binding of

seed-matched sites (Fig. 8a), we identified 5 miRNAs that were differentially expressed between T_{reg} and T_{conv} (Fig. 8b) and showed a significant inverse correlation between SATB1 and miRNA expression (Fig. 8c). Of these 5 miRNAs, miR-155, miR-21, and miR-7 are direct targets of FOXP3 as previously reported for miR-155[29, 42, 43] and miR-21[44] and confirmed by FOXP3-ChIP tiling arrays and ChIP-qPCR (Fig. 8d,e, and Supplementary Fig. 13) as well as functional analysis (Simon Barry, unpublished data). Assessment of miRNA expression levels in FOXP3-overexpressing T_{conv} and FOXP3-silenced T_{reg} could confirm these miRNAs as targets of FOXP3 (Supplementary Fig. 14). For the assessment of functionally relevant binding of the miRNAs to the 3′ UTR of the SATB1 mRNA we fused the SATB1 3′ UTR to a luciferase reporter gene and determined luciferase activity in cells transfected with synthetic miRNAs. Expression of any of the 5 miRNAs significantly repressed constitutive luciferase activity with the 3 miRNAs that are direct targets of FOXP3 clearly showing the strongest effect (Fig. 8f). Mutation of the respective binding motifs resulted in restoration of luciferase activity (Fig. 8f). As exemplified for miR-155, loss of function of a single miRNA only resulted in minor differences in SATB1 mRNA expression in primary human T_{reg} (Supplementary Fig. 15a) indicating that the loss of a single miRNA may be incapable of rescuing SATB1 expression. Complete loss of all miRNAs, however, as achieved in mice by a T_{reg}-specific deletion of DICER[23] clearly leads to up-regulation of SATB1 at both mRNA and protein level (Fig. 8g and Supplementary Fig. 15b). These results suggest that FOXP3 is able to confer T_{reg}-specific downregulation of SATB1 expression not only by direct binding to the SATB1 locus but also using a second layer of regulation using miRNAs.

Decreased T_{reg}-cell function in SATB1 expressing murine T_{reg} *in vivo*

To assess whether SATB1 expression results in reduced regulatory function in murine T_{reg} *in vitro* and *in vivo* we over-expressed SATB1 in murine $CD4^+FOXP3^+$ T_{reg} from DEREG mice using a lentiviral vector carrying the SATB1 full length transcript (Supplementary Fig. 16). Sorted murine $CD4^+FOXP3^+$ T_{reg} or $CD4^+FOXP3^-$ T_{conv} from DEREG mice were expanded for 10-14 days with CD3 and CD28-coated beads in the presence of IL-2. After this initial expansion period, murine expanded T_{reg} were lentivirally transduced with a SATB1-IRES-Thy1.1 construct or control plasmids. Cells were expanded for 4 additional days in the presence of CD3 and CD28-coated beads and IL-2 prior to sorting Thy1.1-positive GFP^+ T_{reg}. Transduced cells showing highly similar FOXP3 expression were used for further analysis (Supplementary Fig. 15a). In contrast to control-transduced T_{reg}, SATB1 over-expressing $FOXP3^+$ T_{reg} cells lost their suppressive function and gained TH1 (IFN-γ) and TH2 (IL-5) effector cytokine expression (Supplementary Fig. 15b-e and Fig. 9b) supporting a reprogramming of T_{reg} cells into $T_{effector}$ in the presence of high levels of SATB1 observed in human T_{reg}.

To assess *in vivo* suppressor capacity of T_{reg} overexpressing SATB1 we transferred these cells together with naïve $CD4^+CD45RB^{high}$ T cells isolated from normal mice into $RAG2^{-/-}$ recipient mice. Transfer of naïve $CD4^+CD45RB^{high}$ T cells alone led to the development of colitis (Fig. 9c-e). As expected, $RAG2^{-/-}$ mice that received naïve $CD4^+CD45RB^{high}$ T cells and control vector-transduced T_{reg} did not lose weight (Fig. 9c-e). In agreement with the reduced suppressor activity observed *in vitro*, SATB1-

overexpressing T_{reg} showed an impairment in suppressor function, reflected in weight loss and colitis development similar to mice receiving only naïve $CD4^{+}CD45RB^{high}$ T cells (Fig. 9c-e). We observed a significant expansion in the number of T_{conv} in mice receiving either no T_{reg} or SATB1-overexpressing T_{reg} in spleen, mesenteric and peripheral lymph nodes (Fig. 9f), while the number of cells that maintained FOXP3 expression in spleen, mesenteric and peripheral lymph nodes was equal in mice receiving control vector-transduced or SATB1-overexpressing T_{reg} (Fig. 9g). Thus, $FOXP3^{+}$ T_{reg} cells in the presence of SATB1 show lower suppressor function with a concomitant gain of $T_{effector}$ programs *in vivo* and *in vitro* suggesting that downregulation of SATB1 in T_{reg} is necessary to maintain a stable suppressive phenotype.

DISCUSSION

In T_{reg} numerous mechanisms have been implicated in their suppressive function upon contact to other immune effector cells, amongst them CTLA4 expression, secretion of inhibitory cytokines, target cell lysis or impaired APC activation[1]. At the same time intrinsic inhibition of $T_{effector}$ function mainly by FOXP3-induced mechanisms - as exemplified by the induction of the transcriptional repressor Eos[15] - seems to be necessary for T_{reg} to exert suppressive function. In this report we identified the repression of SATB1 in T_{reg} to be required for suppressive function and inhibition of effector differentiation of these cells. Inhibition of SATB1 in T_{reg} is conserved between man and mice. In scurfy mice immunopathology is associated with a strong upregulation of SATB1 and downstream effector cytokines in the T_{reg} compartment suggesting that the induction of $T_{effector}$ function by T_{reg} contributes to the immunopathology of these mice. A defining difference in SATB1 regulation in T_{reg} compared to a T_{conv} was the profound lack of upregulation of SATB1 following stimulation. As up-regulation of SATB1 is required for the induction of $T_{effector}$ cytokines in T_{conv} this suggests that FOXP3-mediated suppression of SATB1 plays an important role in inhibiting cytokine production within a T_{reg}. In support of this, the ectopic expression of high levels of SATB1 in T_{reg} led to the induction of $T_{effector}$ cytokines and loss of suppressive function despite the expression of FOXP3 *in vitro* and *in vivo*. Mechanistically, SATB1 expression is controlled directly by FOXP3-mediated transcriptional repression, histone modifications as well as the induction of at least 5 miRNAs binding to the 3'UTR of SATB1. Together these findings establish that continuous active repression of central mechanisms involved in $T_{effector}$ programs provided by SATB1 is necessary for T_{reg} to exert their suppressive function.

Thus a major finding of our study is that T_{reg} not only depend on the induction of FOXP3-mediated genes associated with suppressive function but also on the specific repression of molecules such as SATB1 to prevent $T_{effector}$ function. SATB1 is not only a critical factor in early T-cell development[31], but also plays an important role in $T_{effector}$ differentiation[34, 45]. SATB1 expression at low levels seems to be necessary to retain functional T-cell integrity not only in T_{conv} but also in T_{reg} as complete SATB1 KO have basically no T cells in the periphery[31, 46]. However, in the peripherally under stimulating conditions, the TCR induced upregulation of SATB1 observed in T_{conv} which is important for their differentiation and cytokine secretion is blocked in T_{reg} by both direct FOXP3 binding and indirect mechanisms including miRNA dependent regulation and repressive histone modifications. SATB1 has been shown to delineate specific epigenetic modifications at target gene loci thereby reprogramming chromatin organization and transcriptional programs[33, 46, 47]. Although many reports suggest SATB1 mainly exerts repressor activity[48], SATB1 clearly can function as an activator of transcription[49], particularly in T_{helper} cell differentiation[34, 45]. Similar to our finding in polyclonal naïve human T cells, SATB1 has also been shown to be induced after activation of a T helper type 2 clone[34]. In this context, SATB1 can interact with multiple binding sites across the T helper type 2 cytokine loci to create a highly looped locus conformation bringing different TH2 cytokine loci in close proximity, an apparent pre-requisite for the induction of genes encoding TH2 cytokines. The induction of TH1 as well as TH17 cytokines in polyclonal T_{reg} strongly suggests that SATB1 may play a similar role in other $T_{effector}$ populations. Indeed, repressing SATB1 in naïve $CD4^{+}CD25^{-}$ T cells under polarizing conditions (TH1, TH2, TH17) leads to significantly reduced effector cytokine expression in these cells

(Beyer, Schultze, unpublished data). While FOXP3 clearly dictates the repression of SATB1 in T_{reg} thereby preventing $T_{effector}$ function, we have no evidence so far for an inverse control of FOXP3 by SATB1 in T_{conv}, which together favors a model with $T_{effector}$ programs continually and actively overruled by FOXP3-mediated transcriptional repression within a T_{reg}.

Further evidence for such a model comes from studies elucidating the effect of the transcriptional repressor Eos, which is expressed at elevated levels in T_{reg}[15]. Eos directly interacts with FOXP3 to specifically induce chromatin modifications that result in gene silencing, while genes induced by FOXP3 were not affected by Eos expression and function. Interestingly, loss of Eos function abrogated suppressive T_{reg} function but only partially endowed T_{reg} with $T_{effector}$ functions consistent with the normal repression of $T_{effector}$ differentiation within a T_{reg}. Similarly, loss of Runx1-CBFβ heterodimers, another component of the FOXP3 containing multi-protein complex, by conditional knockout in T_{reg} leads to reduction of FOXP3 expression, loss of suppressor function and gain of IL-4 expression by T_{reg}[50, 51]. FOXP3 as well as Eos and Runx1-CBFβ heterodimers have been shown to directly repress certain effector cytokines such as IFNγ or IL-4 suggesting T_{reg} may use multiple mechanisms to suppress $T_{effector}$ programs[15, 20, 50]. Nevertheless, the ectopic expression of SATB1 in T_{reg} by lentiviral gene transfer at levels comparable with activated T_{conv} was sufficient to induce effector cytokines suggesting that high levels of SATB1 can overcome FOXP3 repression of downstream targets. This might be similarly true in activated T_{conv} that can express lower levels of FOXP3 temporarily during early activation phases.

Recently the FOXO transcription factors Foxo1 and Foxo3 have also been implicated in the inhibition of $T_{effector}$ function in T_{reg}[16]. Interestingly, lack of Foxo1 and Foxo3 in T_{reg} is sufficient to induce TH1 and TH17 effector cytokines but not TH2 cytokines whereas SATB1 seems to have a more profound effect on TH2 cytokines under certain conditions[34, 45]. Limited evidence based on the reported gene expression data derived from $Foxo1^{-/-}$ $Foxo3^{-/-}$ double KO T_{reg} suggests that SATB1 is not a direct target of Foxo1 and Foxo3 indicating that repression of the different $T_{effector}$ cytokine loci in T_{reg} may occur either by separate or multiple mechanisms. Together these findings point to a hierarchy of repressive mechanisms ensuring suppression of $T_{effector}$ function in T_{reg}.

We could establish that epigenetic regulation by altered histone modifications contributes to the lower expression of SATB1 in T_{reg}. We observed less permissive and more repressive histone modifications in human as well as murine T_{reg} suggesting that epigenetic regulation of the SATB1 locus represents an additional layer of regulation present to preserve low levels of SATB1 expression in T_{reg}.

Another finding of our study was the control of SATB1 by at least 5 miRNAs that are all highly upregulated in $FOXP3^{+}$ T_{reg}. These findings are in line with recently suggested concepts of feed forward control of gene transcription by transcriptional repressors and miRNAs that are induced by the same transcriptional repressor[52]. At least 3 of these miRNA are direct targets of FOXP3 as reported previously for miR-155 and miR-21[29, 42-44]. While silencing single miRNAs was not sufficient to significantly change SATB1 protein expression complete loss of miRNAs in T_{reg} by conditional KO of DICER in T_{reg} clearly increased SATB1 expression in these T_{reg}. Although this experiment cannot rule out the possibility of indirect mechanisms leading to elevated SATB1 expression

exerted by the complete loss of miRNAs in these cells, the presence of conserved and functionally important binding sites of these highly upregulated miRNAs in the 3'UTR of the SATB1 mRNA strongly suggests that miRNA control plays an important role in repression of SATB1 in T_{reg}.

In conclusion, we have established FOXP3-mediated repression of SATB1 as a prerequisite for suppressive function and inhibition of $T_{effector}$ mechanisms in T_{reg}. This was not only mediated by direct FOXP3-mediated transcriptional repression but also by epigenetic modifications and the induction of several miRNAs (Supplementary Fig. 17). Together with other previous reports our findings support a model of continuously active regulatory networks shaping the overall function of T cells in the periphery as an alternative to terminal differentiation. An active and continuous blockade of $T_{effector}$ function instead of terminal T_{reg} differentiation allows T cells a higher degree of functional plasticity e.g. under inflammatory conditions where T_{reg} can gain effector function once FOXP3 is switched off[27, 53-55]. Therapeutic manipulation of these regulatory networks may provide new opportunities for T_{reg} associated diseases, including autoimmune diseases and cancer.

REFERENCES

1. Sakaguchi, S., Yamaguchi, T., Nomura, T. & Ono, M. Regulatory T cells and immune tolerance. *Cell* **133**, 775-787 (2008).
2. Lin, W. *et al.* Regulatory T cell development in the absence of functional Foxp3. *Nat Immunol* **8**, 359-368 (2007).
3. Wan, Y.Y. & Flavell, R.A. Regulatory T-cell functions are subverted and converted owing to attenuated Foxp3 expression. *Nature* **445**, 766-770 (2007).
4. Lahl, K. *et al.* Nonfunctional regulatory T cells and defective control of Th2 cytokine production in natural scurfy mutant mice. *J Immunol* **183**, 5662-5672 (2009).
5. Williams, L.M. & Rudensky, A.Y. Maintenance of the Foxp3-dependent developmental program in mature regulatory T cells requires continued expression of Foxp3. *Nat Immunol* **8**, 277-284 (2007).
6. Fontenot, J.D., Gavin, M.A. & Rudensky, A.Y. Foxp3 programs the development and function of CD4+CD25+ regulatory T cells. *Nat Immunol* **4**, 330-336 (2003).
7. Hori, S., Nomura, T. & Sakaguchi, S. Control of regulatory T cell development by the transcription factor Foxp3. *Science* **299**, 1057-1061 (2003).
8. O'Shea, J.J. & Paul, W.E. Mechanisms underlying lineage commitment and plasticity of helper CD4+ T cells. *Science* **327**, 1098-1102 (2010).
9. Murphy, K.M. & Stockinger, B. Effector T cell plasticity: flexibility in the face of changing circumstances. *Nat Immunol* **11**, 674-680 (2010).
10. Feuerer, M., Hill, J.A., Mathis, D. & Benoist, C. Foxp3+ regulatory T cells: differentiation, specification, subphenotypes. *Nat Immunol* **10**, 689-695 (2009).

11. Lee, Y.K., Mukasa, R., Hatton, R.D. & Weaver, C.T. Developmental plasticity of Th17 and Treg cells. *Curr Opin Immunol* **21**, 274-280 (2009).

12. Brunkow, M.E. *et al.* Disruption of a new forkhead/winged-helix protein, scurfin, results in the fatal lymphoproliferative disorder of the scurfy mouse. *Nat Genet* **27**, 68-73 (2001).

13. Bennett, C.L. *et al.* The immune dysregulation, polyendocrinopathy, enteropathy, X-linked syndrome (IPEX) is caused by mutations of FOXP3. *Nat Genet* **27**, 20-21 (2001).

14. Gavin, M.A. *et al.* Foxp3-dependent programme of regulatory T-cell differentiation. *Nature* **445**, 771-775 (2007).

15. Pan, F. *et al.* Eos mediates Foxp3-dependent gene silencing in CD4+ regulatory T cells. *Science* **325**, 1142-1146 (2009).

16. Ouyang, W. *et al.* Foxo proteins cooperatively control the differentiation of Foxp3+ regulatory T cells. *Nat Immunol* **11**, 618-627 (2010).

17. Harada, Y. *et al.* Transcription factors Foxo3a and Foxo1 couple the E3 ligase Cbl-b to the induction of Foxp3 expression in induced regulatory T cells. *J Exp Med* **207**, 1381-1391 (2010).

18. Zheng, Y. *et al.* Regulatory T-cell suppressor program co-opts transcription factor IRF4 to control T(H)2 responses. *Nature* (2009).

19. Chaudhry, A. *et al.* CD4+ regulatory T cells control TH17 responses in a Stat3-dependent manner. *Science* **326**, 986-991 (2009).

20. Ziegler, S.F. FOXP3: of mice and men. *Annu Rev Immunol* **24**, 209-226 (2006).

21. Chong, M.M., Rasmussen, J.P., Rudensky, A.Y. & Littman, D.R. The RNAseIII enzyme Drosha is critical in T cells for preventing lethal inflammatory disease. *J Exp Med* **205**, 2005-2017 (2008).

22. Liston, A., Lu, L.F., O'Carroll, D., Tarakhovsky, A. & Rudensky, A.Y. Dicer-dependent microRNA pathway safeguards regulatory T cell function. *J Exp Med* **205**, 1993-2004 (2008).

23. Zhou, X. *et al.* Selective miRNA disruption in T reg cells leads to uncontrolled autoimmunity. *J Exp Med* **205**, 1983-1991 (2008).

24. Floess, S. *et al.* Epigenetic control of the foxp3 locus in regulatory T cells. *PLoS Biol* **5**, e38 (2007).

25. Li, B. *et al.* FOXP3 interactions with histone acetyltransferase and class II histone deacetylases are required for repression. *Proc Natl Acad Sci U S A* **104**, 4571-4576 (2007).

26. Wei, G. *et al.* Global mapping of H3K4me3 and H3K27me3 reveals specificity and plasticity in lineage fate determination of differentiating CD4+ T cells. *Immunity* **30**, 155-167 (2009).

27. Zhou, X., Bailey-Bucktrout, S., Jeker, L.T. & Bluestone, J.A. Plasticity of CD4(+) FoxP3(+) T cells. *Curr Opin Immunol* **21**, 281-285 (2009).

28. Pfoertner, S. *et al.* Signatures of human regulatory T cells: an encounter with old friends and new players. *Genome Biol* **7**, R54 (2006).

29. Zheng, Y. *et al.* Genome-wide analysis of Foxp3 target genes in developing and mature regulatory T cells. *Nature* **445**, 936-940 (2007).

30. Sugimoto, N. *et al.* Foxp3-dependent and -independent molecules specific for CD25+CD4+ natural regulatory T cells revealed by DNA microarray analysis. *Int Immunol* **18**, 1197-1209 (2006).

31. Alvarez, J.D. *et al.* The MAR-binding protein SATB1 orchestrates temporal and spatial expression of multiple genes during T-cell development. *Genes Dev* **14**, 521-535 (2000).

32. (!!! INVALID CITATION !!!).

33. Cai, S., Han, H.J. & Kohwi-Shigematsu, T. Tissue-specific nuclear architecture and gene expression regulated by SATB1. *Nat Genet* **34**, 42-51 (2003).

34. Cai, S., Lee, C.C. & Kohwi-Shigematsu, T. SATB1 packages densely looped, transcriptionally active chromatin for coordinated expression of cytokine genes. *Nat Genet* **38**, 1278-1288 (2006).

35. Lund, R. *et al.* Identification of genes involved in the initiation of human Th1 or Th2 cell commitment. *Eur J Immunol* **35**, 3307-3319 (2005).

36. Chen, W. *et al.* Conversion of peripheral CD4+CD25- naive T cells to CD4+CD25+ regulatory T cells by TGF-beta induction of transcription factor Foxp3. *J Exp Med* **198**, 1875-1886 (2003).

37. Lahl, K. *et al.* Selective depletion of Foxp3+ regulatory T cells induces a scurfy-like disease. *J Exp Med* **204**, 57-63 (2007).

38. Fontenot, J.D. *et al.* Regulatory T cell lineage specification by the forkhead transcription factor foxp3. *Immunity* **22**, 329-341 (2005).

39. Anz, D. *et al.* Immunostimulatory RNA Blocks Suppression by Regulatory T Cells. *J Immunol* **184**, 939-946.

40. Kuczma, M. *et al.* Foxp3-deficient regulatory T cells do not revert into conventional effector CD4+ T cells but constitute a unique cell subset. *J Immunol* **183**, 3731-3741 (2009).

41. Szymczak, A.L. *et al.* Correction of multi-gene deficiency in vivo using a single 'self-cleaving' 2A peptide-based retroviral vector. *Nat Biotechnol* **22**, 589-594 (2004).

42. Lu, L.F. *et al.* Foxp3-dependent microRNA155 confers competitive fitness to regulatory T cells by targeting SOCS1 protein. *Immunity* **30**, 80-91 (2009).

43. Kohlhaas, S. *et al.* Cutting edge: the Foxp3 target miR-155 contributes to the development of regulatory T cells. *J Immunol* **182**, 2578-2582 (2009).

44. Marson, A. *et al.* Foxp3 occupancy and regulation of key target genes during T-cell stimulation. *Nature* **445**, 931-935 (2007).

45. Ahlfors, H. *et al.* SATB1 dictates expression of multiple genes including IL-5 involved in human T helper cell differentiation. *Blood* (2010).

46. Yasui, D., Miyano, M., Cai, S., Varga-Weisz, P. & Kohwi-Shigematsu, T. SATB1 targets chromatin remodelling to regulate genes over long distances. *Nature* **419**, 641-645 (2002).

47. Galande, S., Purbey, P.K., Notani, D. & Kumar, P.P. The third dimension of gene regulation: organization of dynamic chromatin loopscape by SATB1. *Curr Opin Genet Dev* **17**, 408-414 (2007).

48. Kumar, P.P. *et al.* Functional interaction between PML and SATB1 regulates chromatin-loop architecture and transcription of the MHC class I locus. *Nat Cell Biol* **9**, 45-56 (2007).

49. Kumar, P.P. *et al.* Phosphorylation of SATB1, a global gene regulator, acts as a molecular switch regulating its transcriptional activity in vivo. *Mol Cell* **22**, 231-243 (2006).

50. Kitoh, A. *et al.* Indispensable role of the Runx1-Cbfbeta transcription complex for in vivo-suppressive function of FoxP3+ regulatory T cells. *Immunity* **31**, 609-620 (2009).

51. Rudra, D. *et al.* Runx-CBFbeta complexes control expression of the transcription factor Foxp3 in regulatory T cells. *Nat Immunol* **10**, 1170-1177 (2009).

52. Tsang, J., Zhu, J. & van Oudenaarden, A. MicroRNA-mediated feedback and feedforward loops are recurrent network motifs in mammals. *Mol Cell* **26**, 753-767 (2007).

53. Koch, M.A. *et al.* The transcription factor T-bet controls regulatory T cell homeostasis and function during type 1 inflammation. *Nat Immunol* **10**, 595-602 (2009).

54. Zhou, X. *et al.* Instability of the transcription factor Foxp3 leads to the generation of pathogenic memory T cells in vivo. *Nat Immunol* **10**, 1000-1007 (2009).

55. Oldenhove, G. *et al.* Decrease of Foxp3+ Treg cell number and acquisition of effector cell phenotype during lethal infection. *Immunity* **31**, 772-786 (2009).

METHODS

Methods and any associated references are available in the online version of the paper at http://www.nature.com/natureimmunology/.

Accession codes. GEO: microarray data, GSE15390; tiling array data, GSE20995.

Note: Supplementary information is available on the Nature Immunology website.

ACKNOWLEDGMENTS

We thank M. Mai, S. Keller, N. Kuhn, J. Birke, I. Büchmann, A. Dolf, and P. Wurst for technical assistance, M. Hoch, M. Pankratz, A. Popov, A. Staratschek-Jox as well as all other lab members for discussions and J. Oldenburg for providing us with blood samples from healthy individuals. J.L.S. and M.B. are funded by the German Research Foundation (SFB 832, SFB 704, INST 217/576-1, INST 217/577-1), the Wilhelm-Sander-Foundation, the German Cancer Aid, the German Jose-Carreras-Foundation, the BMBF (NGFN2), and the Humboldt-Foundation (Sofja-Kovalevskaja Award). B.R.B. and K.L.H. are funded by a translational research grant from the Leukemia and Lymphoma Society of America (R6029-07). X.Z., S.L.B.-B., and J.A.B. are funded by the Juvenile Diabetes Research foundation Scholar #16-2008-643, and UCSF Autoimmunity Center of Excellence. S.C.B. supported by NHMRC project grants 339123, 565314

AUTHOR CONTRIBUTIONS

M.B. designed, performed and overlooked experiments, analyzed data, wrote the manuscript; Y.T. performed qPCR, CBA, WB, overexpression experiments and filter retention analysis, analyzed data; R.M. designed and performed reporter assays; S.C. performed experiments, analyzed data; T.S. performed ChIP experiments, analyzed data; K.L. and C.T.M. performed experiments with DEREG mice; S.B. and T.G. performed overexpression experiments; E.S. performed and analyzed immunofluorescence experiments; W.K. performed histone methylation studies, S.L.B.-B. and X.Z. performed experiments with $DICER^{fl/fl}$ mice; A.H. performed bioinformatic analysis; D.S. generated lentiviral contructs; S.D.P. performed microarray experiments; E.E. performed FACS sorting; J.B. and A.L. performed experiments with $RAG2^{-/-}$ mice; P.A.K. was involved in study design; K.L.H. and B.R.B. provided vital analytical tools; R.B. provided vital analytical tools; T.Q. overlooked and analyzed immunofluorescence experiments; C.W: performed IHC; A.W. performed, designed and overlooked DNA methylation experiments; G.M. and M.F. designed and overlooked filter retention experiments; W.K. designed and overlooked experiments, wrote the manuscript; B.S. designed and analyzed reporter assays; S.C.B. designed and overlooked ChIP experiments; T.S. designed and overlooked experiments with DEREG mice, provided vital analytical tools; J.A.B. designed and overlooked experiments with $DICER^{fl/fl}$ mice; J.L.R. designed and overlooked SATB1 overexpression experiments, wrote the manuscript; J.L.S. designed, overlooked and analyzed experiments, wrote the manuscript. All authors discussed the results and commented on the manuscript.

COMPETING FINANCIAL INTERESTS

Research support to J.L.S. and M.B. has in part been provided by Becton Dickinson.

R.B. is currently employed by Becton Dickinson, S.C. by Miltenyi Biotech.

Correspondence and requests for materials should be addressed to J.L.S. (j.schultze@uni-bonn.de).

Published online at http://www.nature.com/natureimmunology/.

Figure Legends

Figure 1. FOXP3-dependent repression of SATB1 expression in human regulatory T cells.

(**a**) Microarray analysis of SATB1 mRNA expression in T_{conv} and T_{reg} (rest=resting, act=activated, TGF=TGFβ treated, exp=expanded). (**b**) Relative SATB1 mRNA expression in freshly isolated T_{reg} and T_{conv} assessed by qRT-PCR (mean±s.d., n=5; * $p<0.05$). (**c**) Western blotting of SATB1 in freshly isolated T_{reg} and T_{conv} (representative donor (left), relative expression (right; n=6, mean±s.d.; * $p<0.05$). (**d**) Flow cytometric analysis of SATB1 expression in freshly isolated T_{reg} and T_{conv} (left: representative donor; right: mean±s.d., n=11; * $p<0.05$) (**e**) Flow cytometry of SATB1 after stimulation of T_{reg} and T_{conv} for 2 days normalized to resting T_{conv} (left: representative donor; right: mean±s.d., n=5; * $p<0.05$). (**f**) qRT-PCR for SATB1 in iT_{reg} on day 5 (mean±s.d.; n=6; * $p<0.05$; T_{unst}=unstimulated; T_{stim}=stimulated; iT_{reg}=induced T_{reg}). (**g**) Flow cytometry of SATB1 in iT_{reg} on day 5 (left: representative experiment; right: n=3, mean±s.d.; * $p<0.05$)). (**h**) Bead assay for IL-4 and IFN-γ secretion in the supernatants of T_{unst}, T_{stim}, and iT_{reg} (mean±s.d.; * $p<0.05$). (**i**) qRT-PCR for FOXP3 (left) and SATB1 (right) in T_{conv} lentivirally transduced with FOXP3 rested for 3 days (mean±s.d., n=5; * $p<0.05$). (**j**) qRT-PCR analysis of IL-5 (left) and IFN-γ (right) expression in T_{conv} lentivirally transduced with FOXP3 rested for 3 days (mean±s.d., n=5, * $p<0.05$).

Figure 2. Rescue of SATB1 expression after silencing of FOXP3 in T_{reg}.

Human T_{reg} were either transfected with control siRNA or FOXP3-specific siRNA and assessed 48 hours post knockdown. (**a**) Flow cytometric analysis of intracellular FOXP3 expression in T_{reg} post FOXP3 knockdown compared to control siRNA transfected T_{reg} (left: representative donor; right: mean±s.d., n=6; * $p<0.05$). (**b**) Suppressive function *in vitro* of control or FOXP3 siRNA treated T_{reg} cultured for 4 d together with CFSE-labeled allogeneic $CD4^+$ T cells at a 1:1 ratio; after stimulation of cultures, CFSE dilution was assessed by flow cytometry. (**c**) qRT-PCR for SATB1 (mean±s.d., n=6; * $p<0.05$) in human T_{reg} after silencong of FOXP3. T_{reg} were transfected and cultivated for 48 hours without stimulation or in the presence of CD3 and IL-2 or CD3 and CD28. (**d**) qRT-PCR for IL-5 and IFN-γ (n=4, mean±s.d.; * $p<0.05$) in siRNA-treated T_{reg} stimulated for 48 hours in the presence CD3 and IL-2. (**e**) Bead assay for IL-4 and IFN-γ (mean±s.d.; * $p<0.05$) in the supernatant of siRNA-treated T_{reg} stimulated for 48 hours in the presence of CD3 and IL-2. (**f**) qRT-PCR for IL-5 and IFN-γ in T_{reg} transfected with FOXP3-specific siRNA alone or FOXP3- and SATB1-specific siRNAs followed by stimulation with CD3 and CD28 for 48 hours (n=4, mean±s.d., one-way ANOVA with LSD; * $p<0.05$).

Figure 3. FOXP3-dependent repression of SATB1 expression in murine regulatory T cells.

(**a**) Flow cytometric analysis of SATB1 in freshly isolated T_{reg} and T_{conv} from spleen from male DEREG mice (left: representative mouse; right: mean±s.d., n=3; * $p<0.05$). MFI values are presented for T_{reg} and T_{conv} respectively. (**b**) Western blot analysis of SATB1 protein expression in murine T_{reg} and T_{conv}. (**c**) Z-projection of immunofluorescence for SATB1 (red) and GFP (green) protein expression in thymocytes from male DEREG mice counterstained with DAPI (blue). White arrow depicts a T_{reg}. (**d**) qRT-PCR of SATB1 in freshly sorted $CD4^+GFP^+$ (T_{reg}) and $CD4^+GFP^-$ (T_{conv}) T cells (♂ DEREG mice; ♂ FOXP3-deficient DEREG x *scurfy* mice). Data are representative of two experiments (mean ± s.d. of three biological replicates; * $p<0.05$). (**e**) qRT-PCR of IL-6 and IFN-γ mRNA production by T_{reg} derived from male DEREG or DEREG x *scurfy* mice. (mean±s.d.; * $p<0.05$; n.d. = not detectable). (**f**) Confocal immunofluorescence for SATB1 (red) and FOXP3 (green) in freshly sorted thymic T_{reg} from female DEREG mice heterozygous for the scurfy mutation counterstained with DAPI (blue). FOXP3 competent: $CD4^+GFP^+FOXP3^+$,($FOXP3^{wt}$ T_{reg}) or FOXP3 incompetent: $CD4^+GFP^+FOXP3^-$ ($FOXP3^{sf}$ T_{reg}). (**g**) Flow cytometry of SATB1 in freshly isolated thymic single positive $FOXP3^+$ (left, dark grey) and $FOXP3^-$ (right, black) GFP^+ T_{reg} from female DEREG mice heterozygous for the scurfy mutation; one representative experiment (left); mean±s.d. (right, n=2). Isotype control shown as solid line.

Figure 4. Direct suppression of SATB1 mRNA transcription by FOXP3.

(**a**) FOXP3 ChIP tiling array data from human expanded cord-blood T_{reg} assessed with a FOXP3 antibody and hybridized to either Affymetrix promoter or Affymetrix tiling arrays. Data were analyzed with MAT and overlayed to the SATB1 locus to identify binding regions (1-13, $p<10^{-5}$ and FDR<0.5%). (**b**) Schematic representation of FOXP3 binding regions (BR) at the human genomic SATB1 locus identified by *in silico* prediction within the indentified regions. (**c**) ChIP-qPCR for FOXP3 binding at the SATB1 locus in human expanded cord-blood T_{reg}. Input DNA and precipitated DNA were quantified by real-time PCR; the same chromatin was used for control ChIP experiments with immunoglobulin G–coupled Dynabeads. Enrichment over input DNA was normalized to control IgG (mean±s.d.; * $p<0.05$; n=3). (**d**) Luciferase reporter assay comparing wildtype to mutated FOXP3 binding regions (mean±s.d.; * $p<0.05$; n=3). FOXP3 binding was assessed by transfecting a reporter construct containing the potential FOXP3 binding region in cells expressing FOXP3 comparison to an empty control. Constructs with mutated motifs were used to demonstrate specificity. (**e**) Determination of the K_D-values of FOXP3 binding to FOXP3 binding motifs in BR9 and BR10 at the SATB1 locus by filter retention analysis.

Figure 5. SATB1 expression in T_{reg} reprograms T_{reg} into effector T cells.

(**a**) Analysis of suppressive function of human T_{reg} lentivirally transduced with SATB1 (blue) or control vector (DsRED, red) cultured for 4 d together with CFSE-labeled allogeneic PBMC at a 1:1 ratio *in vitro*; after stimulation of cultures, CFSE dilution of human $CD8^+$ T cells was assessed by flow cytometry. Left: representative experiment; right: mean±s.d., n=3; * $p<0.05$. (**b**) Bead assay for IL-4 and IFN-γ secretion of human T_{reg} lentivirally transduced with SATB1 or control vector assessed 4 and 16 hours after stimulation with CD3/CD28-coated beads (mean±s.d.; * $p<0.05$). qRT-PCR analysis of (**c**) IL-5, (**d**) IFN-γ, and (**e**) IL-17A expression in T_{conv} activated for 16 hrs with CD3/CD28 coated beads (grey) as well as human T_{reg} lentivirally transduced with SATB1 (blue) or control vector (DsRED, red) (mean±s.d., n=3, * $p<0.05$).

Figure 6. Transcriptional $T_{effector}$ programs are induced in SATB1 expressing T_{reg}

(**a**) Up- and down-regulated genes in T_{reg} lentivirally transduced with SATB1 or control vector after 16 hours stimulation with CD3/CD28-coated beads. Data were z-score normalized. (**b**) Cross annotation analysis using 4 classes: Genes associated with T_{conv} but not T_{reg} cells (yellow), with T cell activation (green), common T-cell genes (orange), and SATB1-induced genes (black). (**c**) Visualization of gene expression levels of genes previously associated with TH1, TH2, or TH17 differentiation; data were z-score normalized. p-values for TH associated genes determined by χ^2 test in comparison to the complete data set (= TH specific gene enrichment) were p = 3.236e-06 (TH1), p = 9.017e-15 (TH2), resp. p = 1.157e-06 (TH17). (**d**) Changes in genes associated with the human T_{reg} signature in T_{reg} lentivirally transduced with SATB1 in comparison to control vector transduced T_{reg}. The mean log2 fold-changes of the comparison T_{reg} to T_{conv} (red dots) and SATB1 to control-transduced Treg (blue dots) were plotted and both comparisons were ranked by fold change in the T_{reg} vs. T_{conv} comparison.

Figure 7. Epigenetic regulation o**f** SATB1 in T_{reg}.

(**a**) DNA methylation of the predicted CpG-islands in the genomic region of SATB1 in T_{reg} and T_{conv}. (**b**) Histone ChIP sequencing data from human expanded T_{reg} and T_{conv} for the permissive histone modifications H3K4me3 and H4Ac and the repressive histone modification H3K27me3. Data were analyzed with MACS and overlayed to the SATB1 locus histone marks ($-10\log_{10}$ p>100 and FDR<0.5%). (**c**) Confirmation of histone marks for H3K4me3, H4Ac, and H3K27me3 in human expanded T_{reg} and T_{conv} by ChIP-qPCR. Quantitative PCR was performed using primer sets corresponding to the marked regions and histone antibody or control IgG precipitated chromatin isolated from T_{reg} and T_{conv}. Relative enrichment of FOXP3 Chip over input normalized to IgG were calculated. (mean±s.d.; * p<0.05; n=3) Primer sequences are listed in table S10.

Figure 8. SATB1 is repressed by miRNA in T_{reg}.

(**a**) Representation of the human genomic SATB1 3′ UTR and the conserved miRNA binding sites. (**b**) qPCR for miR-155, miR-21, miR-7, miR-34a, and miR-18a in human T_{reg} (mean±s.d., n=5; * $p<0.05$). (**c**) Correlation of miRNA expression with SATB1 mRNA expression is plotted against miRNA fold change (T_{reg} vs. T_{conv}) for all 735 miRNA assessed by microarrays. Highlighted are miR-155, miR-21, miR-7, miR-34a, and miR-18a. (**d**) FOXP3 ChIP tiling array data for miR-155, miR-21, and miR-7. (**e**) Confirmation of FOXP3 binding to the miR-155 and miR-21 loci by ChIP-qPCR. Quantitative PCR was performed using primer sets corresponding to the marked regions and FOXP3 antibody or control IgG precipitated chromatin isolated from T_{reg}. Relative enrichment of FOXP3 Chip over input normalized to IgG were calculated. The AFM locus was used as a negative control. Primer sequences are listed in table S5. (**f**) Luciferase reporter assays comparing the WT SATB1 3′ UTR to a version containing mutated miRNA-binding sites (mean±s.d.; * $p<0.05$, n=3). Functional miRNA binding was assessed by transfecting a reporter construct containing the WT SATB1 3′ UTR in cells transfected with miRNA mimics. Constructs with mutated motifs were used to demonstrate specificity. (**h**) Western blot of SATB1 in sorted T_{reg} from mice with a T_{reg}-specific complete DICER loss ($DICER^{fl/fl}$) in comparison to $DICER^{wt/fl}$ T_{reg}.

Figure 9. Ectopic expression of SATB1 in T_{reg} results in reduced suppressive function *in vivo*.

(**a**) Analysis of suppressive function of murine expanded T_{reg} lentivirally transduced with SATB1 (blue) or control vector (red) cultured for 4 d together with eFluor 670-labeled $CD4^+$ T cells at a the indicated ratio *in vitro*; after stimulation of cultures, eFluor 670 dilution of $CD4^+$ T cells was assessed by flow cytometry. Left: representative experiment; right: mean±s.e.m. Data are representative of two independent experiments (mean and s.e.m. of triplicate cultures). (**b**) qRT-PCR analysis of IL-5 and IFN-γ in murine T_{reg} lentivirally transduced with SATB1 (blue) or control vector (red) (mean±s.d., n=3, * $p<0.05$). (**c**) Hematoxylin and eosin staining of colon sections. Colons from mice that received naïve $CD4^+CD45RB^{high}$ T cells only or together with SATB1-overexpressing T_{reg} displayed infiltrates of inflammatory cells. In colons from mice that received naïve $CD4^+CD45RB^{high}$ T cells and control T_{reg} no inflammatory changes were evident. (**d**) Histology scores of sections of the colon at 8 weeks after cell transfer. (**e**) Body weight of $RAG2^{-/-}$ recipients of naïve $CD4^+CD45RB^{high}$ T cells transferred alone or together with control- or SATB1-transduced T_{reg}, presented relative to initial body weight. Data are pooled from two independent experiments (average and s.d. of four to five recipient mice). (**f**) Recovery of T_{conv} cells from spleens mesenteric and peripheral lymph nodes. (**g**) Recovery of T_{reg} cells from spleens mesenteric and peripheral lymph nodes.

Figures

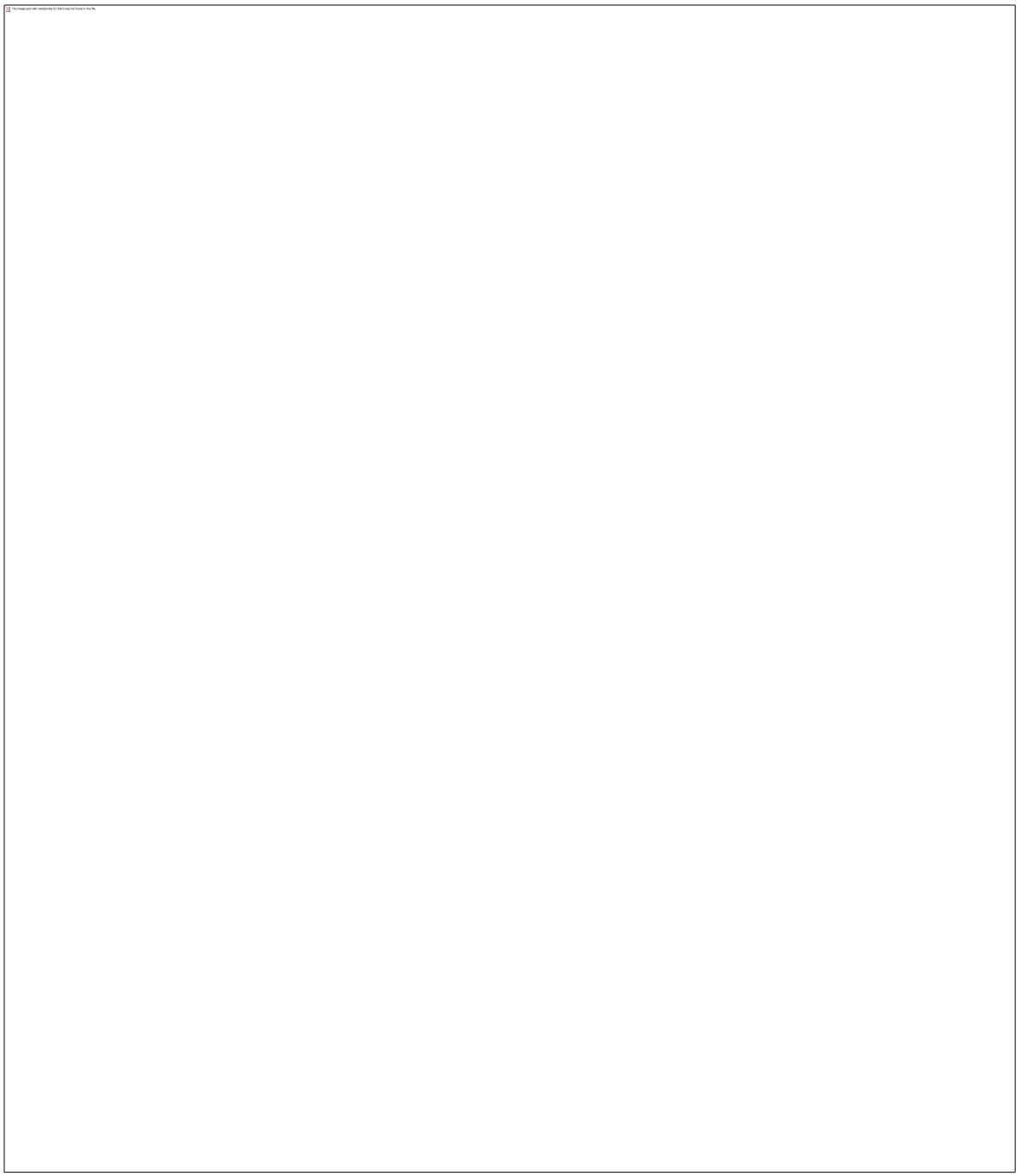

Fig. 2

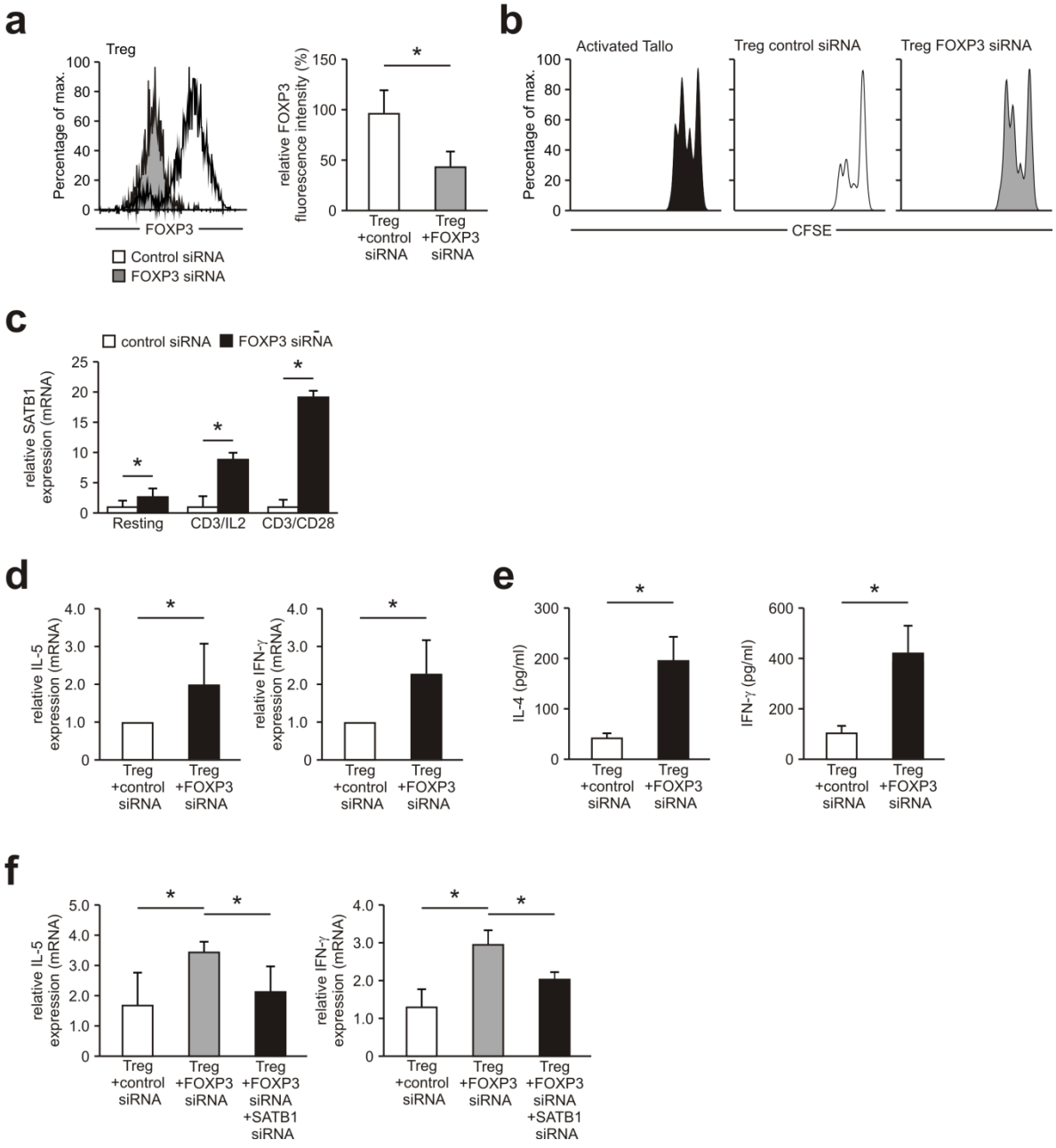
a
Treg
Percentage of max.
FOXP3
Control siRNA
FOXP3 siRNA
relative FOXP3 fluorescence intensity (%)
Treg +control siRNA
Treg +FOXP3 siRNA
b
Activated Tallo
Treg control siRNA
Treg FOXP3 siRNA
Percentage of max.
CFSE
c
control siRNA
FOXP3 siRNA
relative SATB1 expression (mRNA)
Resting
CD3/IL2
CD3/CD28
d
relative IL-5 expression (mRNA)
relative IFN-γ expression (mRNA)
Treg +control siRNA
Treg +FOXP3 siRNA
e
IL-4 (pg/ml)
IFN-γ (pg/ml)
Treg +control siRNA
Treg +FOXP3 siRNA
f
relative IL-5 expression (mRNA)
relative IFN-γ expression (mRNA)
Treg +control siRNA
Treg +FOXP3 siRNA
Treg +FOXP3 siRNA +SATB1 siRNA

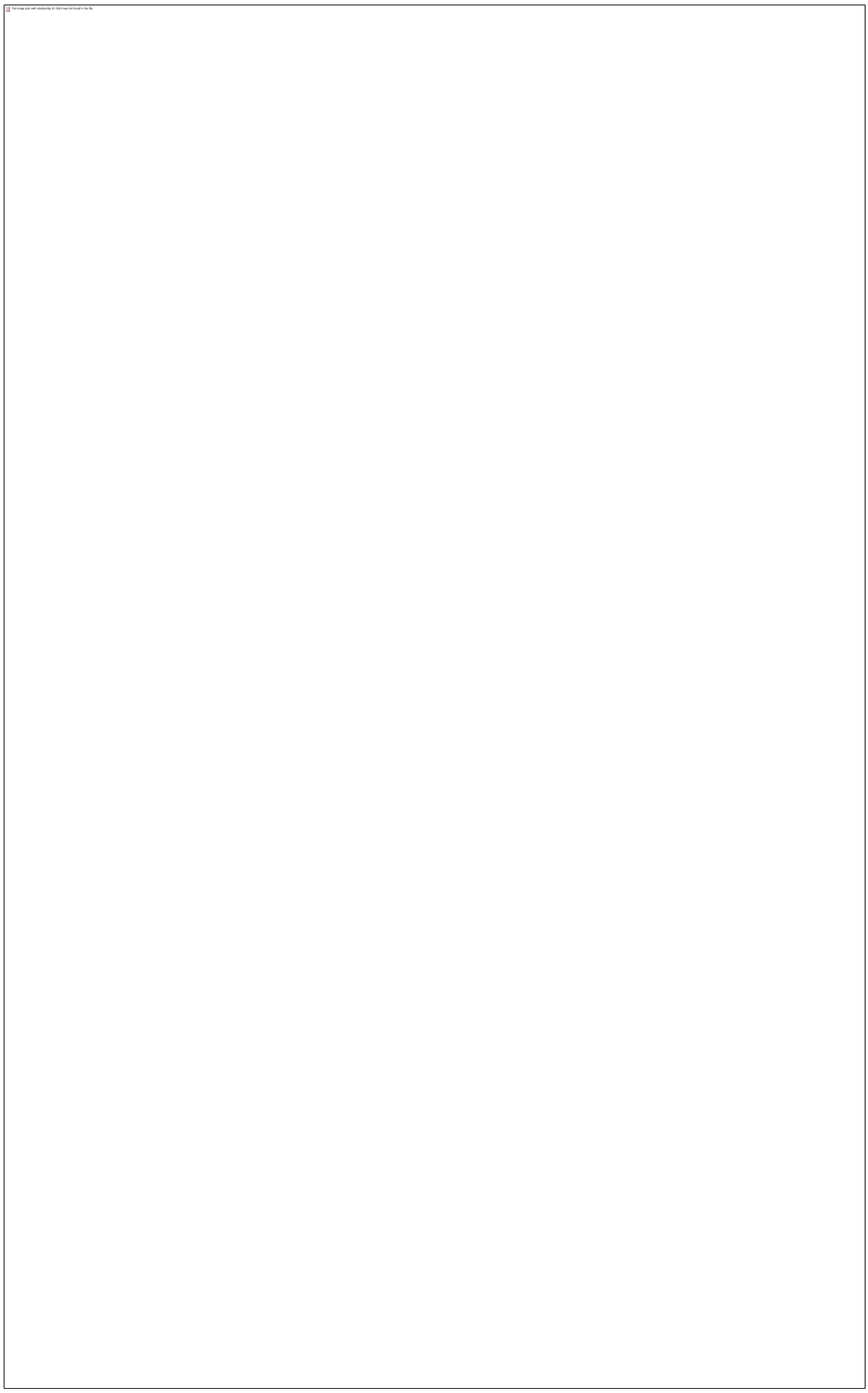
The image path with relationship ID rId3 was not found in the file.

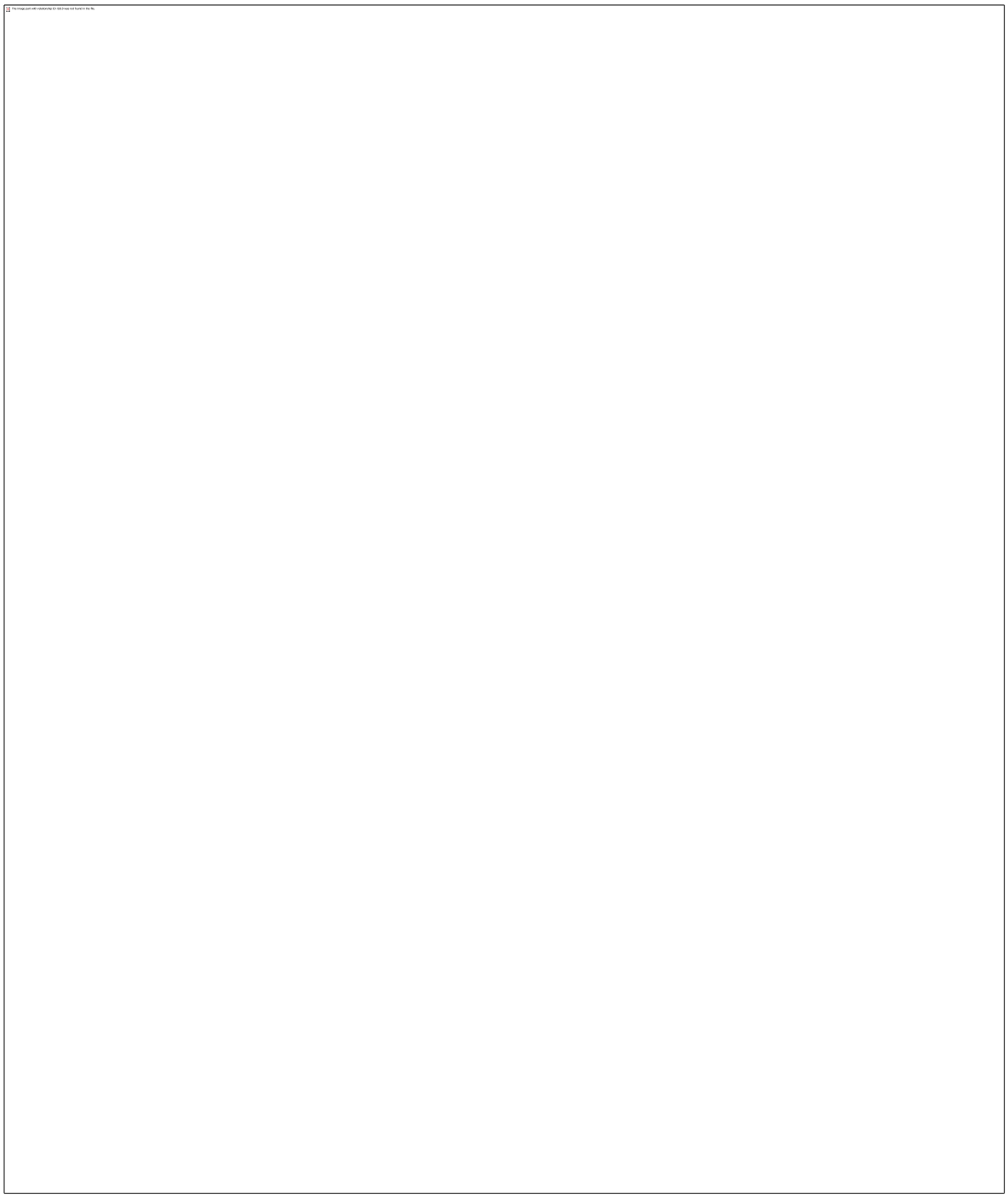
The image path with relationship ID rId3 was not found in the file.

Fig. 5

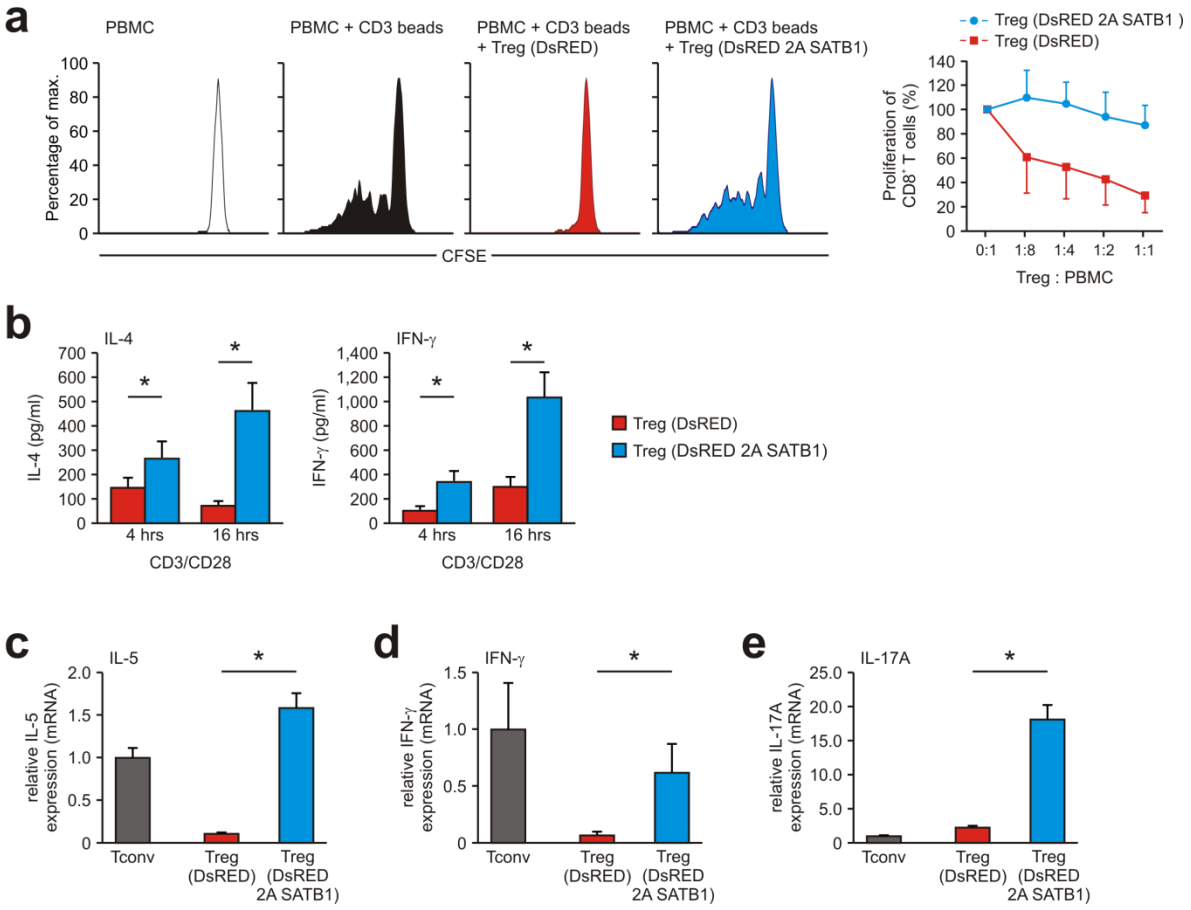
a
PBMC
PBMC + CD3 beads
PBMC + CD3 beads + Treg (DsRED)
PBMC + CD3 beads + Treg (DsRED 2A SATB1)
Percentage of max.
CFSE
Treg (DsRED 2A SATB1)
Treg (DsRED)
Proliferation of CD8+ T cells (%)
Treg : PBMC
b
IL-4
IL-4 (pg/ml)
IFN-γ
IFN-γ (pg/ml)
4 hrs
16 hrs
CD3/CD28
Treg (DsRED)
Treg (DsRED 2A SATB1)
c
IL-5
relative IL-5 expression (mRNA)
d
IFN-γ
relative IFN-γ expression (mRNA)
e
IL-17A
relative IL-17A expression (mRNA)
Tconv
Treg (DsRED)
Treg (DsRED 2A SATB1)

Fig. 6

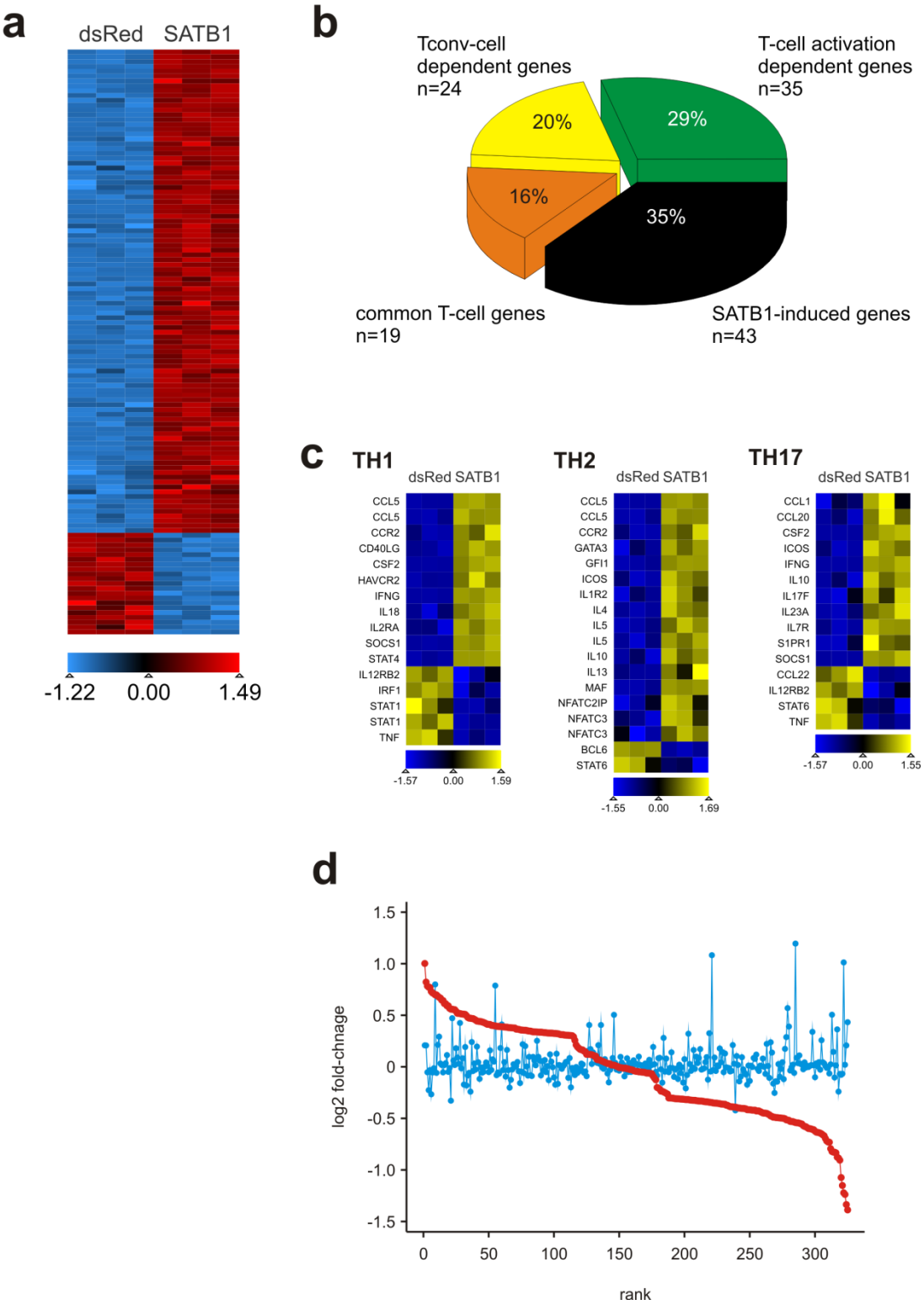
a
dsRed SATB1
-1.22 0.00 1.49
b
Tconv-cell dependent genes n=24
T-cell activation dependent genes n=35
20%
29%
16%
35%
common T-cell genes n=19
SATB1-induced genes n=43
c
TH1
dsRed SATB1
CCL5
CCL5
CCR2
CD40LG
CSF2
HAVCR2
IFNG
IL18
IL2RA
SOCS1
STAT4
IL12RB2
IRF1
STAT1
STAT1
TNF
-1.57 0.00 1.59
TH2
dsRed SATB1
CCL5
CCL5
CCR2
GATA3
GFI1
ICOS
IL1R2
IL4
IL5
IL5
IL10
IL13
MAF
NFATC2IP
NFATC3
NFATC3
BCL6
STAT6
-1.55 0.00 1.69
TH17
dsRed SATB1
CCL1
CCL20
CSF2
ICOS
IFNG
IL10
IL17F
IL23A
IL7R
S1PR1
SOCS1
CCL22
IL12RB2
STAT6
TNF
-1.57 0.00 1.55
d
log2 fold-chnage
1.5
1.0
0.5
0
-0.5
-1.0
-1.5
0
50
100
150
200
250
300
rank

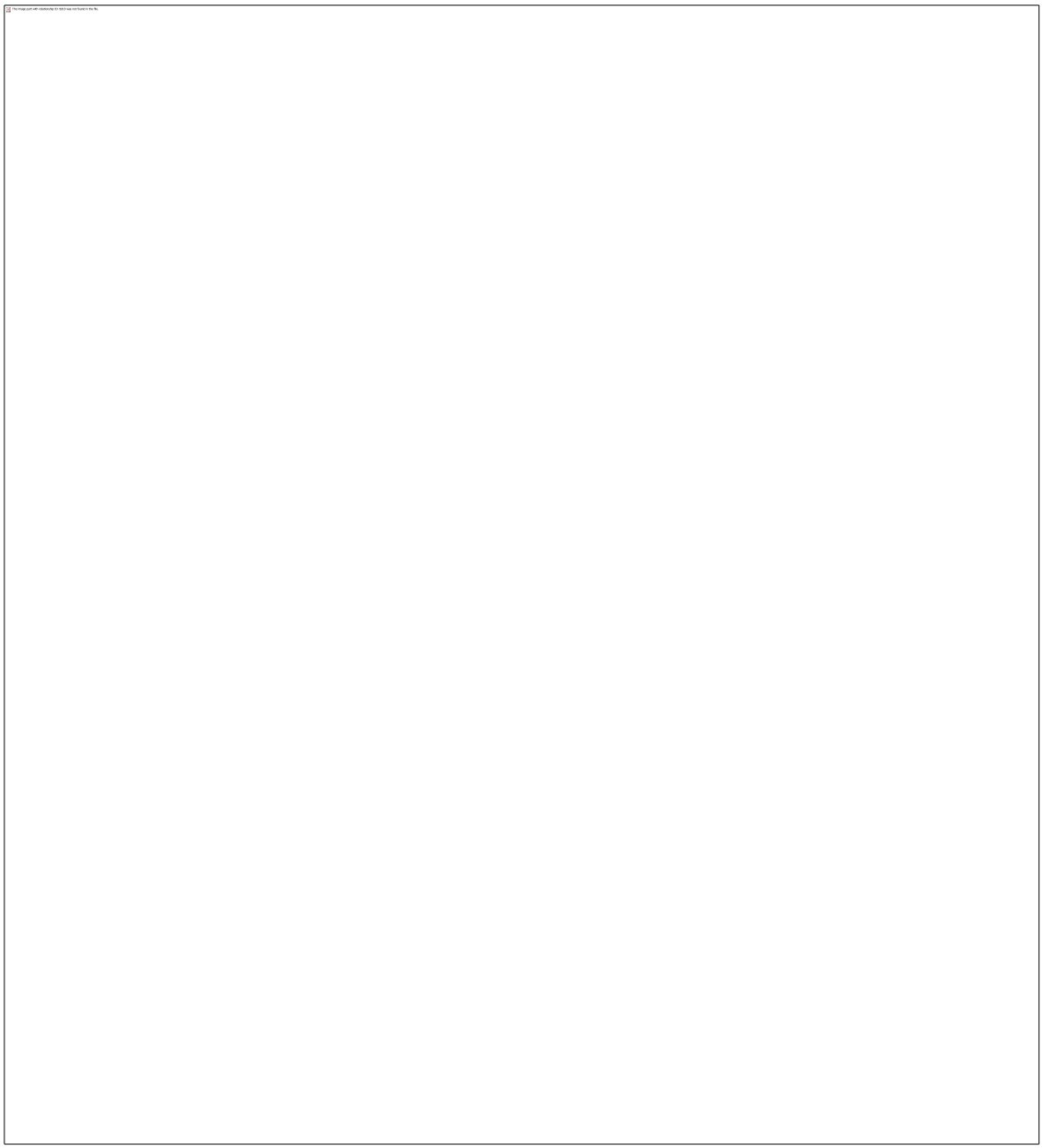
The image path with relationship ID rId3 was not found in the file.

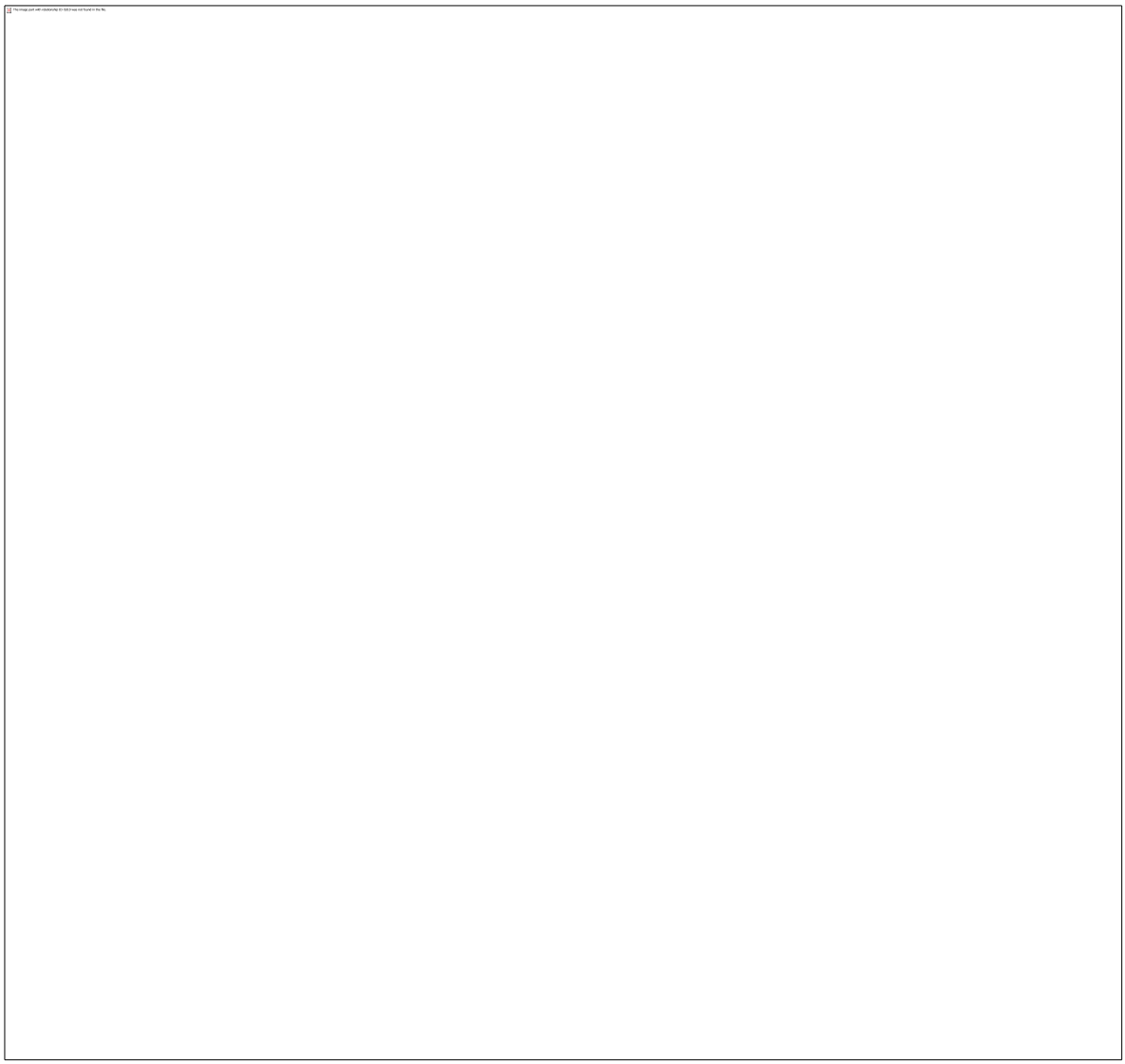
The image path with relationship ID rId3 was not found in the file.

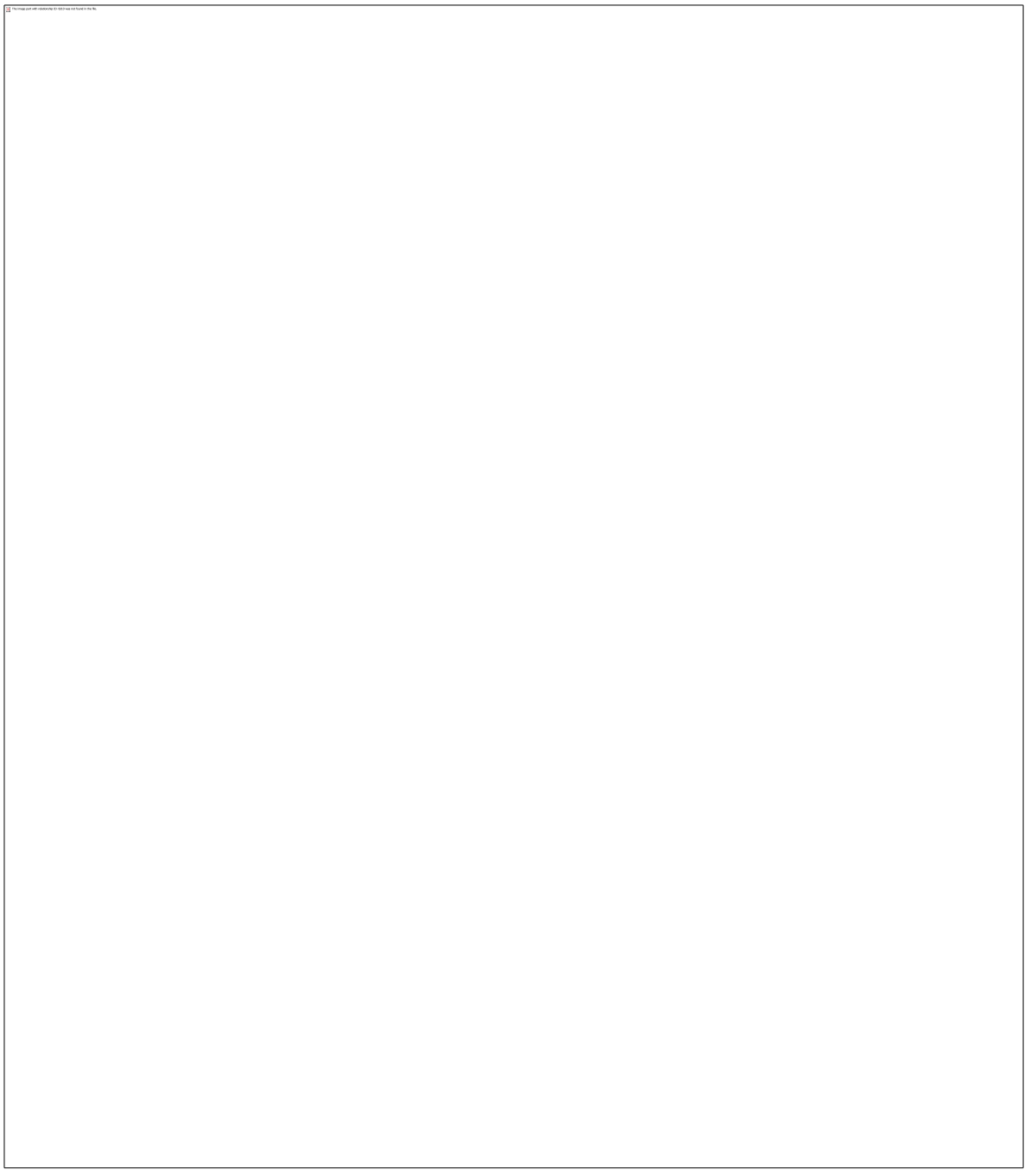
The image part with relationship ID rId3 was not found in the file.

SUPPLEMENTARY MATERIAL

SUPPLEMENTARY FIGURES

Supplementary Fig. 1

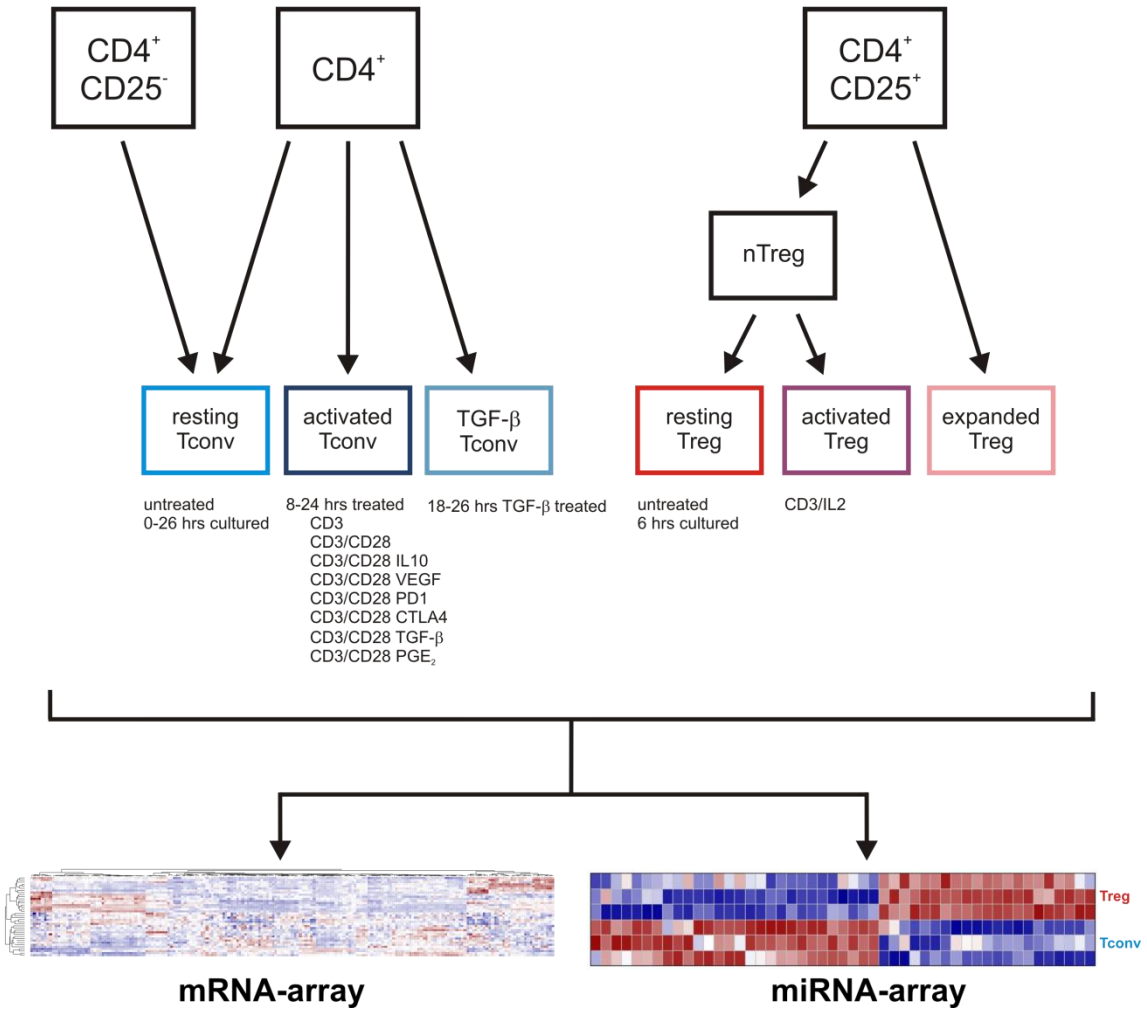

Supplementary Fig. 1. Layout of microarray experiments

Human $CD4^+$ T cells resp. $CD4^+CD25^-$ T_{conv}, were assessed either directly after isolation or after up to 26 hours of cell culture without further stimulation (resting T_{conv}), after culture in the presence of TGF-β for 18 to 26 hours (TGF-β T_{conv}), or

after activation for 8 to 24 hours by various stimuli (T_{conv} activated) including also $CD4^+$ T cells stimulated in the presence of inhibitory signals including IL-10, prostaglandin-E2 (PGE_2), PD1, or CTLA-4 (see also Supplementary Table 1). Human T_{reg} were analyzed either directly after isolation or after culture for up to 6 hours without further stimulation (resting T_{reg}), after culture in the presence of CD3/IL-2 for 24 hours (activated T_{reg}), or after expansion (expanded T_{reg}).

Supplementary Fig. 2

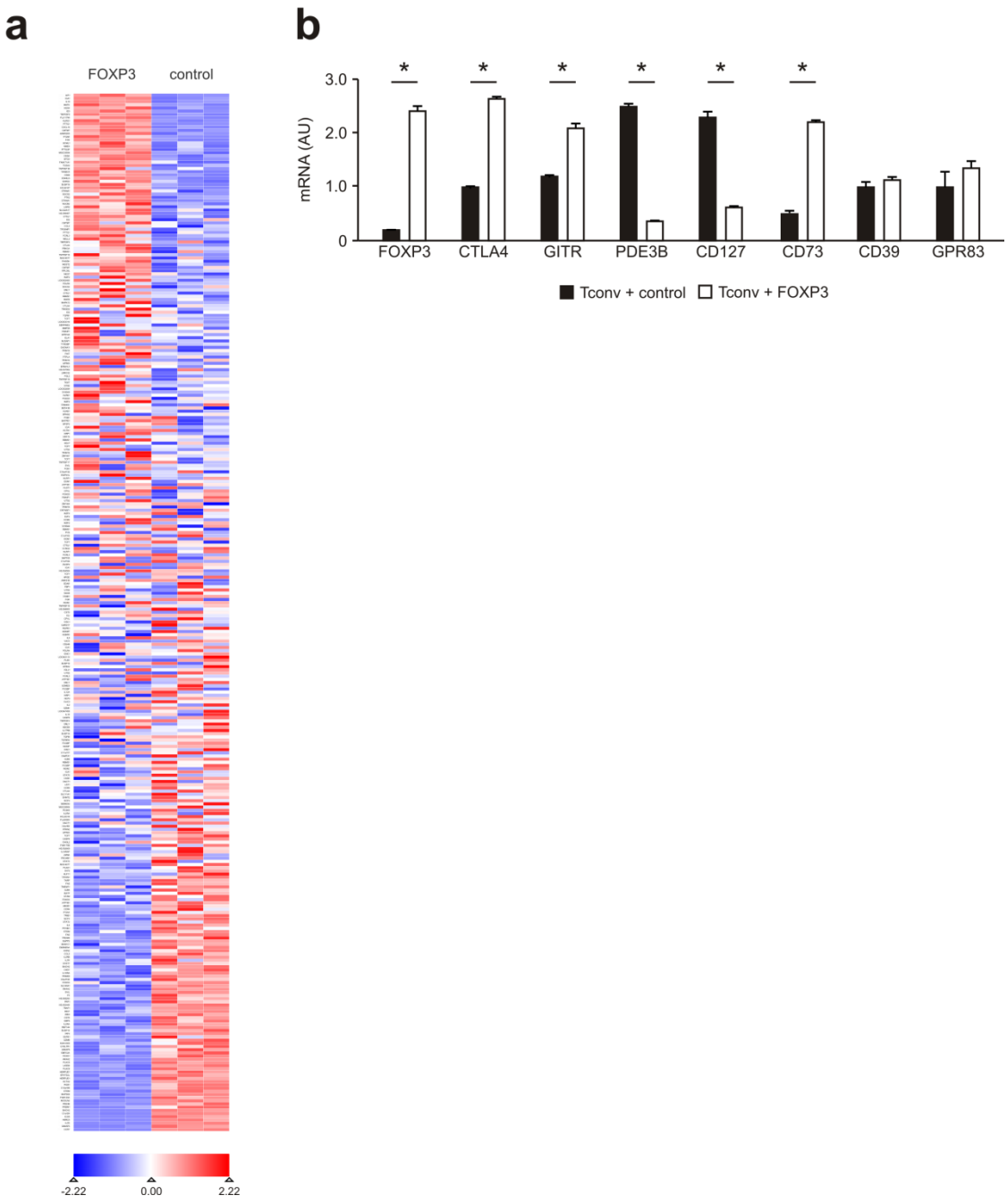

Supplementary Fig. 2. Expression of T_{reg}-cell genes in FOXP3-transduced T_{conv}. To assess whether FOXP3 overexpression induces typical T_{reg}-cell associated genes, we transduced T_{conv} with a lentivirus containing the full length human FOXP3 cDNA. T_{reg}-cells gene signatures were assessed by (**a**) whole genome

transcriptome analysis and subsequent visualization of expression of the T_{reg}-cell gene signature and (**b**) qRT-PCR of a set of known T_{reg}-cell marker genes (mean±s.d., n=3; * $p<0.05$).

Supplementary Fig. 3

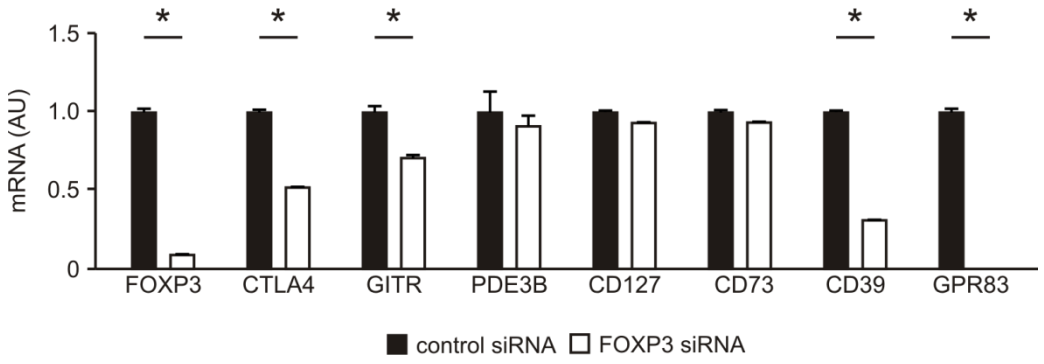

Supplementary Fig. 3. T_{reg}-cell associated gene expression in FOXP3-silenced human T_{reg}.

To assess whether silencing of FOXP3 reverses the phenotype of T_{reg}, we isolated T_{reg} and performed siRNA-mediated knockdown of FOXP3 and analyzed mRNA expression after stimulation for 48 hours with CD3 and CD28 (mean±s.d., n=3; * $p<0.05$).

Supplementary Fig. 4

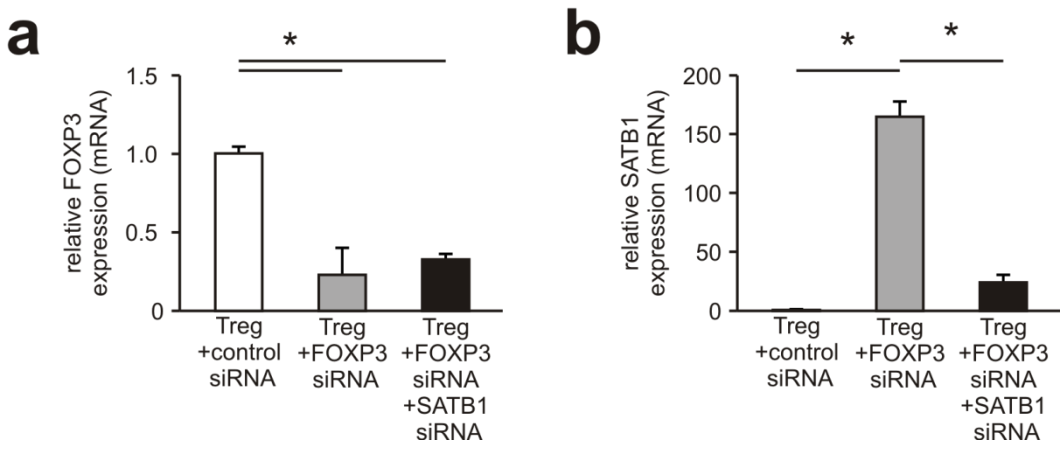

Supplementary Fig. 4. FOXP3 and SATB1 mRNA expression in FOXP3/SATB1-silenced human T_{reg}.

To assess whether SATB1 is responsible for the increased production of T-helper cytokines, we isolated T_{reg} and performed siRNA-mediated knockdown of FOXP3 or FOXP3 and SATB1 and analyzed SATB1 mRNA expression after stimulation for 48 hours with CD3 and CD28. qRT-PCR for (**a**) FOXP3, and (**b**) SATB1 in nT_{reg} transfected with FOXP3-specific siRNA alone or FOXP3- and SATB1-specific siRNAs followed by stimulation with CD3 and CD28 (mean±s.d., one-way ANOVA with LSD; * $p<0.05$).

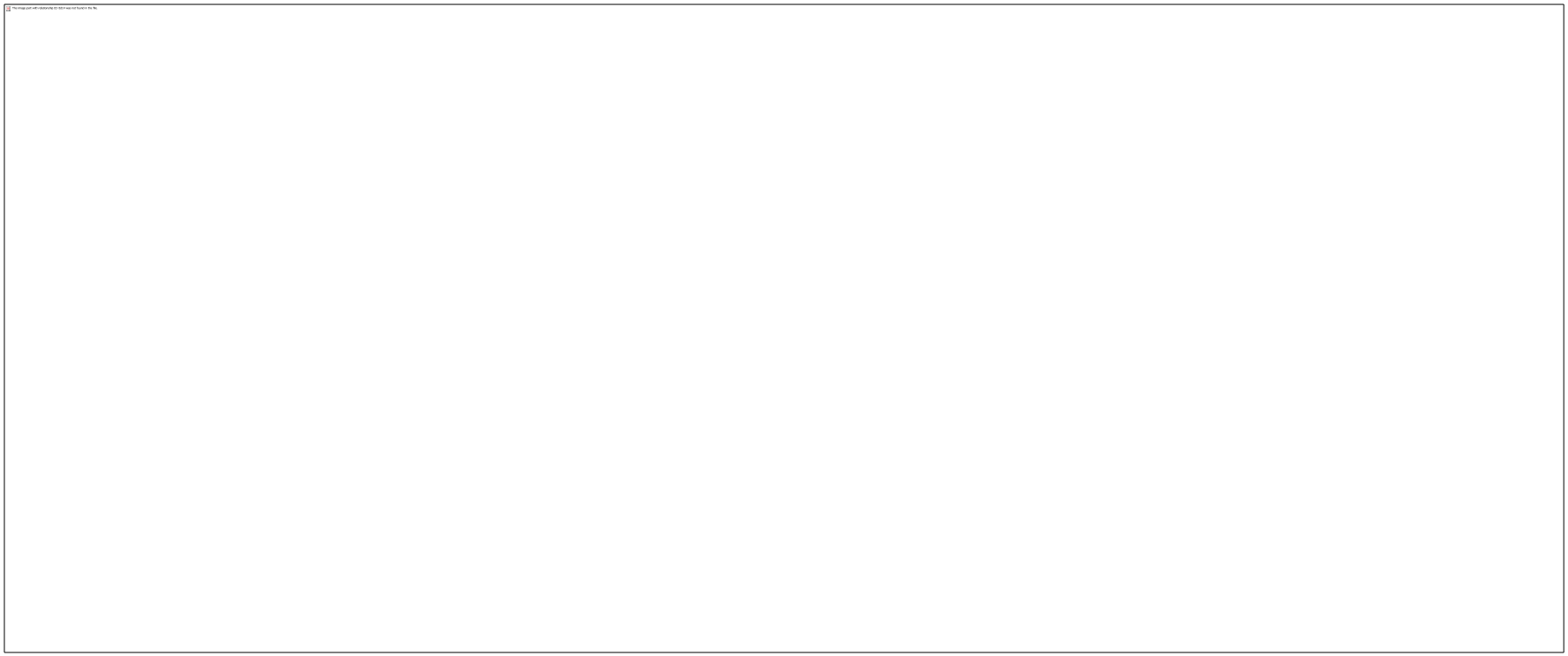

Supplementary Fig. 5. Experimental protocol for combined silencing of SATB1 and FOXP3 in expanded human T_{reg} with artificial miRNA.

FACS-sorted human $CD4^{+}CD25^{high}CD127^{low}CD45RA^{+}$ T_{reg} were expanded for 14 days with CD3 and CD28-coated beads in the presence of IL-2. After this initial expansion, T_{reg} were lentivirally transduced with miRNA against FOXP3, FOXP3 and SATB1 or control plasmids containing EmGFP, expanded for 3 additional days in the presence of CD3 and CD28-coated

beads and IL-2. Cells sorted on EmGFP-positivity using a FACS Aria III sorter (BD Biosciences) showing highly similar EmGFP expression were used for further analysis. Relative (**a**) FOXP3, (**b**) SATB1, (**c**) IL-5, and IFN-γ mRNA expression in transduced T_{reg} was assessed by qRT-PCR (mean±s.d., n=3; * $p<0.05$). (**d**) Cytokine secretion was assessed using cytometric bead arrays.

Supplementary Fig. 6

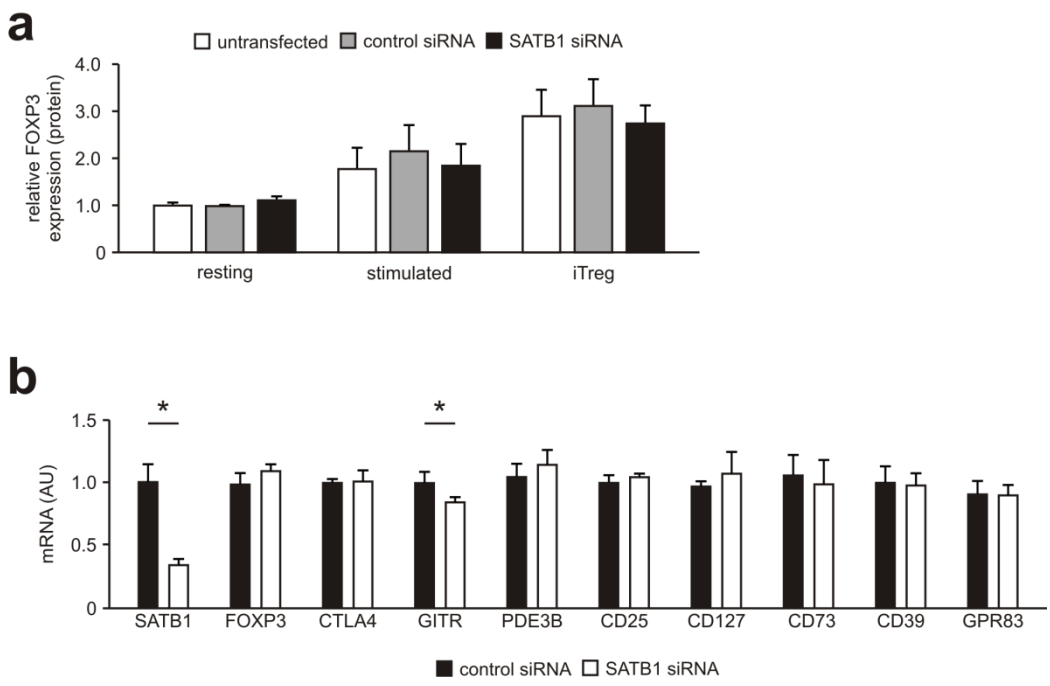

Supplementary Fig. 6. Assessment of induction of T_{reg}-cell associated genes in human $CD4^+$ T_{conv} after silencing of SATB1.

(**a**) To assess whether silencing of SATB1 induces FOXP3, we isolated naïve $T_{conv,}$ performed siRNA-mediated knockdown of SATB1, rested them (resting), stimulated them with CD3/CD28 coated beads (stimulated) or cultivated them in the presence of CD3/CD28 coated beads, TGF-β and IL-2 to induce iT_{reg} (iTreg). We analyzed FOXP3 expression by flow cytometry (mean±s.d., n=4; * $p<0.05$). (**b**) To assess whether silencing of SATB1 induces other genes associated with the T_{reg}-cell phenotype, we isolated $T_{conv,}$ performed siRNA-mediated knockdown of SATB1, stimulated them with CD3/CD28 coated beads and analyzed mRNA expression for a set of known T_{reg}-cell marker genes (mean±s.d., n=3; * $p<0.05$).

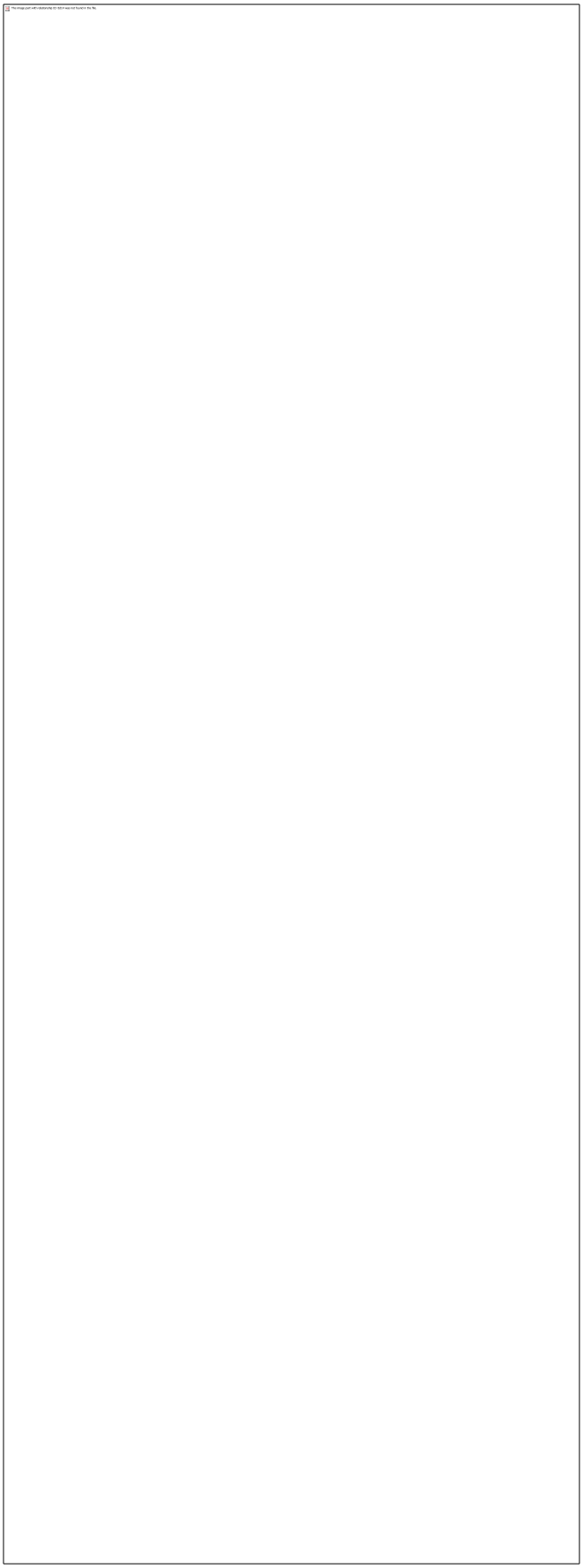
The image path with relationship ID: rId14 was not found in the file.

Supplementary Fig. 7. Array and ChIP-qPCR results for FOXP3 binding to SATB1 and known FOXP3 target genes.

(**a**) FOXP3 binds to the promoter region of the human SATB1 locus. FOXP3 ChIP-on-chip experiments and data analysis using MAT were previously described[1]. Each bar represents the signal intensity of an individual oligonucleotide probe on Affymetrix Human Promoter 1.0 (upper panel) or Human Tiling 2.0R Array (lower panel). (**b**) FOXP3 binds to the human CTLA4 locus. (**c**) FOXP3 binds to the human IL7R locus. (**e**) No FOXP3 binding to the human AFM locus. (**e**) FOXP3 binds to the human PDE3B locus. (**f**) Confirmation of FOXP3 binding by ChIP-qPCR. Quantitative PCR was performed using primer sets corresponding to the marked regions and FOXP3 antibody or control IgG precipitated chromatin isolated from T_{reg} cells. Relative enrichment of FOXP3 Chip over input normalized to IgG were calculated. The AFM locus or intron 10 of PDE3B was used as a negative control. Primer sequences are listed in Supplementary Table 5.

Supplementary Fig. 8. Experimental protocol for overexpression of SATB1 in primary human T_{reg}.

MACS-isolated human $CD4^{+}CD25^{high}$ T_{reg} or $CD4^{+}CD25^{-}$ T_{conv} were stimulated for 24 hours with CD3 and CD28-coated beads in the presence of IL-2. After this initial stimulation, T_{reg} were lentivirally transduced with pELNS DsRED 2A SATB1 or control plasmids containing DsRED expressed at a ratio of 1:1 to the transgene[2], expanded for 6 days in the presence of CD3 and

CD28-coated beads and IL-2. Cells sorted for DsRED-positivity using a MoFlo sorter (DakoCytomation) showing highly similar DsRED expression were used for further analysis. Relative (**a**) FOXP3 and (**b**) SATB1 mRNA expression in DsRED- rSATB1-transduced T_{reg} was assessed by qRT-PCR and compared with freshly isolated T_{conv} (mean±s.d., n=3; * $p<0.05$). (**c**) Relative SATB1 protein expression in DsRED- SATB1-transduced T_{reg} was assessed by flow cytometry and compared with freshly isolated T_{conv} (mean±s.d., n=3; * $p<0.05$).

Supplementary Fig. 9

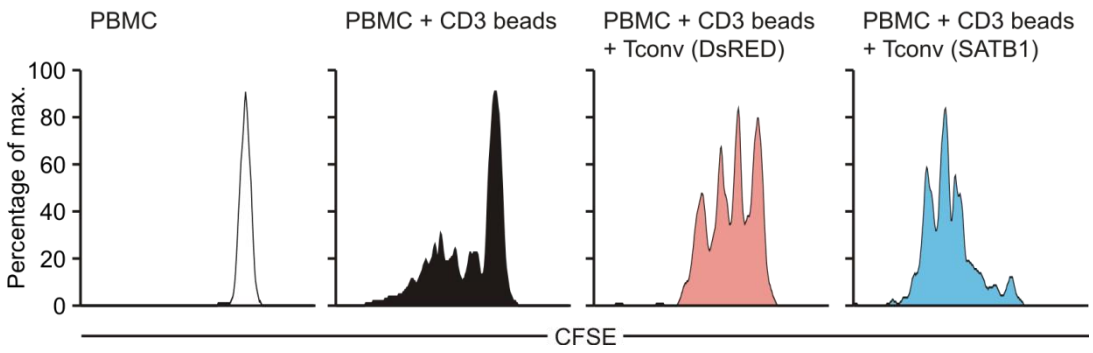

Supplementary Fig. 9. Human T_{conv} transduced with SATB1 show no suppressive function.

PBCM were cultured in the presence of CD3 beads together with human T_{conv} lentivirally transduced with SATB1 (light blue) or control vector (DsRED, light red) at a 1:1 ratio. Analysis of proliferation of human $CD8^+$ T cells as determined by flow cytometry using CFSE staining.

Supplementary Fig. 10

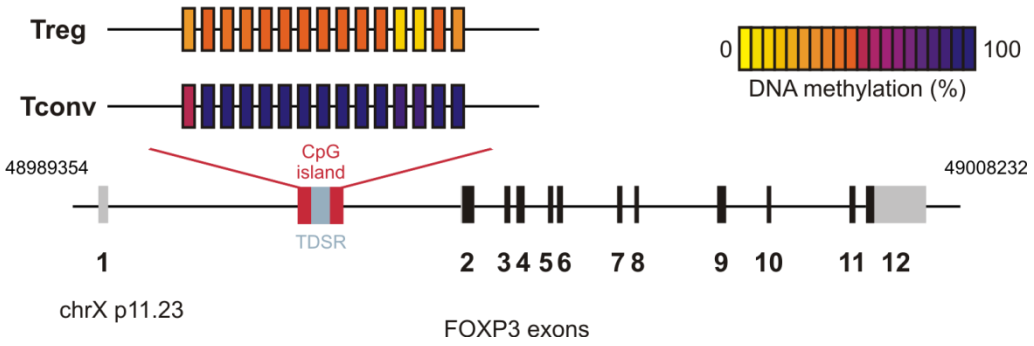

Supplementary Fig. 10. DNA methylation of the CpG island of the FOXP3 locus in freshly isolated T_{reg} and T_{conv}.

As a positive control, DNA methylation of the described CpG-islands in the human FOXP3 promoter was assessed in T_{reg} and T_{conv}[3].

Supplementary Fig. 11

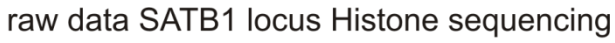

Supplementary Fig. 11. Histone methylation at the human SATB1 gene locus. Presence of H3K4me, H3K27me3, and H4Ac at the SATB1 locus in human expanded T_{conv} and T_{reg}. Each bar represents the cumulative frequency of matching sequences aligned to the human SATB1 locus with a sliding window of 10bp.

Supplementary Figure 12

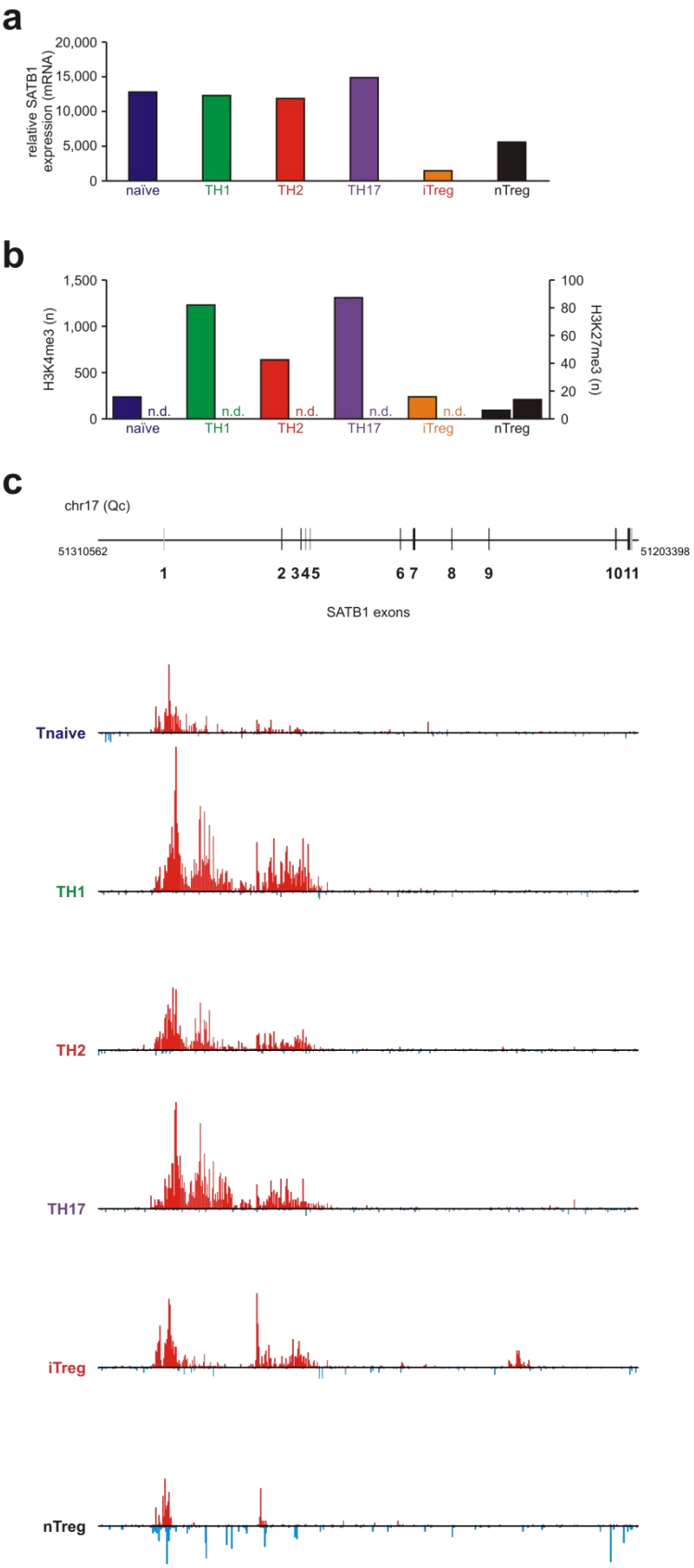

Supplementary Fig. 12. Histone methylation at the murine SATB1 gene locus.

Recently published data on genome-wide histone methylation were reanalyzed for SATB1 expression and histone methylation maps in murine naive T cells, $T_{effector}$ (TH1, TH2, resp. TH17), iT_{reg} and nT_{reg}[4]. (**a**) expression of SATB1 as assessed by microarray analysis. (**b**) and (**c**) ChIP-sequencing data were re-analyzed over the SATB1 locus. Trimethylation of H3K4 (b, left) is associated with gene activation, whereas di- and trimethylation of H3K27 (b, right) are associated with gene repression. Low to absent trimethylation of H3K27 was detected in the $T_{effector}$ subsets analyzed, while T_{reg} showed this repressive histone mark. In contrast, $T_{effector}$ showed high levels of H3K4 trimethylation while in T_{reg} lower trimethylation of H3K4 could be observed. **b,** cumulative data for H3K4 (left) and H3K27 (right) in T_{naive}, TH1, TH2, TH17. iT_{reg}, and nT_{reg} (n.d. = not detectable). **c,** analysis of trimethylation islands (red: H3K4, blue: H3K27) mapped to the genomic SATB1 locus.

Supplementary Fig. 13

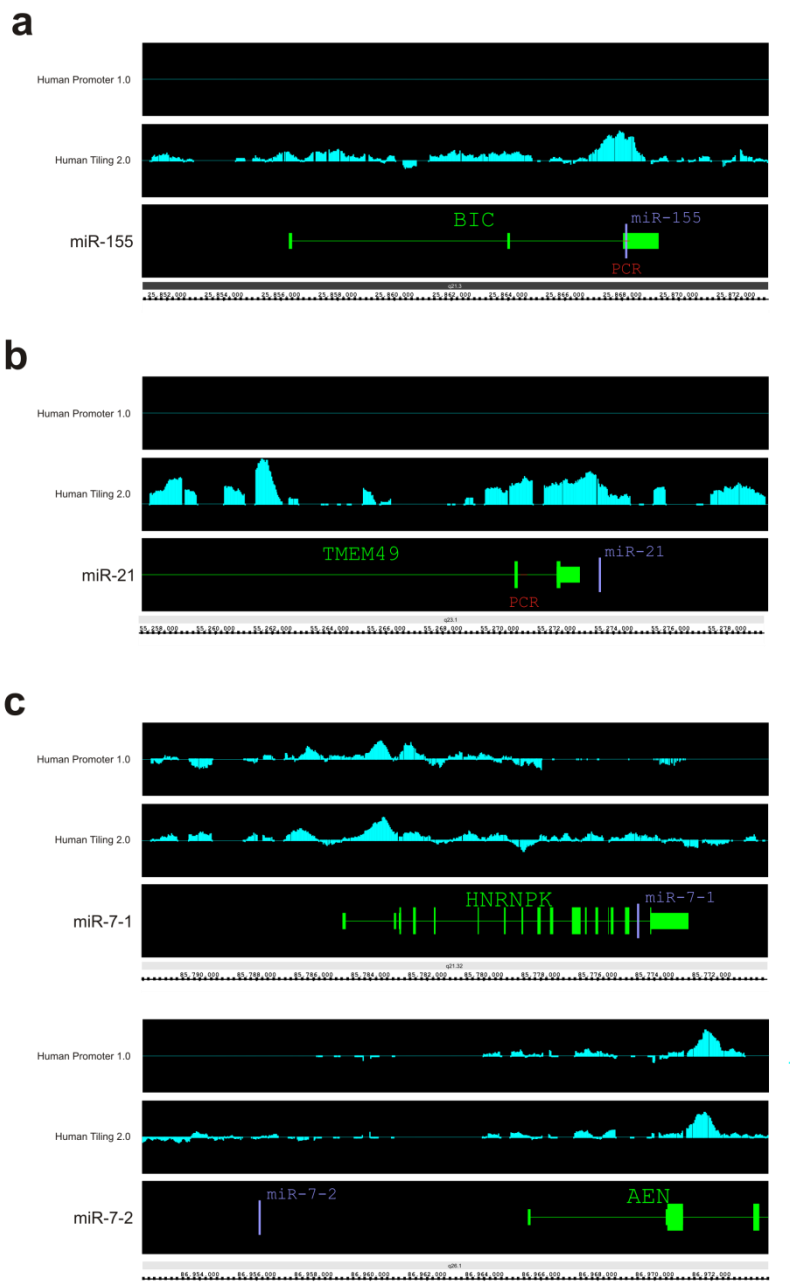

Supplementary Fig. 13. Results for FOXP3 binding to miRNA genes.

FOXP3 binds in close proximity of (**a**) the human miR-155, (**b**) the human miR-21, and (**c**) the two human miR-7 loci. FOXP3 ChIP-on-chip experiments and data analysis using MAT were previously described[1]. Each bar represents the signal

intensity of an individual oligonucleotide probe on Affymetrix Human Promoter 1.0 (upper panel) or Human Tiling 2.0R Array (lower panel).

Supplementary Fig. 14

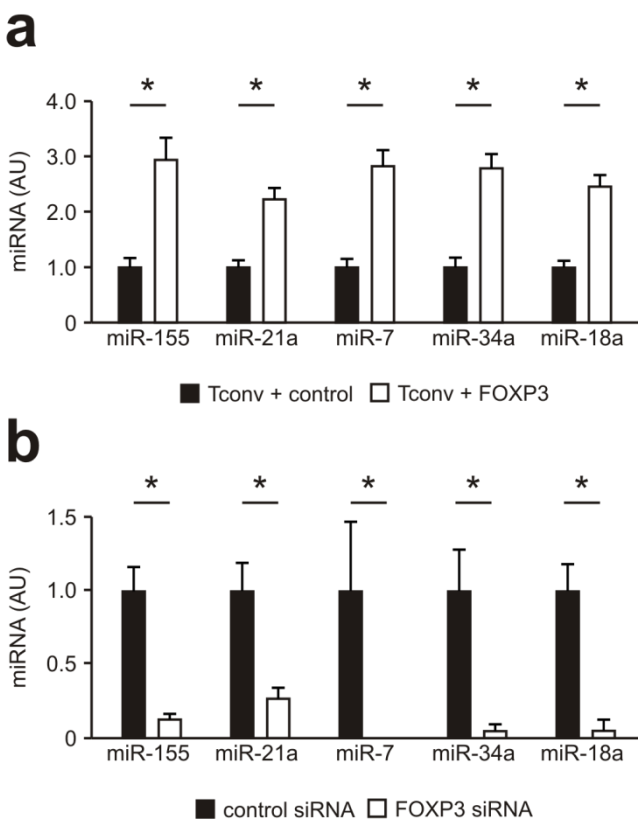

Supplementary Fig. 14. Expression of miRNAs in FOXP3-overexpressing T_{conv} and T_{reg} after silencing of FOXP3.

To assess whether FOXP3 is responsible for the increased expression of miR-155, miR-21a, miR-7. miR-34a, and miR-18a, (**a**) we transduced T_{conv} with a lentivirus containing the full length human FOXP3 cDNA and analyzed miRNA expression or (**b**) isolated T_{reg} and performed siRNA-mediated knockdown of FOXP3 and analyzed miRNA expression after stimulation for 48 hours with CD3 and IL-2 (mean +/- s.d., n=3, * $p<0.05$)

Supplementary Fig. 15

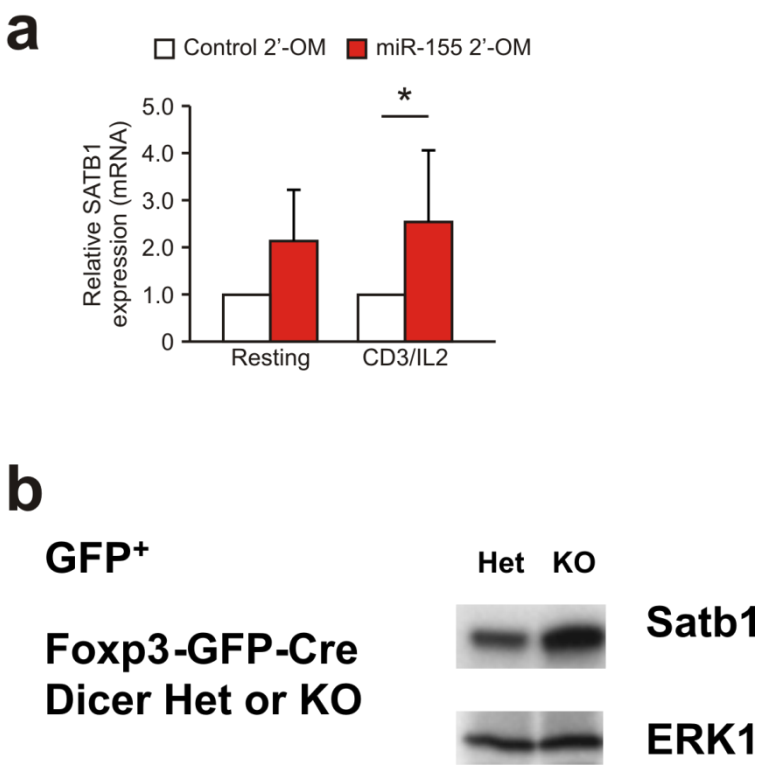

Supplementary Fig. 15. SATB1 expression after inhibition of miRNA in T_{reg}.

(**a**) MACS-purified human natural T_{reg} were transfected with either a control or miR-155 inhibitor and regulation of SATB1 mRNA expression was assessed 48 hours post knockdown by qRT-PCR (mean +/- s.d., n=5, * $p<0.05$) in unstimulated or CD3 and IL-2 stimulated T_{reg}. (**b**) Western blot analysis of SATB1 protein expression in sorted freshly isolated T_{reg} from mice with a T_{reg}-specific complete DICER loss ($DICER^{fl/fl}$) in comparison to $DICER^{wt/fl}$ T_{reg}.

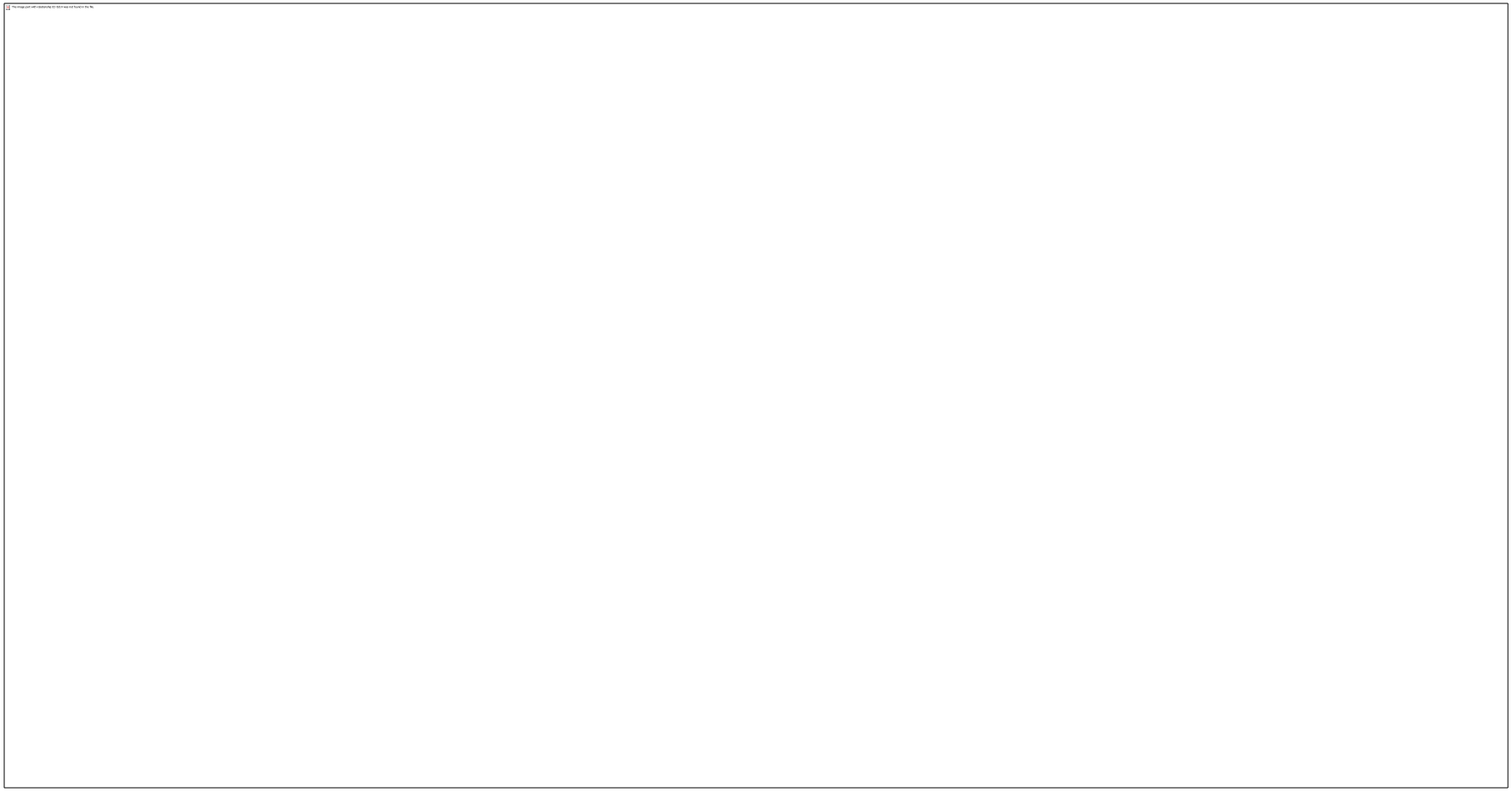

Supplementary Fig.16. Experimental protocol for overexpression of SATB1 in murine human T_{reg}.

FACS sorted murine $CD4^{+}GFP^{+}$ T_{reg} from DEREG mice were expanded for 10-14 days with CD3/CD28-coated beads in the presence of IL-2. After this expansion period, T_{reg} were transduced with pLVTHM-SATB1-IRES-Thy1.1 or control lentivirus

and cultivated in the presence of CD3/CD28 coated beads and IL-2 for 3 to 4 days. SATB1-Thy1.1-transduced, control-transduced or non-transduced expanded T_{reg} were sorted on GFP and Thy1.1 expression or GFP expression alone on a FACS Aria III (BD). (**a**) FOXP3 protein expression in SATB1-Thy1.1-transduced, control-transduced or non-transduced expanded T_{reg} was assessed by flow cytometry. (**b**) SATB1 and (**c**) IL-5, and IFN-γ mRNA expression in SATB1-Thy1.1-transduced Thy1.1-positive, SATB1-Thy1.1-transduced Thy1.1-negative, control-transduced or non-transduced expanded T_{reg} was assessed by qRT-PCR (mean±s.d., n=3; * $p<0.05$). (**d**) Thy1.1 protein expression before and after sorting of SATB1-Thy1.1-transduced T_{reg} into SATB1-Thy1.1-transduced Thy1.1-positive and SATB1-Thy1.1-transduced Thy1.1-negative T_{reg} was assessed by flow cytometry. (**e**) Comparison of suppressive function of SATB1-Thy1.1-transduced Thy1.1-positive, SATB1-Thy1.1-transduced Thy1.1-negative, control-transduced or non-transduced expanded T_{reg} at a ratio of 5:1 of T_{conv} to T_{reg}.

Supplementary Fig. 17

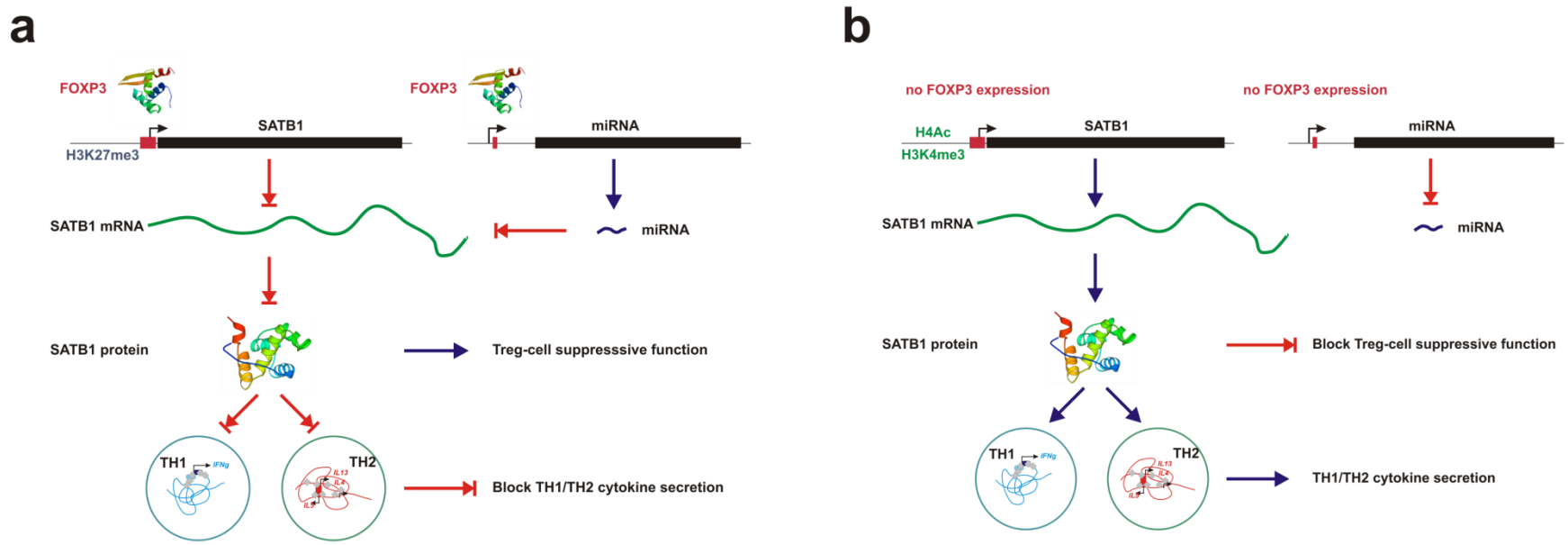

Supplementary Fig. 17. Model for the mode of action of FOXP3.

A, B, Model for the FOXP3- and miRNA-mediated SATB1-dependent remodelling of the respective genomic loci for the release of TH1 and TH2 cytokines and the induction of suppressive function of T_{reg}.

ONLINE METHODS

Mice.

C57BL/6 (B6) mice were purchased from the Jackson Laboratory. RAG2$^{-/-}$, *DEREG*, *scurfy* and *DEREG x scurfy* mice were previously described[5-8]. The male *DEREG x scurfy* mice were indistinguishable from *scurfy* mice in regard to the immunological and clinical manifestations of autoimmunity, while female *DEREG* mice heterozygous for the FOXP3 mutation were symptom free. Mice were housed under specific pathogen-free conditions at the TWINCORE, Centre for Experimental and Clinical Infection Research or at the LIMES Institute, University of Bonn and used in accordance with the German legislation governing animal studies following The Principles of Laboratory Animal Care (NIH publication No. 85-23, revised in 1996).

FoxP3-GFP-hCre BAC Dicer$^{lox/lox}$ mice and FoxP3-GFP-hCre BAC Dicer$^{lox/lox}$ ROSA26R-loxP-Stop-loxP-YFP mice have been previously described[9]. Mice were housed and bred under specific pathogen-free conditions at the UCSF Animal Barrier Facility of the University of California, San Francisco. All animal experiments were approved by the Institutional Animal Care and Use Committee of the University of California, San Francisco.

Antibodies and FACS analysis.

Fluorescent-dye-conjugated antibodies were purchased from Becton Dickinson, BioLegend, or eBioscience. Alexa 647-conjugated mouse anti-human SATB1 monoclonal antibody (clone 14) cross-reactive to murine SATB1 was prepared by R. Balderas (BD Biosciences). FACS data were acquired on a FACSCanto II and LSR II flow cytometer

(Becton Dickinson) and analyzed using FlowJo software package (Tri-Star). Intracellular staining of human and murine FOXP3 and SATB1 was conducted using either the human or mouse FOXP3 Regulatory T-cell Staining Kit (BioLegend) with the addition of FcR-blocking reagents (CD16/CD32 or human IgG) 15 min before intranuclear staining.

Purification and sorting of human T_{reg}.

Human T_{reg} and $T_{effector}$ were purified from whole blood of healthy human donors in compliance with institutional review board (IRB) protocols by negative selection using CD4-RosetteSep (Stem Cell), followed by positive-selection using CD25-specific MACS beads (Miltenyi Biotech) or sorting on a FACSDiVa or Aria III cell sorter (Becton Dickinson) after incubating cells with combinations of fluorochrome-labeled monoclonal antibodies to CD4, CD25, and CD127. For experiments with non-sorted cells, only samples with >95% T_{reg} were used.

Purification and sorting of murine $CD4^+$ T_{reg}.

Murine GFP^+ T_{reg} were purified from thymus, spleen, or peripheral lymph nodes by sorting on a MoFlo high performance cytometer (Beckman Coulter) or FACSDiVA or Aria III cell sorter for CD3 and CD4 stained GFP^+ cells directly or following enrichment of $CD4^+$ T cells using the CD4 negative isolation kit (Invitrogen or Miltenyi Biotech).

Generation of iT_{reg}.

Human $CD4^+$ lymphocytes were purified from whole blood of healthy human donors by negative selection using CD4-RosetteSep (Stem Cell). After negative selection with CD25-specific MACS beads (Miltenyi Biotech), conventional $CD4^+$ lymphocytes were

incubated with CD45RA-specific MACS beads (Miltenyi Biotech). Naïve conventional T cells were obtained by passing the cell mixture over LS magnetic separation columns in a MidiMACS (Miltenyi Biotech) and collecting the $CD4^+CD25^-CD45RA^+$ T cells. Naive T_{reg}-depleted $CD4^+$ T cells (5×10^4 cells $well^{-1}$) were stimulated in serum-free Aim-V/X-Cell (50%/50% V/V) medium with 5×10^4 magnetic beads coated with 5% CD3 (OKT3, Ortho Biotech), 12% CD28 (9.3), and 83% anti-MHC-I (W6/32) monoclonal antibody $well^{-1}$ and TGFβ1 (R&D systems) 5 ng ml^{-1} for a period of 7 days in the absence of IL-2. The described composition of beads was optimized for the induction of iT_{reg} cells.

qRT–PCR on human samples.

Total RNA extracted using TRIZOL (Invitrogen) from T_{conv}, T_{reg}, or iT_{reg} was used to generate cDNA along with the Transcriptor First Strand cDNA synthesis kit (Roche Diagnostics). qRT–PCR was performed using the LightCycler Taqman master kit and the Universal Probe Library assay specific for SATB1, FOXP3, IL-5, IFN-γ, T_{reg}-cell specific genes and beta-2 microglobulin (B2M; Roche Diagnostics) on a LightCycler 480 II (Roche Diagnostics). For each experiment at least two technical replicates were performed. Results were normalized to B2M expression. PCR primer sequences are listed in table S3.

Western blot analysis.

Cell lysates from purified human T_{conv} and T_{reg} and murine T_{reg} and T_{conv} as well as $DICER^{fl/fl}$ or $DICER^{wt/fl}$ T_{reg} were prepared as previously described[10] followed by western blotting with SATB1 antibody as well as human beta-actin or murine ERK antibodies as loading control.

Whole-genome gene expression in human cells.

All RNA was extracted using TRIZOL (Invitrogen) and purified in our laboratory using standard methods. Sample amplification, labelling and hybridization on Illumina WG6 Sentrix BeadChips V1 were performed for all arrays shown in Fig. 1a according to the manufacturer's instructions (Illumina) using an Illumina BeadStation. All data analyses were performed by using Bioconductor for the statistical software R (http://www.r-project.org). Expression values were normalized and summarized by using the IlluminaGUI package[11]. From the resulting data sets we extracted a list of genes with a significant different expression in T_{reg} compared to T_{conv}. Microarray data can be accessed under GSE15390.

For SATB1-transduced T_{reg} as well as FOXP3-transduced T_{conv} Illumina WG6 Sentrix BeadChips V3 were used according to the manufacturer's instructions (Illumina) using an Illumina BeadStation All data analyses were performed by using Bioconductor for the statistical software R (http://www.r-project.org). Expression values were normalized and summarized by using the IlluminaGUI package[11]. From the resulting data sets we extracted a list of genes with a significant different expression in SATB1-transduced T_{reg} compared to control-transduced T_{reg}. These were analyzed in comparison to a dataset consisting of $CD4^+CD25^+$ T_{reg}, $CD4^+CD25^-$ T_{conv}, naive $CD4^+CD25^-CD45RA^+$ T cells activated for 5 days with CD3/CD28-coated beads, as well as unstimulated naive T cells to define T_{conv}-dependent genes (differentially expressed between T_{conv} and T_{reg}), T-cell activation dependent genes (differentially expressed between activated and unstimulated naive T cells), and common T-cell genes (changed in the same direction in both comparisons). For enrichment analysis of TH gene sets, the expression dataset was filtered for expressed probes and significance of enrichment was calculated using χ^2 statistic implemented in R. For verification of SATB1, FOXP3, IL-5, IFN-γ, and IL17A mRNA expression in these

samples by qRT-PCR, total RNA was extracted using TRIZOL. First strand complementary DNA was synthesized with the Transcriptor First Strand cDNA synthesis kit (Roche Diagnostics). qRT–PCR was performed using the LightCycler Taqman master kit and the Universal Probe Library assay specific for SATB1, FOXP3, IL-5, IL-17-A, IFN-γ and beta-2 microglobulin (B2M; Roche Diagnostics) on a LightCycler 480 II (Roche Diagnostics). For each experiment at least three technical replicates were performed. Results were normalized to B2M expression. PCR primer sequences are listed in table S3.

Immunofluorescence microscopy.

Unpurified lymphocytes from male *DEREG* or $CD4^+$ GFP^+ T_{reg} from female heterozygous *DEREG x scurfy* mice purified from thymus were fixed in cold paraformaldehyde for 10 min, washed with PBS, permeabilized with Triton-X and pre-blocked in PBS containing 10% normal goat serum and 1% gelatine from cold water fish skin for 30 min. Slides were then incubated in combinations of primary antibodies (rabbit anti-GFP, mouse anti-FOXP3, mouse anti-SATB1-AF647) for 60 min, washed twice, and incubated with secondary antibodies (anti-rabbit-AF488, anti-mouse-AF555) for 60 min, stained with DAPI and fluorescence was examined using an Olympus FluoView FV1000 or Zeiss LSM 5 LIVE confocal microscope.

qRT–PCR of murine T_{reg}.

Total RNA was extracted with TRIZOL reagent from FOXP3-competent and FOXP3-incompetent $CD4^+$ GFP^+ T_{reg} from female heterozygous *DEREG x scurfy* mice, $CD4^+$ GFP^- T_{conv} FACS-purified from male *DEREG* and *DEREG x scurfy* mice, as well as SATB1-, control-, on non-transduced expanded T_{reg}, respectively. Complementary DNA was

synthesized (Miltenyi Biotech). qPCR was performed using the LightCycler Taqman master kit and the Universal Probe Library assay (Roche Diagnostics) on a LightCycler 480 II (Roche Diagnostics). PCR primer sequences are listed in table S4.

Chromatin immunoprecipitation, whole genome arrays, ChIP qPCR, and electromobility shift assays.

Expanded cord blood T_{reg} were cultured overnight in X-Vivo 15 media supplemented with 20 mM HEPES, pH 7.4, 5% heat inactivated pooled human serum (Lonza), 2 mM glutamine and 100 U/ml rhIL-2 prior to re-stimulation (2 hours) with 1 µM Ionomycin (Sigma) before cross-linking for 10 minutes in 1% formaldehyde solution (50 mM HEPES KOH, pH 7.5, 100 mM NaCl, 1 mM EDTA, 0.5 mM EGTA and 1% formaldehyde). Cell lysis, chromatin immunoprecipitation (ChIP) and DNA isolation steps for human FOXP3 ChIP-on-chip experiments were carried out as previously described[12], using $5x10^7$ cells per immunoprecipitation with either a rabbit anti-FOXP3 IgG_1 (Novus Biochem) or ChIP grade control rabbit IgG_1 Sera (Abcam). Chromatin shearing conditions consisted of 12 repeats of 30 second pulses amplitude 90% with 90 seconds between pulses with a Misonix S-4000 ultrasonic processor (Misonix) with a microtip. Total input chromatin was also purified from an aliquot (100 µl) of cross-linked material and the concentration determined using a Nanodrop UV spectrophotometer (Thermo Scientific).

Amplification of immunoprecipitated and Input chromatin (10 ng) for labelling and hybridisation to either Affymetrix Human Tiling 2.0R or Human Promoter 1.0 arrays was achieved by whole genome amplification (WGA; Sigma GenomePlex WGA kit) adapted for Affymetrix labelling systems by the inclusion of 0.1 mM dUTP (Promega Corp) in the amplification reaction[13]. Amplified material was purified using a PCR clean up kit

(QIAGEN). Labelling and hybridization of amplified material was carried out at the Biomolecular Resource Facility (John Curtin School of Medical Research, Australian National University).

Data were analyzed in MAT[14]. A false discovery rate (FDR) of 0.5% and a score of >100.0 was used to identify significantly enriched regions in FOXP3 immunoprecipitated material relative to input chromatin. Gene accessions were assigned to an individual ChIP region if the peak of the enriched region fell within a window beginning 5kb upstream of a transcription start site (TSS). Annotation information was obtained using gene accessions from both UCSC and NCBI, encompassing RefSeqs, mRNAs and miRNAs. Tiling array data can be accessed under GSE20995.

Validation of FOXP3 binding to genomic regions was carried out by ChIP-qPCR. Reactions were performed using a RT2 SYBRgreen/ROX qPCR master mix (SABiosciences). The relative enrichment of target regions in FOXP3 immunoprecipitated material relative to input chromatin analysis was carried out using the $2^{-\Delta\Delta CT}$ method. Immunoprecipitations using rabbit IgG were used to normalize for non-specific background. PCR primer sequences are listed in table S5.

Gene-specific mRNA silencing, miRNA knockdown and agonistic miRNA.

All siRNAs as well as the miRNA mimics and inhibitors were purchased from Biomers or Dharmacon. miRNA mimics were designed according to the sequences published in miRBase and resembling the double-stranded Dicer-cleavage products. miRNA-inhibitors were designed as single-stranded antisense 2'OM oligonucleotides[15]. These were used for transfection of freshly isolated primary human T_{reg} with nucleofection as previously described[16]. For luciferase assays, HEK293T cells were transfected with both

the reporter plasmids and the small RNA duplexes using Lipofectamine 2000 in a 96-well format and luciferase activity was measured 24 h later. Sequences are listed in tables S6 and S7.

***In vitro* suppression assays after FOXP3 silencing.**

For *in vitro* suppression assays, CFSE-labeled $T_{effector}$ (1 x 10^5 cells $well^{-1}$) were co-cultured with PKH-26-labeled natural or induced T_{reg} at indicated ratios in the presence of CD3/CD28/MHC-I-coated magnetic beads (3.3 x 10^4 beads $well^{-1}$) in 96-well plates in X-Vivo-15 medium supplemented with 10% FCS for 72 h. CFSE dilution was measured on a FACSCanto II flow cytometer.

Cytokine cytometric bead array.

IL-4 and IFN-gamma concentrations were measured using the human TH1/TH2 cytokine kit II (BD Pharmingen).

miRNA profiling and miRNA qRT–PCR.

All RNA were extracted using TRIZOL (Invitrogen) and purified in our laboratory using standard methods. Sample amplification, labelling and hybridization on Illumina miRNA array matrix were performed with the human v1 MicroRNA Expression Profiling kit for all arrays in this study according to the manufacturer's instructions (Illumina) using an Illumina BeadStation. All data analyses were performed by using Bioconductor for the statistical software R (http://www.r-project.org). Expression values were normalized and summarized by using the IlluminaGUI package[11]. From the resulting data sets we extracted a list of miRNAs with a significant different expression in T_{reg} compared to T_{conv}. For

miRNA-specific qRT-PCR, total RNA from freshly isolated T_{reg} and T_{conv}, FOXP3- or control-transduced T_{conv}, as well as control or FOXP3 siRNA tranfected freshly isolated T_{reg} was extracted using TRIZOL. First strand complementary DNA for each miRNA assessed was synthesized by using the TaqMan MicroRNA RT kit and the corresponding miRNA specific kit (Applied Biosystems). Levels of miRNA were measured by qPCR using the TaqMan Universal PCR MasterMix (Applied Biosystems) on a LighCycler 480 II (Roche Diagnostics). Ubiquitously expressed U6 small nuclear RNA or miR-26b were used for normalization.

Cloning of SATB1 3'UTR constructs.

The SATB1 3'UTR was amplified by PCR using human genomic DNA as source material. The full length 3'UTR construct was amplified with primers SATB1 3'UTR F1 and R1, covering the full 1.2 kB region. After digestion with Xho I and Not I the fragment was cloned into the psiCHECK II vector (Promega) to generate psiCHECK II–SATB1–3'UTR.

SATB1 3'UTR F1: ATACTCGAGGATAAAAGTATTTGTTTCGTT

SATB1 3'UTR R1: ATAGCGGCCGCACGATACAAACAATTTTAA

A mutated construct was generated with PCR-based mutagenesis or the QuikChange Lightning Multi Site-Directed mutagenesis kit (Stratagene) following the manufacturer's conditions. MiRNA binding sites were changed by swapping four nucleotides in the seed region as follows:

miR-155 site at +333 3'UTR: AGCATTA to AGCTAAT

Forward primer: TAATTACCTTCTGTGATTATGATT

Reverse primer: GCTTGTTTGAGGCTCCGGAA

miR-34a site at +538 3'UTR: CACTGCC to CACACGG

Primer miR-34a:

CTTTTATTTCCAAAATAAAAACAAATTTGAATTACCCGTGTGCCATATAATACAA

GGCATTTGTTGGCATATG

miR-21 site I at +886 3'UTR: ATAAGCT to ATATCGA

Primer miR-21 I:

GTAAAAATTGCATACAACAATAAGAGTGATCGATATAGTATGAATTGCTTGGAT

AACATAGAGCACTTTTTA

miR-21 site II at +932 3'UTR: ATAAGCT to ATATCGA

Primer miR-21 II:

CATTCGTGATCTATTAGTTTTATTTACCTATCGATATTTGCATGATAGTAAAAAT

TGCATACAACAATAAGAGTG

miR-18a site at +961 3'UTR: CACCTTA to CACGAAT

Primer miR-18a:

GCAAACATCAATTATTTTCACATTAATTGCATAATTTTCATTCGTGATCTATTAG

TTTTATTTACCTAAGCTTATTTGCATG

miR-7 site at +1012 3'UTR: GTCTTCC to GTCAAGG

Primer miR-7:

TACAGATGTAGCTTTAAAATTGATTGTAAACCAAACCTTGACACATTGCAAACA

TCAATTATTTTCACATTAAT

Cloning of SATB1 constructs with potential FOXP3 binding regions.

The corresponding SATB1 genomic regions were amplified by PCR using human genomic DNA as source material. The full length FOXP3 binding site constructs were amplified with the following primers:

FOXP3 BR1 (251 bp, -3947 - -3697)

FOXP3 BR1 F1: ATATGGTACCATGCTCATTTATTCTGTT

FOXP3 BR1 R1: ATATAAGCTTGAAATAAAATATTGTAAACA

FOXP3 BR2 (401 bp, -3110 - -2710)

FOXP3 BR2 F1: ATATGGTACCGCTATTAGAGTGATATATT

FOXP3 BR2 R1: ATATAAGCTTGTTCATGTAAAAATAAAG

FOXP3 BR3 (401 bp, +269 - +669)

FOXP3 BR3 F1: ATATGGTACCGTGTTTCTGTTTCTAGATAG

FOXP3 BR3 R1: ATATAGATCTGAGTTTCTTTTGAGTTACACGT

FOXP3 BR4 (401 bp, +3336 - +3736)

FOXP3 BR4 F1: ATATGGTACCGACTGAATTAAATATAATGG

FOXP3 BR4 R1: ATATAAGCTTTCCAAGTTGTTAAACTGCA

FOXP3 BR5 (200 bp, +6303 - +6502)

FOXP3 BR5 F1: ATATGGTACCTAATTTGTTTGGACACAA

FOXP3 BR5 R1: ATATAAGCTTGCAATGAATGCAGAATTAC

FOXP3 BR6 (117 bp, +6653 - +6769)

FOXP3 BR6 F1: ATATGGTACCCACAGTGAATCTCTTGTG

FOXP3 BR6 R1: ATATAAGCTTCTATCAAAAAGATGAAGAAGAA

After digestion with Acc65 I and Hind III resp. Bgl II for FOXP3 BR 3 the fragments were cloned into the pGL4.24 vector with a minP element upstream of the potential binding motif and a destabilized downstream Firefly luciferase.

Mutated constructs were generated with either PCR-based mutagenesis or the QuikChange Lightning Multi Site-Directed mutagenesis kit (Stratagene) following manufacturer's conditions. FOXP3 binding regions were changed as follows:

FOXP3 BR1

FOXP3 BR1 site I + II at -3933: ATTCTGTTTATCATTTT to CGTGCGGCCGCAGGACA

FOXP3 BR1 site I + II:

TAAGGACTGACATGGCCTTGGTGTCCTGCGGCCGCACGAAATGAGCATGGTACC

GGCCAGTTAGGCCAGAG

FOXP3 BR1 site III + IV at -3718: ATGTTTAC to GGTCCGTG

FOXP3 BR1 site III + IV:

TATACCCTCTAGTGTCTAAGCTTGAAATAAAATATTCACGGACCGCTTATTACAT

CATTTTACAGAAATAAATAAGAC

FOXP3 BR2

FOXP3 BR2 site I at -3001: GTAATGTAAACAGTGTG to TGTCCTGCGGCCGCACG

FOXP3 BR2 site I:

GCTCTGTAAAGCCACCAATACACTCTTAGGCGTGCGGCCGCAGGACAAAATCTA

AAGAAAAGCCAAAAGGTAAAGCAGAAAAGTG

FOXP3 BR2 site II at -2881: CAAAATGTTTATCTGAC to TCGTCCCTGCAGGCCGG

FOXP3 BR2 site II:

GAATTTGCTGGTAGGGAAAAGAGAAAAATCACCGGCCTGCAGGGACGATTACA

CATAAAAAAGCAACAAGTTAGCACAAGTACTGAGATAAAAGGG

FOXP3 BR2 site III at -2843: TGAAAAATAATTCTTGT to CGTGGCTGGCGAAGAGC

FOXP3 BR2 site III:

CCATTTTAGCACCCTGAAGGCAGTTAATCATTAACAAAAAGCTCTTCGCCAGCC

ACGGAATTTGCTGGTAGGGAAAAGAGAAAAATCAGTCAG

FOXP3 BR2 site IV at -2733: AATATTCTTTATTTTTA to GCTGGCGGCGCCGCGCG

FOXP3 BR2 site IV + V:

GCTGGAAGTCGAGCTTCCATTATATACCCTCTAGTGTCTAAGCTTGCAATCACGC
GCGGCGCCGCCAGCACAATGTAACCCAAAATAGAAATGCCTCATTTATCGCTTA
GG

FOXP3 BR2 site V at -2727: CTTTATTTTTACATGAA to GGCGCCGCGCGTGATTG

FOXP3 BR2 site IV + V:
GCTGGAAGTCGAGCTTCCATTATATACCCTCTAGTGTCTAAGCTTGCAATCACGC
GCGGCGCCGCCAGCACAATGTAACCCAAAATAGAAATGCCTCATTTATCGCTTA
GG

FOXP3 BR3

FOXP3 BR3 site I at +511: ATAATTGTTGTTACTGA to CGTGCGGCCGCAGGACA

FOXP3 BR3 site I:
CTAAGACCATATATGATAATTACTGAATAAAACAGTGAACCGTGCGGCCGCAGG
ACATTCCTTTAAAAGGAAAGAAAATCTCGAAATTCTAGTTTTTTAGG

FOXP3 BR4

FOXP3 BR4 site I at +3343: TTAAATATAATGGTTTT to CCGGCGCGCCACCGCGA

FOXP3 BR4 site I:
CACCTTTTGAATGGACCCTGCCAAAACTTCGCGGTGGCGCGCCGGTTCAGTCGG
TACCGGCCAGTTAGGCCAGAGAAATG

FOXP3 BR4 site II at +3538: GGTAATGTTATTTTTTG to CATCCCTGCAGGGACCA

FOXP3 BR4 site II:

CTGCTAATGAATTTGCTCTTAAGAAAATAAGCCATGGTCCCTGCAGGGATGAAA

CTTCTACATAAGATGTCCAAGATCTCTGAAACTGCCCTAC

FOXP3 BR4 site III at +3583: TAGCAGTAAAAAATCTG to GCTCGCGGCCGCCGAGT

FOXP3 BR4 site III:

CCCAATTAAAACAAAAATAAAAAACTAGAATCATACTCGGCGGCCGCGAGCAT

GAATTTGCTCTTAAGAAAATAAGCCATGGTCCCTGCAGGGATG

FOXP3 BR5

FOXP3 BR5 site I at +6398: ATGTTTGC to CGGTCCGTG

FOXP3 BR5 site I forward primer: ATACTGTATACTACTCATAGCAAA

FOXP3 BR5 site I reverse primer: CACGGACCGAACTCACCATTTATCTTCAG

FOXP3 BR6

FOXP3 BR6 site I + II at +6670: GATTATTTATTT to TCGGCGGCCGCG

FOXP3 BR6 site I + II:

GGAAATATTAGCCATGACGCGGCCGCCGAACAAGAGATTCACTGTGGGTACCG

GCCAGTTAGGCC

FOXP3 BR6 site III at +6728: GATTATTTATTT to CCGGCGCGCCAC

FOXP3 BR6 site III:

CTATCAAAAAGATGAAGAAGAAGAGATGGAGTGGCGCGCCGGTTCAGAAATAC
AGCTTGGGGGTGGC

Luciferase assays.

Human embryonic kidney (HEK) 293T (ATCC CRL-11268) cells were maintained in DMEM containing 10% heat-inactivated fetal bovine serum.

To assess regulation of SATB1 expression by binding of miRNA to the 3'UTR of SATB1, the 3'UTR of human SATB1 was amplified using PCR and cloned into the psiCHECK II vector (Promega) to generate psiCHECK II–SATB1–3'UTR (see above). To control for specific miRNA-binding, miRNA seed motifs were mutated using the QuickChange mutagenesis kit (Promega). These constructs were transfected into HEK293T cells in 96-well plates together with miRNA mimics for either miR-155, miR-7, miR-21, miR-34a, miR-18a or a scrambled control miRNA.

To assess regulation of SATB1 expression by binding of FOXP3 to the genomic locus of SATB1, the six potential FOXP3 binding regions were amplified using PCR and cloned into the pGL4.24 vector with a minP element upstream of the potential binding motif and a destabilized downstream Firefly luciferase (see above). To control for specific FOXP3-binding, FOXP3 binding motifs were mutated using the QuickChange mutagenesis kit (Promega). These constructs were transfected separately into HEK293T cells in 96-well plates together with control plasmid or plasmids expressing FOXP3 as well as a plasmid encoding renilla luciferase for normalization.

Lysis and analysis were performed 24 hours post transfection using the Promega Dual Luciferase Kit. Luciferase activity was counted in a Mithras plate reader (Berthold).

Lentiviral vector production.

For transduction of human T cells cDNA encoding SATB1 and FOXP3 were obtained from Open Biosystems and placed into the 2nd position of a T2A expression vector as previously described[17]. High titer lentiviral vector supernatant encoding DsRED T2A SATB1, YFP T2A FOXP3 and control plasmids alone was collected as previously described[18]. For silencing of FOXP3 and SATB1 in human T_{reg}, artificial miRNA against FOXP3 and SATB1 were designed, cloned into the pcDNA6.2-GW+EmGFP-miR vector, chained and recombined with pDONR221 and pLenti6.3 to generate miRNA containing pLenti6.3 expression vectors (all from Invitrogen). Oligonucleotide sequences are listed in table S11. For transduction of murine expanded T_{reg}, SATB1 was cloned into the pLVTHM expression vector in front of an IRES-Thy1.1 sequence[19]. High titer lentiviral vector supernatant encoding miRNAs and murine SATB1 was generated as previously described[18, 19].

Lentiviral FOXP3 and SATB1 transductions of human $CD4^+$ T cells.

T_{reg}-depleted human $CD4^+$ T_{conv} were lentivirally transduced with a pELNS YFP T2A FOXP3 or control plasmids containing GFP as previously described[17] and assessed after a resting period of 72-120 h for SATB1, FOXP3, cytokine gene, and T_{reg}-cell associated gene expression, miRNA expression as well as whole genome expression analysis using Illumina WG6 Sentrix BeadChips V3.

MACS-isolated human $CD4^+CD25^+$ T_{reg} were stimulated for 24 hours with CD3 and CD28-coated beads in the presence of IL-2. After this initial stimulation, T_{reg} were lentivirally transduced with a pELNS DsRED 2A SATB1 or control plasmids containing

DsRED as previously described[17] resulting in a 1:1 expression of DsRED and the transgene[2], expanded for 6 days in the presence of CD3 and CD28-coated beads and IL-2, sorted on DsRED-positive cells on a MoFlo sorter (DakoCytomation) and used for suppression assays directly after isolation, cytokine assessment after 4 and 16 hours of CD3/CD28 stimulation, SATB1, FOXP3 and cytokine gene expression by qPCR and whole genome expression analysis using Illumina WG6 Sentrix BeadChips V3 after 16 hours of CD3/CD28 stimulation[20].

***In vitro* suppression assays of human SATB1-transduced T_{reg}.**

Following the harvest of SATB1-transduced T_{reg}, varying numbers of T_{reg} were plated in round-bottom, 96-well plates (Corning). Frozen autologous PBMCs were thawed and CFSE labelled. 1 x 10^5 CFSE-labelled PBMC were added together with CD3-coated beads (Invitrogen) at a ratio of one bead per cell[20]. Cultures were harvested 4 days later and stained with allophycocyanin-conjugated CD8 (BD Pharmingen). Data were acquired on a FACSCalibur (BD Biosciences) flow cytometer using CellQuest Pro software and analyzed using FlowJo software (Tree Star).

Bisulphite sequencing.

Genomic DNA from human T_{reg} cells and conventional T cells purified by negative selection using CD4-RosetteSep (Stem Cell), followed by sorting on a FACSDiVa cell sorter (Becton Dickinson) after incubating cells with a combination of fluorochrome-labelled monoclonal antibodies to CD4, CD25, and CD127 was isolated using phenol/chloroform extraction. Sodium bisulphate treatment of genomic DNA was performed resulting in the deamination of unmethylated cytosines to uracil, whereas methylated

cytosines remain unchanged. After amplification PCR products were purified and sequenced in both directions. PCR primer sequences are listed in tableS7.

Filter retention analysis.

Each individual ^{32}P-radiolabeled dsDNA sequence (14 nM) was incubated with increasing concentrations of FOXP3 protein for 30 min at 37°C in 25 µl of binding buffer (KCl-Tris, pH 7.6, 5% Glycerol, 3 mM $MgCl_2$, 2 mM DTT) in the presence of 1µg/ml tRNA (Roche) and 50µg/ml BSA. After incubation, the binding reaction was filtered through pre-wet 0.45µm nitrocellulose filter membrane (Millipore) to co-retain protein and bound DNA. Membranes were washed and the amount of bound DNA-protein complexes determined by autoradiography[21]. Data analysis was done with Origin 8G software using non-linear curve fitting (Hill1-model). Oligonucleotide sequences are listed in table S9.

Expansion of murine T_{reg}

$CD4^+CD25^+GFP^+$ T_{reg} were isolated from lymph nodes and spleens of DEREG mice. Cells were pre-enriched with the mouse $CD4^+$ T-cell isolation kit according to manufacturer's instructions (Miltenyi Biotech). Following enrichment, cells were stained with CD4, CD25, CD3, and CD8α. Cells were sorted on a FACS Aria III (BD) (purity > 98.0%). Cells were expanded *in vitro* by activation with Dynabead mouse T cell activator CD3/CD28 coated microbeads (3:1 bead to T_{reg} ratio, Invitrogen) with exogenous IL-2 (2000 IU/ml, Proleukin) as previously described[22].

Lentiviral transductions of murine T_{reg} cells.

After expansion for 10 to 14 days in the presence of CD3/CD28 coated beads and IL-2, murine T_{reg} were lentivirally transduced with a pLVTHM-SATB1-IRES-Thy1.1 plasmid or control plasmids. Therefore, 2.5×10^5 cells per well were transduced in 500 µl total volume of fresh culture media in a 24-well plate containing lentivirus (20 TU/cell) and protamine sulfate (8 µg/ml; Sigma-Aldrich). Cells were spin-inoculated by centrifugation at 1000×g for 90 min at 30°C, fresh medium was added and cells were incubated for an additional 2 hours at 37°C. Afterwards, cells were washed several times and cultivated in the presence of CD3/CD28 coated beads and IL-2. Transgene expression was assessed no earlier than 72 hours post-transduction. SATB1-Thy1.1-transduced, control-transduced or non-transduced expanded T_{reg} were sorted on GFP and Thy1.1 expression or GFP expression alone on a FACS Aria III (BD) and used for suppression assays, cytokine gene expression by qPCR or adoptive transfer experiments directly after isolation.

***In vitro* suppression assays of murine SATB1-transduced T_{reg}.**

After the harvest and sorting of transduced T_{reg}, varying numbers of SATB1-Thy1.1-transduced Thy1.1$^+$ or Thy1.1$^-$, control transduced or non-transduced expanded T_{reg} were plated in round-bottom 96-well plates. Freshly isolated splenic CD4$^+$ T cells from C57BL/6 mice were labelled with eFlour 670 (eBiosciences). 1 x 10^5 eFlour 670-labelled CD4$^+$ T cells were added together with CD3/CD28-coated beads (Invitrogen) at a ratio of one bead per 3 cells. Cultures were harvested 4 days later, acquired on a LSR II flow cytometer and analyzed using FlowJo software (Tree Star).

Induction and assessment of colitis.

Splenocyte samples were enriched for $CD4^+$ T cells by negative selection on MACS columns with the $CD4^+$ T-cell isolation kit II (Miltenyi Biotec). Cells were then stained with CD45RB, CD25, CD4, CD8α, and CD3 (all from BD) and naïve $CD4^+CD25^-CD45RB^{high}$ T cells were sorted on a FACS Aria III. IBD was induced by the adoptive transfer of 600,000 naïve $CD4^+CD45RB^{high}$ T cells that were purified from C57BL/6 mice into $RAG2^{-/-}$ animals by tail vain injection. Mice that received 100,000 control-transduced expanded $CD4^+GFP^+$ T_{reg} from DEREG mice at the same time as the naïve $CD4^+CD45RB^{high}$ T cells served as controls. To test the function of SATB1-expressing T_{reg}, mice received 100,000 SATB1-transduced expanded $CD4^+GFP^+$ T_{reg} from DEREG mice together with the naïve $CD4^+CD45RB^{high}$ T cells. Recipient mice were weighed 3 times per week and monitored for signs of illness. After 8 weeks, the animals were killed, and the mesenteric and peripheral LNs as well as spleen were analyzed by flow cytometry. For histological analysis, the large intestine (from the ileo-ceco-colic junction to the anorectal junction) was removed, fixed in 10% buffered formalin solution, and routinely processed for histological examination. Sections were stained with hematoxylin and eosin and assigned scores as described (Zitat Claudia). All samples were coded and assigned scores by researchers 'blinded' to the experimental conditions.

Expansion of human T_{reg}.

$CD4^+CD25^{high}CD127^{low}CD45RA^+$ T_{reg} as well as $CD4^+CD25^-CD127^+CD45RA^+$ T_{conv} were isolated on a FACS Aria III and plated at 2.5×10^5 T_{reg} or T_{conv} per well in a 24-well plate and activated with CD3/ CD28 coated microbeads (Invitrogen) at a 3:1 bead to cell. Cultures were grown in the presence of IL-2 and continuing throughout the expansion period (300 IU/ml, Proleukin). Cells were resuspended and fresh media and IL-2 (300

IU/ml) added at days 5, 7, 9, and 12 assuming consumption of IL-2. On day 8, cells were restimulated with fresh CD3/CD28 coated beads. Cultured cells were harvested at day 14 for analysis by FACS (only cultures with >95% FOXP3 expression were used for further studies), functional studies, lentiviral transductions with miRNAs against FOXP3 and SATB1 as well as analysis of histone modifications.

Lentiviral transductions of expanded human T_{reg}.

Expanded human T_{reg} were lentivirally transduced with pLenti6.3-EmGFP-miRNA-FOXP3, pLenti6.3-EmGFP-miRNA-FOXP3-miRNA-SATB1 or control plasmids containing EmGFP as previously described[17], expanded for 3 further days in the presence of CD3 and CD28-coated beads and IL-2, sorted on EmGFP-positive cells on a FACS Aria III sorter (BD) and used directly after isolation for cytokine gene expression by qPCR or for cytokine assessment after 16 hours of CD3/CD28 stimulation.

Assessment of histone modifications in expanded human $CD4^+$ T cells

ChIP-Seq experiments were performed as described previously. In brief, expanded T_{reg} and T_{conv} were harvested on days 14, treated with MNase to generate approximately 80% mononucleosomes and 20% dinucleosomes. Chromatin from 2.5×10^6 cells was used for each ChIP experiment, which yielded approximately 500 pg of DNA. Antibodies against histone H4Ac, H3K4me3 and H3K27me3 (Millipore) were used. The ChIP DNA fragments were blunt-ended, ligated to the Illumina adaptors, and sequenced with the Illumina HiScan. Sequenced reads of mostly 25 bp were obtained with the Solexa Analysis Pipeline. All reads were mapped to the human genome (hg18) using CASAVA 1.7 (Illumina) and only uniquely matching reads were retained. Data were further analyzed in MACS[23]. A false

discovery rate (FDR) of 0.5% and a p-value ($-10\log_{10}$) of >100.0 was used to identify significantly enriched regions in histone immunoprecipitated material from T_{reg} relative to T_{conv} and vice versa at the SATB1 locus.

Validation of histone binding to the SATB1 locus was carried out by ChIP-qPCR. Reactions were performed using SYBR green qPCR master mix (Fermentas). The relative enrichment of target regions in histone immunoprecipitated material relative to input chromatin analysis was carried out using the $2^{-\Delta\Delta CT}$ method. Immunoprecipitations using control IgG were used to normalize for non-specific background. PCR primer sequences are listed in table S10.

To confirm histone modifications observed at the SATB1 locus in human expanded T_{reg}, previously published murine data were reanalyzed for SATB1 expression and histone methylation in naive T cells, Teffector (ThH1, TH2, resp. TH17), iT_{reg} and nT_{reg}[4].

Statistical analysis.

Student's t-tests and ANOVA with LSD were performed with SPSS 19.0 software.

SUPPLEMENTARY TABLES.

Table 1 Experimental conditions for microarray analysis

ID	n	donor	subset	celltype	experimental condition
1	4	healthy	activated Tconv	CD4+	8 hrs CD3CD28
2	4	healthy	activated Tconv	CD4+	8 hrs CD3CD28 + TGF-β
3	4	healthy	activated Tconv	CD4+	8 hrs CD3CD28 + VEGF
4	4	healthy	activated Tconv	CD4+	8 hrs CD3CD28 + IL-10
5	4	healthy	activated Tconv	CD4+	8 hrs CD3CD28 + PGE_2
6	4	healthy	activated Tconv	CD4+	8 hrs CD3CD28 + PD1
7	4	healthy	activated Tconv	CD4+	8 hrs CD3CD28 + CTLA-4
8	4	healthy	activated Tconv	CD4+	8 hrs CD3
9	4	healthy	activated Tconv	CD4+	24 hrs CD3/IL-2
10	3	healthy	TGF-β-treated Tconv	CD4+	18 hrs cultured + 1 hr TGF-β
11	3	healthy	TGF-β-treated Tconv	CD4+	18 hrs cultured + 2 hrs TGF-β
12	3	healthy	TGF-β-treated Tconv	CD4+	18 hrs cultured + 8 hrs TGF-β
13	4	healthy	TGF-β-treated Tconv	CD4+	12 hrs cultured + 8 hrs TGF-β (1ng/ml)
14	4	healthy	TGF-β-treated Tconv	CD4+	12 hrs cultured + 8 hrs TGF-β (10ng/ml)
15	3	healthy	TGF-β-treated Tconv	CD4+	18 hrs TGF-β
16	4	healthy	resting Tconv	CD4+	8 hrs cultured
17	4	healthy	resting Tconv	CD4+	12 hrs cultured
18	3	healthy	resting Tconv	CD4+	18 hrs cultured

19	3	healthy	resting Tconv	CD4+	19 hrs cultured
20	6	healthy	resting Tconv	CD4+	20 hrs cultured
21	3	healthy	resting Tconv	CD4+	26 hrs cultured
22	7	healthy	resting Tconv	CD4+	Untreated
23	4	healthy	resting Tconv	CD4+CD25-	Untreated
24	2	healthy	resting Tconv	CD4+CD25-	Untreated
25	2	healthy	resting Tconv	CD4+CD25-	Untreated
26	3	healthy	resting Tconv	CD4+CD25-	6 hrs cultured
27	2	healthy	resting Tconv	CD4+CD25-	Untreated
28	3	healthy	resting Tconv	CD4+CD25-	Untreated
29	3	healthy	resting Tconv	CD4+CD25-	Untreated
30	4	healthy	resting Tconv	CD4+CD25-	Untreated
31	4	CLL	resting Treg	CD4+CD25+	Untreated
32	4	healthy	resting Treg	CD4+CD25+	Untreated
33	4	healthy	resting Treg	CD4+CD25+	Untreated
34	2	healthy	resting Treg	CD4+CD25+	Untreated
35	2	healthy	resting Treg	CD4+CD25+	6 hrs cultured
36	4	healthy	activated Treg	CD4+CD25+	24 hrs CD3/IL-2
37	4	CLL	activated Treg	CD4+CD25+	24 hrs CD3/IL-2
38	4	healthy	expanded Treg	CD4+CD25+	expanded
39	4	healthy	expanded Treg	CD4+CD25+	expanded with Rapamycin
40	4	healthy	expanded Treg	CD4+CD25+	expanded + 6 hrs CD3CD28

Table 2 FOXP3 binding regions

Tiling array region	start	stop	length (bp)	FOXP3 binding motifs	MAT score	p-value ($-10\log_{10}$)	FOXP3 binding region	FOXP3 binding motifs	start	stop	length (bp)
B1	-19933	-18711	1223	9	7.05	154.29	**BR1**	7	-19337	-18711	626
B2	-17526	-15898	1629	15	5.25	90.42	**BR2**	6	-16970	-16592	379
B3	-15767	-14637	1131	7	5.16	87.58	**BR3**	2	-15692	-15439	254
B4	-13165	-12161	1005	5	6.43	130.41	**BR4**	4	-22566	-12161	406
B5	-12160	-11018	1143	8	4.89	79.92	**BR5**	4	-11490	-11217	274
B6	-11017	-9639	1379	14	6.02	115.69	**BR6**	6	-10161	-9818	345
B7	-8491	-6303	2189	13	6.88	147.33	**BR7**	4	-7085	-6865	221
B8	-5995	-4369	1627	15	5.47	97.25	**BR8**	5	-5181	-4896	286
B9	-4356	-1861	2496	27	12.86	483.42	**BR9**	4	-3947	-3697	251
							BR10	5	-3110	-2710	401
B10	-854	1465	2320	13	7.88	189.63	**BR11**	1	+269	+669	401
B11	+2895	+6146	3252	29	7.96	193.47	**BR12**	3	+3336	+3736	401
B12	+6505	+7653	1149	9	5.59	101.04	**BR13**	1	+6303	+6502	200
							BR14	3	+6653	+6769	117
B13	+11598	+13006	1409	12	6.93	149.36	**BR15**	7	+12260	+12760	501
B14	+20356	+22256	1901	20	11.38	381.62	**BR16**	6	+21031	+21431	401

Table 3 human qPCR oligonucleotides

SATB1 Forward	CGATGAACTGAAACGAGCAG
SATB1 Reverse	CGGAGGATTTCTGAAAGCAA
FOXP3 Forward	ACCTACGCCACGCTCATC
FOXP3 Reverse	TCATTGAGTGTCCGCTGCT
IL-5 Forward	GGTTTGTTGCAGCCAAAGAT
IL-5 Reverse	TCTTGGCCCTCATTCTCACT
IFN-γ Forward	CACTGAAGAAATCTTTCAGGGAAT
IFN-γ Reverse	CCGTCTTTCTTCTCCACACTTT
IL-17A Forward	TGGGAAGACCTCATTGGTGT
IL-17A Forward	GGATTTCGTGGGATTGTGAT
CTLA4 Forward	TTCATCCCTGTCTTCTGCAA
CTLA4 Reverse	AGTGGCTTTGCCTGGAGAT
GITR Forward	AGGCCAGGGGGTACAGTC
GITR Reverse	AAGGTTTGCAGTGGCCTTC
PDE3B Forward	AACAATGGTATAAGCCTCATTATCAA
PDE3B Reverse	CGAGCCTCATTTAGCACTGA
CD25 Forward	ACGGGAAGACAAGGTGGAC
CD25 Reverse	TGCCTGAGGCTTCTCTTCA
CD127 Forward	AAAGTTTTAATGCACGATGTAGCTT
CD127 Reverse	TGTGCTGGATAAATTCACATGC
CD73 Forward	TGATCCTCCCAAACTTCCTG

CD73 Reverse	AACCACGTTGATATCTTGGTCA
CD39 Forward	AAGGCCACAGCTGGCTTAC
CD39 reverse	GGAAAGGCGATGCTTTAAATAC
GPR83 Forward	TCTGCCAGAAATTATTTACCTTCA
GPR83 Reverse	AGCTGGCTCAGGGAAGTCT
β-2 microglobulin Forward	TTCTGGCCTGGAGGCTAT
β-2 microglobulin Reverse	TCAGGAAATTTGACTTTCCATTC

Table 4 murine qPCR oligonucleotides

satb1 Forward	AGGAGTGCCCCCTTTCAC
satb1 Reverse	TGCTGCTGAGACATTTGCAT
foxp3 Forward	ACCACACTTCATGCATCAGC
foxp3 Reverse	CCAGTGGCAGCAGAAGGT
IL-5 Forward	CAAACTGGTAATGTAGCCAAGGAT
IL-5 Reverse	CTGTAACCTCAGCCTTCAGGA
IL-6 Forward	GCTACCAAACTGGATATAATCAGGA
IL-6 Reverse	CCAGGTAGCTATGGTACTCCAGAA
IFN-γ Forward	CCTTTGGACCCTCTGACTTG
IFN-γ Reverse	AGCGTTCATTGTCTCAGAGCTA
β-actin Forward	CTAAGGCCAACCGTGAAAAG
β-actin Reverse	ACCAGAGGCATACAGGGACA

Table 5 ChIP-PCR oligonucleotides

SATB1 BR1 Forward	GAACAGTAGTACATTCATATACTGG
SATB1 BR1 Reverse	TTAAGATGCCTATTCATGCTATTCC
SATB1 BR2 Forward	GAAAGTTATGTTTCAGCATGATGAG
SATB1 BR2 Reverse	CTGGTATTTACTTCAGGAAGGTAAG
SATB1 BR3 Forward	TCAACACATTAACACACATTATTTC
SATB1 BR3 Reverse	ATAACTTGAAAGCATAAAAATAGGC
SATB1 BR4 Forward	CAAACAGAGCACTCCCCTGAG
SATB1 BR4 Reverse	GGAAAGAACGCATAGAAGGTCAATC
SATB1 BR5 Forward	TCTCATTTCCTCTTGTTTATTGTTG
SATB1 BR5 Reverse	ATAATAAGGTTAAGTAGGCTTCTCC
SATB1 BR6 Forward	TTCTACTGTGGCATTATTTATCAAC
SATB1 BR6 Reverse	GCATATCCAGTTACCTATCTTGTAG
SATB1 BR7 Forward	TCTCCCAAAACAAACATAAACATTG
SATB1 BR7 Reverse	TTTCCCTAATTACTTGGCATAGAT
SATB1 BR8 Forward	AAAGTGTTATGGTGGTAAGCATTG
SATB1 BR8 Reverse	CAGAGAAAGCATTTAGAATTCGAGTG
SATB1 BR9 Forward	ATAGTCATTCTTAGATGCCTTTATG
SATB1 BR9 Reverse	CTGTTGGGCAAAATAAAATTTAAAC
SATB1 BR10 Forward	ATTGGTGGCTTTACAGAGCTTAAT
SATB1 BR10 Reverse	AATTTGCTGGTAGGGAAAAGAGAA
SATB1 BR11 Forward	GTTTCAGGTCGGTTTTGCTAATTT

SATB1 BR11 Reverse	GATTGTGCCCTTATCCATTCCATA
SATB1 BR12 Forward	TAGGCAGCTGTTTCTTCAAACTAA
SATB1 BR12 Reverse	CTGAAACTGCCCTACAACTAAGAA
SATB1 BR13 Forward	GCAGTAGAAAGGTGGGTTCTTC
SATB1 BR13 Reverse	GCAATGAATGCAGAATTACCTTT
SATB1 BR14 Forward	GCCTGTACTGTACCCAGTC
SATB1 BR14 Reverse	CATATTCAATGGCGTTTTCATAATG
SATB1 BR15 Forward	AGGTCAGCTATTACTTCTACCAGC
SATB1 BR15 Reverse	GGAAGGTAAAAATGCGCAAATCAG
SATB1 BR16 Forward	TTTTGTAGATGCTCTTGCTACCTC
SATB1 BR16 Reverse	TCATATGATCTACATGCTTGCGTT
SATB1 -15kb ChIP Forward	AGCAAGATTTAATTGCTGGTCCTG
SATB1 -15kb ChIP Reverse	TGCAATTGAAAAGACAAAGCCCTA
CTLA4 Forward	AAGGCTTTCTATTCAAGTGCCTTC
CTLA4 Reverse	TGTTCAGGTCTTCAGGAAGTAGAG
PDE3B Intron 1 BS1 Forward	GPH002163(+)02A
PDE3B Intron 1 BS1 Reverse	GPH002163(+)02A
PDE3B Intron 1 BS2 Forward	TATGCATTCCGTATGCGTGGTAG
PDE3B Intron 1 BS2 Reverse	AATGAACCTACAACAAGCAGCCT
PDE3B Intron 10 Forward	GTTTTGTGTGCAAACATGGGTCT
PDE3B Intron 10 Reverse	TGGAAAATGTTCTCAAGGTGGCT
IL7RA Promoter Forward	CAGGGAATATCCAGGAGGAA

IL7RA Promoter Reverse	TGTGTGAGCCAGTGTGTATGAA
AFM Intron 1 Forward	GCAGAACCTAGTTCCTCCTTCAAC
AFM Intron 1 Reverse	AGTCATCCCTTCCTACAGACTGAGA
hsa-miR-155 Forward	TGCTAATCGTGATAGGGGTTTTTG
hsa-miR-155 Reverse	GCCTGAAGTCTAAGTTTATCCAGC
hsa-miR-21 Forward	CACCACAGGTAAGACTTTAATCCG
hsa-miR-21 Reverse	AAATGTGAGTGAGAGCTGTGAATG
hsa-miR-7-1 Forward	GPH026342(+)01A
hsa-miR-7-1 Reverse	GPH026342(+)01A

Table 6 siRNA

FOXP3 sense	GCACAUUCCCAGAGUUCCUdTdT
FOXP3 antisense	AGGAACUCUGGGAAUGUGCdTdT
control sense	UUCUCCGAACGUGUCACGUdTdT
control antisense	ACGUGACACGUUCGGAGAAdTdT
SATB1 siRNA pool 1 sense	GAAGGAAACACAGACAUUA
SATB1 siRNA pool 1 antisense	UAAUGUCUGUGUUUCCUUC
SATB1 siRNA pool 2 sense	GGAAUGCUCUGAAGGACUU
SATB1 siRNA pool 2 antisense	AAGUCCUUCAGAGCAUUCC
SATB1 siRNA pool 3 sense	GCAAAUGUCUCAGCAGCAA
SATB1 siRNA pool 3 antisense	UGCUGCUGAGACAUUUGC
SATB1 siRNA pool 4 sense	UCAGAAAUGUCUAACAAUG
SATB1 siRNA pool 4 antisense	CAUUGUUAGACAUUUCUGA

Table 7 miRNA mimics and inhibitors

miR-155 guide	UUAAUGCUAAUCGUGAUAGGGGU
miR-155 passenger	UCCUACAUAUUAGCAUUAACA
miR-7 guide	UGGAAGACUAGUGAUUUUGUUGU
miR-7 passenger	CAACAAAUCACAGUCUGCCAUA
miR-21 guide	UAGCUUAUCAGACUGAUGUUGA
miR-21 passenger	CAACACCAGUCGAUGGGCUGU
miR-34a guide	UGGCAGUGUCUUAGCUGGUUGU
miR-34a passenger	CAAUCAGCAAGUAUACUGCCCU
miR-18a guide	UAAGGUGCAUCUAGUGCAGAUAG
miR-18a passenger	ACUGCCCUAAGUGCUCCUUCUG
control guide	AAUUCUCCGAACGUGUCACGU
control passenger	GUGACACGUUCGGAGAAUUAC
2'OM miR-155	ACCCCUAUCACGAUUAGCAUUAA
2'OM control	CAAACACCAUUGUCACACUCCA

Table 8 bisulphite sequencing oligonucleotides

SATB1 CpG A Forward	TCTCCCTGTGCCACCCAG
SATB1 CpG A Reverse	ACCACAATGGCACTAGGAC
SATB1 CpG B Forward	TAACTCCTCATAATTTAAAA
SATB1 CpG B Reverse	GGGAGTTATTAGGAAGTGGT
SATB1 CpG C Forward	CTCTCCCTATACCACCCAA
SATB1 CpG C Reverse	TATTATAATGGTATTAGGAT
FOXP3 Forward	TGTTGTAGGATAGGGTAGTT
FOXP3 Reverse	CATAAAAATAATCTATCTAA

Table 9 oligonucleotides for filter retention

SATB1 BR1 motif 3 sense	GATGTAATAAGCATGTTTACAATATTTTATTTCAGTC
SATB1 BR1 motif 3 antisense	GACTGAAATAAAATATTGTAAACATGCTTATTACATC
SATB1 BR1 motif 3 (mutated) sense	GATGTAATTCAATTACGAATTGTATTTAATTTCAGTC
SATB1 BR1 motif 3 (mutated) antisense	GACTGAAATTAAATACAATTCGTAATTGAATTACATC
SATB1 BR2 motif 1 sense	TTAGATTTGTAATGTAAACAGTGTGCCTAAGAG
SATB1 BR2 motif 1 antisense	CTCTTAGGCACACTGTTTACATTACAAATCTAA
SATB1 BR2 motif 1 (mutated) sense	TTAGATTTAGTGTGGATAAATCATGCCTAAGAG
SATB1 BR2 motif 1 (mutated) antisense	CTCTTAGGCATGATTTATCCACACTAAATCTAA

Table 10 Histone ChIP-PCR oligonucleotides

SATB1 -25kb Forward	TTAATGGCGGTAAGTAGTAAGTTC
SATB1 -25kb Reverse	TAAGACCAGAGGAATCAGAGATC
SATB1 -24kb Forward	GCCCATGTGCTTTCTATACAAGAC
SATB1 -24kb Reverse	ACTCATCTGCTTCCCCAAGTTATC
SATB1 -23kb Forward	TCCCTCCTGCTTCCATAGTTTC
SATB1 -23kb Reverse	TTGGCAAGAAGTGTAGTTAGGTTC
SATB1 -22kb Forward	GCACACACACTACAGTAACC
SATB1 -22kb Reverse	CGCACTCCTCCTCTTGTC
SATB1 -21kb Forward	GTCCATGCCTGAGTGAGTTCTG
SATB1 -21kb Reverse	ACGAGGAGTGGGTGCTACG
SATB1 -20kb Forward	TGACCTCAGAAGACCAACAG
SATB1 -20kb Reverse	GAGAAAGTTCGCCAAGGAAG
SATB1 -19kb Forward	GGATTTCCCTCCTAAAGTAC
SATB1 -19kb Reverse	GGTCTTCTTTCTCTATCTTCC
SATB1 -17.5kb Forward	ACCTTCAGATATTTCAGAGAGCAG
SATB1 -17.5kb Reverse	AAGCACAAACCACACAAAACTG
SATB1 -13.5kb Forward	AGCAGTTAATCACAGAGGTAGTTC
SATB1 -13.5kb Reverse	TTGTCTAAGTAAGCCTAAGTCCAG
SATB1 -9.5kb Forward	TGTGTAGCATAGACTGGACTGTAG
SATB1 -9.5kb Reverse	GCCAAGCCTCAGAGAAACAATG
SATB1 -6.5kb Forward	TTGTGCTGCTTTAAGAGTGTAGAG

SATB1 -6.5kb Reverse	TCCGCCAGTGACTGTGTTAG
SATB1 -4kb Forward	TCCCGTGATCTTTGTTTAGTGGTG
SATB1 -4kb Reverse	GCCAGGCAATGTCACCTCAAG
SATB1 -3kb Forward	TCAGGGTGCTAAAATGGTAGAAC
SATB1 -3kb Reverse	CACTTCTGCTGTAATCTAGGGTAG
SATB1 -2kb Forward	CCGCCTCACTCTAATCAAG
SATB1 -2kb Reverse	AAAGCCGAAAGACAAGTAAC
SATB1 -1kb Forward	CTTCTGATCTTCCTCCTCCTC
SATB1 -1kb Reverse	CTCTCCCTGCCCATTGAC
SATB1 0kb Forward	GTCGGTTTTGCTAATTTCACTCAG
SATB1 0kb Reverse	GCTGGATCGCCTCCTTCG
SATB1 +1kb Forward	ATGGGACCTCTATCAACGGTAAAC
SATB1 +1kb Reverse	GGGCAGCAATGTTAATCTGGAAG
SATB1 +2kb Forward	CACATCTTTGGCCCAAAACTTG
SATB1 +2kb Reverse	AGAAGGTAACAAACATCTAACTGC

Table 11 oligonucleotides for miRNAs against human SATB and FOXP3

SATB1 miRNA sense	TGCTGATTCACTGCATACTGCTGGTTGTTTTGGCCACTGACTGAC AACCAGCAATGCAGTGAAT
SATB1 miRNA antisense	CCTGATTCACTGCATTGCTGGTTGTCAGTCAGTGGCCAAAACAAC CAGCAGTATGCAGTGAATC
FOXP3 miRNA sense	TGCTGAAAGCACTTGTGCAGACTCAGGTTTTGGCCACTGACTGAC CTGAGTCTACAAGTGCTTT
FOXP3 miRNA antisense	CCTGAAAGCACTTGTAGACTCAGGTCAGTCAGTGGCCAAAACCTG AGTCTGCACAAGTGCTTTC

SUPPLEMENTARY REFERENCES

1. Sadlon, T.J. *et al.* Genome-Wide Identification of Human FOXP3 Target Genes in Natural Regulatory T Cells. *J Immunol* (2010).
2. Szymczak, A.L. *et al.* Correction of multi-gene deficiency in vivo using a single 'self-cleaving' 2A peptide-based retroviral vector. *Nat Biotechnol* **22**, 589-594 (2004).
3. Floess, S. *et al.* Epigenetic control of the foxp3 locus in regulatory T cells. *PLoS Biol* **5**, e38 (2007).
4. Wei, G. *et al.* Global mapping of H3K4me3 and H3K27me3 reveals specificity and plasticity in lineage fate determination of differentiating CD4+ T cells. *Immunity* **30**, 155-167 (2009).
5. Brunkow, M.E. *et al.* Disruption of a new forkhead/winged-helix protein, scurfin, results in the fatal lymphoproliferative disorder of the scurfy mouse. *Nat Genet* **27**, 68-73 (2001).
6. Lahl, K. *et al.* Selective depletion of Foxp3+ regulatory T cells induces a scurfy-like disease. *J Exp Med* **204**, 57-63 (2007).
7. Lahl, K. *et al.* Nonfunctional regulatory T cells and defective control of Th2 cytokine production in natural scurfy mutant mice. *J Immunol* **183**, 5662-5672 (2009).
8. Shinkai, Y. *et al.* RAG-2-deficient mice lack mature lymphocytes owing to inability to initiate V(D)J rearrangement. *Cell* **68**, 855-867 (1992).
9. Zhou, X. *et al.* Selective miRNA disruption in T reg cells leads to uncontrolled autoimmunity. *J Exp Med* **205**, 1983-1991 (2008).

10. Classen, S. *et al.* Human resting CD4+ T cells are constitutively inhibited by TGF beta under steady-state conditions. *J Immunol* **178**, 6931-6940 (2007).

11. Schultze, J.L. & Eggle, D. IlluminaGUI: graphical user interface for analyzing gene expression data generated on the Illumina platform. *Bioinformatics* **23**, 1431-1433 (2007).

12. Lee, T.I., Johnstone, S.E. & Young, R.A. Chromatin immunoprecipitation and microarray-based analysis of protein location. *Nat Protoc* **1**, 729-748 (2006).

13. O'Geen, H., Nicolet, C.M., Blahnik, K., Green, R. & Farnham, P.J. Comparison of sample preparation methods for ChIP-chip assays. *Biotechniques* **41**, 577-580 (2006).

14. Johnson, W.E. *et al.* Model-based analysis of tiling-arrays for ChIP-chip. *Proc Natl Acad Sci U S A* **103**, 12457-12462 (2006).

15. Meister, G., Landthaler, M., Dorsett, Y. & Tuschl, T. Sequence-specific inhibition of microRNA- and siRNA-induced RNA silencing. *RNA* **10**, 544-550 (2004).

16. Mantei, A. *et al.* siRNA stabilization prolongs gene knockdown in primary T lymphocytes. *Eur J Immunol* **38**, 2616-2625 (2008).

17. Basu, S., Golovina, T., Mikheeva, T., June, C.H. & Riley, J.L. Cutting edge: Foxp3-mediated induction of pim 2 allows human T regulatory cells to preferentially expand in rapamycin. *J Immunol* **180**, 5794-5798 (2008).

18. Parry, R.V., Rumbley, C.A., Vandenberghe, L.H., June, C.H. & Riley, J.L. CD28 and inducible costimulatory protein Src homology 2 binding domains show distinct regulation of phosphatidylinositol 3-kinase, Bcl-xL, and IL-2 expression in primary human CD4 T lymphocytes. *J Immunol* **171**, 166-174 (2003).

19. Wiznerowicz, M. & Trono, D. Conditional suppression of cellular genes: lentivirus vector-mediated drug-inducible RNA interference. *Journal of virology* **77**, 8957-8961 (2003).

20. Golovina, T.N. *et al.* CD28 costimulation is essential for human T regulatory expansion and function. *J Immunol* **181**, 2855-2868 (2008).

21. Klug, S.J., Huttenhofer, A., Kromayer, M. & Famulok, M. In vitro and in vivo characterization of novel mRNA motifs that bind special elongation factor SelB. *Proc Natl Acad Sci U S A* **94**, 6676-6681 (1997).

22. Tang, Q. *et al.* In vitro-expanded antigen-specific regulatory T cells suppress autoimmune diabetes. *The Journal of experimental medicine* **199**, 1455-1465 (2004).

23. Zhang, Y. *et al.* Model-based analysis of ChIP-Seq (MACS). *Genome biology* **9**, R137 (2008).